

NITRATO COMPLEXES
OF MANGANESE(III)

by

DAVID WILLIAM JOHNSON

B.Sc., University of Alberta, Calgary, 1966

A THESIS SUBMITTED IN PARTIAL FULFILMENT
OF THE REQUIREMENTS FOR THE DEGREE OF
DOCTOR OF PHILOSOPHY
in the Department of
Chemistry

©

DAVID WILLIAM JOHNSON
SIMON FRASER UNIVERSITY

AUGUST, 1972.

APPROVAL

Name: David William Johnson

Degree: Doctor of Philosophy

Title of Thesis: Nitrate Complexes of Manganese(III)

Examining Committee:

Chairman: T.N. Bell

D. Sutton, Senior Supervisor

F.W.B. Einstein

C.H.W. Jones

L.K. Peterson

N. Paddock,
Professor,
University of British Columbia
Vancouver, B.C.

Date Approved: August 2nd 1972.

Abstract

The thesis describes a study of the reactions of a variety of manganese compounds with N_2O_4 or N_2O_5 leading to the synthesis of new manganese compounds with coordinated nitrate groups and other ligands. The aim of this work, to synthesise the first reported nitrate-complexes of manganese in an oxidation state higher than the common state (II), has been achieved.

Manganese(III) trinitrate, $Mn(NO_3)_3$, has been prepared by reaction of manganese(III) trifluoride and dinitrogen pentoxide in dinitrogen tetroxide. Manganese(III) trinitrate is stable indefinitely below $-14^\circ C$, but rapidly evolves N_2O_4 at room temperature and fumes in moist air. The properties indicate that all nitrate groups are strongly coordinated and suggest that the compound is polymeric with bridging nitrate groups. The bipyridyl, o-phenanthroline, triphenylphosphine oxide and acetonitrile complexes of $Mn(NO_3)_3$ have been prepared; all are stable at room temperature in a dry atmosphere and their magnetic moments are normal for high spin d^4 complexes.

Cesium and nitronium tetranitratomanganate(III) and sodium and potassium tetranitratomanganate(II) have been prepared. This makes the manganese-nitrate system unique

among transition metal nitrate complexes, since tetranitrato-complexes for two oxidation states of manganese exist, but have not been found for any other transition metal.

The crystal and molecular structure of trinitrato-2,2'-bipyridylmanganese(III), $\text{Mn}(\text{NO}_3)_3 \cdot \text{bipy}$, was determined. $\text{Mn}(\text{NO}_3)_3 \cdot \text{bipy}$ forms monoclinic crystals, space group $P2_1/c$ with four molecules in a unit cell with dimensions of $a = 7.311(3)$, $b = 18.022(7)$, $c = 11.704(4) \text{ \AA}$ and $\beta = 108.73(3)^\circ$. The manganese atom is seven coordinate, with approximate pentagonal bipyramidal geometry. The equatorial ligand atoms consist of one nitrogen of the bipyridyl group and four oxygens from two bidentate nitrate groups; the remaining bipyridyl nitrogen and the coordinated oxygen of the unidentate nitrate group are at the apices. This is the first nitrate complex to be shown by crystallography to possess three distinctly different coordinated nitrate groups. One nitrate group is unidentate with $\text{Mn}-\text{O} = 1.896(8) \text{ \AA}$, one is symmetric bidentate with $\text{Mn}-\text{O} = 2.236(8)$ and $2.201(8) \text{ \AA}$ and one asymmetric bidentate with $\text{Mn}-\text{O} = 2.112(8)$ and $2.400(9) \text{ \AA}$.

The Raman spectra of a number of powdered anhydrous metal nitrates have been determined and a technique to obtain the depolarization ratios of powdered samples by immersion in a liquid of identical refractive index has been examined and found to be impractical for this work.

To my three girls, Edna Mae, Janice and Bonnie.

ACKNOWLEDGEMENTS

I would like to express my sincere thanks to my Research Director, Dr. Derek Sutton, for his helpful guidance and advice throughout the five years of this work.

My sincere thanks are also extended to:

Dr. F.W.B. Einstein for his aid in the X-ray crystallography involved in this thesis and the continuing interest and many hours of friendly discussion of my progress while at Simon Fraser;

The faculty, staff and fellow-students of the Chemistry Department at Simon Fraser University, especially Mr. Alan Gilchrist for always being ready to discuss chemistry over another cup of coffee and for proof reading this thesis;

and my wife, Edna Mae, who has managed to put up with me and still find the many hours necessary to type and proof read this thesis.

Table of Contents

Chapter	Page
1. Review of Metal-Nitrate Complexes and Definition of the Research	1
1.1. Introduction	1
1.2. Preparative Techniques	3
1.3. Determination of the Nature of the Metal Nitrate Bond	8
1.3.1. Diffraction Techniques	8
1.3.2. Vibrational Spectroscopy	23
1.4. Research Proposal	28
1.4.1. Preparative Chemistry	28
1.4.2. Investigation of the Coordination of Nitrates by Spectroscopic Techniques	33
 2. Anhydrous Manganese(III) Nitrate	 35
2.1. Introduction	35
2.2. Preparation of Manganese(III) Nitrate	36
2.2.1. Reaction of MnF_3 and N_2O_5	36
2.2.2. Reaction of MnF_3 and $AgNO_3$	39
2.2.3. Reaction of MnF_3 and N_2O_4	40
2.2.4. Reaction of MnO_2 and N_2O_5 or N_2O_4	40
2.2.5. Reactions of K_2MnO_4 and $BaMnO_4$ with N_2O_4	42

2.2.6.	Reaction of KMnO_4 and N_2O_4	43
2.2.7.	Physical Measurements	45
2.3.	Properties of Manganese(III) Trinitrate	46
2.3.1.	Physical Properties	46
2.3.2.	X-Ray Powder Patterns	47
2.3.3.	Solubility and Electronic Spectrum	50
2.3.4.	Infrared Spectrum	52
2.3.5.	Magnetic Susceptibility	54
2.3.5.	Chemical Properties	55
3.	Complexes of Manganese(III) Trinitrate	64
3.1.	Introduction	64
3.2.	Trinitrato-2,2'-bipyridylmanganese(III)	65
3.2.1.	Preparation	65
3.2.2.	Physical Measurements	66
3.2.3.	Discussion	66
3.3.	Trinitrato- α -phenanthroline manganese(III)	72
3.4.	Trinitratomanganese(III) bistriphenylphosphineoxide	74
3.5.	Trinitratomanganese(III)·acetonitrile	75
3.6.	Reaction of Manganese(III) Trinitrate with Pyridine	79
3.7.	Reaction of Manganese(III) Trinitrate with Triphenylphosphine	80

3.8.	Discussion	80
4.	The Crystal and Molecular Structure of Trinitrato-2,2'-bipyridylmanganese(III)	82
4.1.	Introduction	82
4.2.	Determination of the Structure	84
4.2.1.	Crystal Mounting	84
4.2.2.	Photographs	84
4.2.3.	Data Collection	86
4.2.4.	Solution of the Structure	88
4.3.	Results and Discussion	99
4.3.1.	Mn(NO ₃) ₃ ·bipy Crystal Data	99
4.3.2.	Description of the Structure	99
4.3.3.	Discussion of the Structure	105
5.	Tetranitratomanganates	113
5.1.	Introduction	113
5.2.	Tetranitratomanganates(II)	114
5.2.1.	Potassium Tetranitratomanganates(II)	114
5.2.2.	Sodium Tetranitratomanganates(II)	114
5.2.3.	Discussion	115
5.3.	Tetranitratomanganates(III)	119
5.3.1.	Nitronium Tetranitratomanganate(III)	119

5.3.2.	Cesium	
	Tetranitratomanganate(III)	120
5.3.3.	Reaction of Cs_2MnCl_5 and N_2O_5	120
5.3.4.	Discussion	121
6.	Raman Spectra of Anhydrous Metal Nitrates	129
6.1.	Introduction	129
6.2.	Experimental Technique	131
6.2.1.	Sample Mounting and Calibration	131
6.2.2.	Immersion Media	132
6.3.	Results	133
6.3.1.	Barium Nitrate	133
6.3.2.	Sodium Sulfate	140
6.3.3.	Discussion	144
6.4.	Raman Spectra	146
6.4.1.	Experimental	147
6.4.2.	Main Group Metal Nitrates	149
6.4.3.	Transition Metal Nitrates	155
6.5.	α - and β -Copper(II) Nitrates	160
6.5.1.	α -Copper Nitrate	161
6.5.2.	β - $\text{Cu}(\text{NO}_3)_2$	166
Appendix A.		170
Bibliography		175

List of Tables.

	Page.
1.1. Anhydrous Metal Nitrate and Nitrate Complexes.	9
1.2. Nitrate Vibrational Modes	25
1.3. Compounds and Complexes of Manganese(III)	32
2.1. X-Ray Powder Patterns for Manganese Nitrate Species	51
2.2. Infrared Spectra of Metal Nitrates	54
2.3. Magnetic Moments of Some Metal Nitrates	55
2.4. Determination of the Oxidation State of Manganese	56
3.1. Infrared Spectra of Some Complexes of $Mn(NO_3)_3$	69
3.2. X-Ray Powder Patterns for Several Mn(III) Complexes	71
3.3. Analysis of $Mn(NO_3)_3 \cdot xMeCN$	77
4.1. Density of $Mn(NO_3)_3 \cdot bipy$	86
4.2. Final Fractional Coordinates and Thermal Parameters	94
4.3. Observed and Calculated Structure Factors (20 x F absolute) for $Mn(NO_3)_3 \cdot bipy$	96
4.4. Interatomic Distances and Angles	100
4.5. Mean Planes as $Ax + By + Cz + D = 0$	103
4.6. Interatomic distances in Unidentate Nitrates	111
5.1. Infrared and Raman Spectra of $Na_2Mn(NO_3)_4$ and $K_2Mn(NO_3)_4$	116
5.2. Infrared Spectra of the Tetranitratomanganate(III) Anion	123

5.3.	X-Ray Powder Photographs of Tetranitratomanganate(III) Anion	124
6.1.	Reference Spectra of the Immersion Liquids.	134
6.2.	Variation of Apparent Depolarization Ratios for $\text{Ba}(\text{NO}_3)_2$ with Refractive Index of the Liquid Phase	137
6.3.	Raman Active $\text{SO}_4^{=}$ Modes in Na_2SO_4	141
6.4.	Variation of Apparent Depolarization Ratio for the A_1 Mode of Na_2SO_4 with Refractive Index of the Liquid Phase	142
6.5.	Preparation of Anhydrous Nitrates	148
6.6.	Raman Spectra of Alkali Metal and Silver Nitrates	150
6.7.	Raman Spectra of Calcium, Strontium, Barium and Lead Nitrates	151
6.8.	Vibrational Spectra of $\text{Be}(\text{NO}_3)_2$, $\text{Mg}(\text{NO}_3)_2$, $\text{Be}(\text{NO}_3)_2 \cdot 2\text{N}_2\text{O}_4$ and $\text{Mg}(\text{NO}_3)_2 \cdot \text{N}_2\text{O}_4$	153
6.9.	Raman Spectra of Sn and Tl Nitrates	156
6.10.	Raman Spectra of Mn, Co, Zn, Cd, and Hg Dinitrates	159
6.11.	Infrared and Raman Spectra of $\alpha\text{-Cu}(\text{NO}_3)_2$	164
6.12.	Infrared and Raman Spectra of $\beta\text{-Cu}(\text{NO}_3)_2$	168

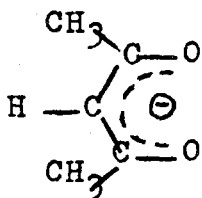
List of Figures.

	Page.
1.1. Unidentate coordination - the tetranitratoaurate(III) ion	15
1.2. Symmetric bidentate coordination- titanium tetranitrate	15
1.3. Bridging coordination - α -copper nitrate	16
1.4. Modes of nitrate coordination	18
2.1. The apparatus used for the generation of dinitrogen pentoxide	38
2.2. Gravimetric analysis of $Mn(NO_3)_3$ at 22°C	48
2.3. Infrared spectrum of $Mn(NO_3)_3$	53
3.1. Infrared spectrum of $Mn(NO_3)_3 \cdot bipy$	68
3.2. Infrared spectrum of $Mn(NO_3)_3 \cdot o\text{-phen}$	73
3.3. Infrared spectrum of $Mn(NO_3)_3 \cdot 2OPPh_3$	76
3.4. Infrared spectrum of $Mn(NO_3)_3 \cdot xMeCN$	78
4.1. The molecular configuration of $Mn(NO_3)_3 \cdot bipy$	104
4.2. A stereoscopic view showing the molecular packing	106
5.1. Infrared spectrum of $K_2Mn(NO_3)_4$	117
5.2. Infrared spectrum of $Na_2Mn(NO_3)_4$	118
5.3. Infrared spectrum of $NO_2^+Mn(NO_3)_4^-$	122
5.4. Thermal gravimetric analysis of $NO_2^+Mn(NO_3)_4^-$	127
6.1(a) 1047 cm^{-1} band of powdered $Ba(NO_3)_2$	136
(b) 1047 cm^{-1} band of powdered $Ba(NO_3)_2$ immersed in a liquid of $\eta = 1.572$	136

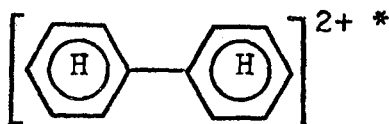
6.2.	Variation of apparent depolarization ratio for the 1047 cm^{-1} band of $\text{Ba}(\text{NO}_3)_2$ with refractive index of the liquid	138
6.3.	Variation of apparent depolarization ratio for the 733 cm^{-1} band of $\text{Ba}(\text{NO}_3)_2$ with refractive index of the liquid	139
6.4.	Variation of apparent depolarization ratio for the 993 cm^{-1} band of Na_2SO_4 with refractive index of the liquid	143
6.5.	Raman spectrum of $\text{Ti}(\text{NO}_3)_4$	157
6.6.	Raman spectrum of $\alpha\text{-Cu}(\text{NO}_3)_2$	162
6.7.	Raman spectrum of $\beta\text{-Cu}(\text{NO}_3)_2$	163

Abbreviations

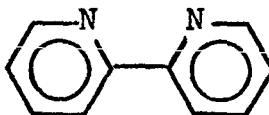
acac Acetylacetonato



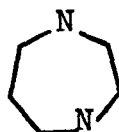
bipH₂ Biphenyl



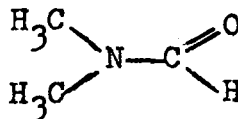
bipy 2-2'-bipyridyl



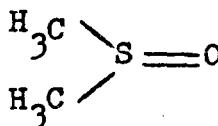
dach 1,4-diazacycloheptane



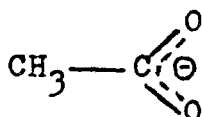
DMF N,N-Dimethylformamide



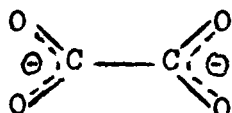
DMSO Dimethylsulfoxide



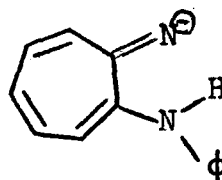
OAc Acetato



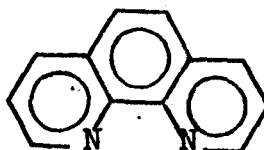
ox Oxalato



pati N-phenylaminoironiminato



o-phen o-phenanthroline



Chapter 1
Review of Metal-Nitrate Complexes
and Definition of the Research.

1.1. Introduction.

Until 1958, when Addison and Hathaway reported the preparation of anhydrous copper(II) nitrate, which they showed to contain covalent nitrate groups (1), the nitrate group was considered to be only a weak ligand, capable of forming only ionic complexes with metals. There were two obvious reasons for this. Firstly, most syntheses of metal nitrates had utilized aqueous media, and the nitrate ligands were unable to replace the water of solvation around the metal and secondly, the only nitrates which crystallized anhydrous from aqueous solution were the ionic nitrates of the alkali metals (sodium through cesium), silver, barium, lead and thallium(I) (see references 2 and 3 and the references therein). Furthermore, the only anhydrous metal nitrates produced by thermal dehydration of the hydrates were the ionic nitrates of calcium, strontium, cadmium etc. Therefore in the late 1950's, it was a very reasonable assumption that nitrate groups were weak ligands, and the synthetic methods in use up till that time offered little prospect for the synthesis and study of compounds containing

coordinated nitrate groups. The unusual properties of anhydrous copper(II) nitrate, (e.g., its volatility, and reactivity (1)) and the recognition that similar anhydrous nitrates and nitrate complexes could be readily obtained in similar fashion from reactions in liquid dinitrogen tetroxide have prompted a rapid growth in the synthesis and, in particular, the structural investigation of this class of compounds. In general, the compounds prepared have been restricted to the common and reasonably easily accessible oxidation states of the metals. The work reported in this thesis is concerned with (i) an attempt to synthesise and characterise nitrate compounds for a metal, manganese, in a less common oxidation state, here (III), and (ii) a study of the reactions of a variety of compounds of manganese in various oxidation states with a variety of potentially nitrate-producing solvent systems in order to judge the course of the reactions and the oxidation states achieved.

Before the results of this study are described, a review of the principal techniques and the major accomplishments in metal nitrate research in the recent past will be presented, concluding with an outline of the aims of the present work.

1.2. Preparative Techniques.

Up to the present time only a limited number of species containing coordinated nitrate groups have been prepared from aqueous media. One class of nitrate complexes which has been produced from aqueous solution were the double nitrates of the trivalent lanthanides of the general formulas $M^{II}_3Ln^{III}_2(NO_3)_{12} \cdot 24H_2O$ (where $M = Mg, Zn$ and $Ln = La, Ce, Pr, Nd, Sm, Eu, Gd, Er$) or $M^I_2Ln^{III}(NO_3)_5 \cdot 12H_2O$ (where $M = Na, K, Rb, Cs, Tl, NH_4, PPh_4$ and $Ln = La, Ce, Pr, Nd$) (4, 5). (Throughout this thesis the term "nitrate" will be used to designate an anionic nitrate species and "metal nitrate", a neutral species.) The crystal structure of $Mg_3Ce_2(NO_3)_{12} \cdot 24H_2O$ has been determined, and the cerium atoms are coordinated by twelve oxygen atoms from six bidentate nitrates (6).

Partial dehydration of the hexahydrates of the transition metal nitrates by heating in vacuo or by addition of dinitrogen tetroxide has produced lower hydrates containing coordinated nitrates such as $Ni(NO_3)_2 \cdot 4H_2O$ and $Cr(NO_3)_2 \cdot 2H_2O$ (7 - 10) but attempts to completely remove the water of hydration resulted in the evolution of nitric acid and the production of a metal oxide or hydroxide. From the above it can be seen that

only a very limited range of nitrate complexes may be prepared from aqueous solution or from metal nitrate hydrates. Therefore, non-aqueous solvent systems have been utilized to prepare the majority of the complexes containing coordinated nitrate groups. The solvent systems that have been used are: organic solvents such as acetone, acetonitrile etc., with silver nitrate as the source of nitrate; anhydrous nitric acid; dinitrogen tetroxide; dinitrogen pentoxide, or various combinations of these.

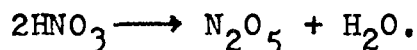
Reactions between metal halides and silver nitrate in organic solvents have been frequently used to prepare nitrate complexes, as the desired counter ion may be included in the reaction solution. Thus the reaction:



was used to prepare the tetranitratoferrate(III) complex (11). However when similar reactions were attempted to prepare anhydrous metal nitrates, addition compounds with the organic solvents tended to crystallize from solution. The removal of the coordinated solvent may be as difficult as the removal of water from hydrated species (2).

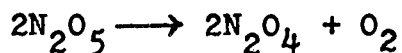
The use of nitric acid has met with little success

for the preparation of anhydrous transition metal nitrates, since in all of the reactions studied hydrated metal nitrates were produced (12). The authors felt that an equilibrium between nitric acid, its acid anhydride and water was responsible for the water of hydration, i.e.,



The high aquation energy of the transition metals would then promote the formation of the hydrate at the expense of the anhydrous nitrate. Recently anhydrous nitric acid, saturated with dinitrogen pentoxide has been used to prepare $\text{Cs}[\text{Al}(\text{NO}_3)_4]$ and $\text{Cs}_2[\text{Al}(\text{NO}_3)_5]$ (13, 14). The latter complex is the first reported example of a complex containing more than four nitrate groups for a metal having $Z < 40$.

One of the most useful routes to anhydrous metal nitrates is by reactions involving dinitrogen pentoxide. In the solid state dinitrogen pentoxide is completely ionized into NO_2^+ and NO_3^- ions (15, 16), but the liquid is non-conducting and hence more likely to be similar to the vapor which is O_2NONO_2 (16). Pure dinitrogen pentoxide melts at 31°C , but the solid readily sublimes at 25°C at one atmosphere pressure. Furthermore, at room temperature, dinitrogen pentoxide decomposes according to the equation:

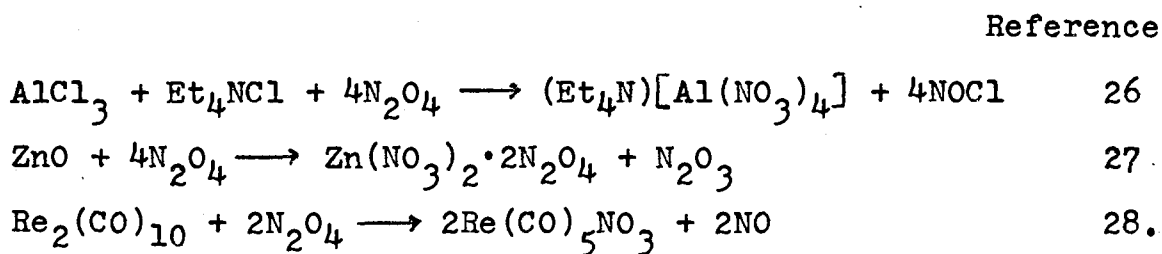


The lack of a convenient liquid range, the ease of sublimation of the solid and the decomposition of the dinitrogen pentoxide may be considered to detract from its usefulness as a preparative reagent for anhydrous metal nitrates. Its usefulness arises from the facts that it is a strong oxidant, it may react in the solid state, or it may usefully be diluted with other solvents. Solid dinitrogen pentoxide reacts with metals, metal halides or hydrated nitrates to yield anhydrous metal nitrates, as illustrated by the following reactions:

	Reference
$\text{Cu} + 2\text{N}_2\text{O}_5 \longrightarrow \text{Cu}(\text{NO}_3)_2 + 2\text{NO}_2$	17
$\text{CoF}_3 + 3\text{N}_2\text{O}_5 \longrightarrow \text{Co}(\text{NO}_3)_3 + 3\text{NO}_2\text{F}$	18
$\text{NO}^+\text{GaCl}_4^- + 5\text{N}_2\text{O}_5 \longrightarrow \text{NO}_2^+\text{Ga}(\text{NO}_3)_4^- + 4\text{NO}_2\text{Cl} + 2\text{NO}_2$	19
$\text{Ti}(\text{NO}_3)_4 \cdot x\text{H}_2\text{O} + x\text{N}_2\text{O}_5 \longrightarrow \text{Ti}(\text{NO}_3)_4 + 2x\text{HNO}_3$	20

Dinitrogen pentoxide in liquid dinitrogen tetroxide has been used to prepare $\text{Sn}(\text{NO}_3)_6^{2-}$ (21) and $\text{Zr}(\text{NO}_3)_4$ (22). Also pure dinitrogen pentoxide can be used in inert organic solvents; hence it has been used in carbon tetrachloride to prepare $\text{Cr}(\text{NO}_3)_3$ (23) and $(\text{CH}_3)_2\text{Ge}(\text{NO}_3)_2$ (24).

The other route to anhydrous metal nitrates is by reactions involving dinitrogen tetroxide. The physical and chemical properties of dinitrogen tetroxide have been reviewed by Addison (25). It has a convenient liquid range, -11.2°C to 21.2°C and has been shown to be O₂N-NO₂ in the solid and gaseous states. In the liquid state, homolytic dissociation ^{occurs} does occur to produce nitrogen dioxide. As well as homolytic dissociation, heterolytic dissociation occurs in the liquid state to produce NO⁺ and NO₃⁻, i.e., O₂N-NO₂ → [NO₂⁺][NO₂⁻] → [NO⁺][NO₃⁻]. This self dissociation provides the necessary source of nitrate ions. Dinitrogen tetroxide reacts with metal halides, metal oxides and metal carbonyls as illustrated by the following equations:



With pure dinitrogen tetroxide adducts are often formed; in some cases the dinitrogen tetroxide may be easily removed in vacuo (i.e., Zn(NO₃)₂·2N₂O₄), whereas in other cases decomposition of the entire nitrate occurs as well. Thus, Fe(NO₃)₃·N₂O₄ decomposes to FeO(NO₃) instead of producing

$\text{Fe}(\text{NO}_3)_3$ (29).

The ionization, and hence the reactivity, of dinitrogen tetroxide may be increased by using organic solvents with high dielectric constants and good electron donor ability to promote its self-dissociation. Thus, dinitrogen tetroxide in ethyl acetate reacts with metallic copper (1) and ferric chloride (29) whereas neither react with pure dinitrogen tetroxide.

The anhydrous nitrates which have been prepared are presented in table 1.1.

1.3. Determination of the Nature of the Metal-Nitrate Bond.

1.3.1. Diffraction Techniques.

As more compounds containing coordinated nitrates have been prepared, an ever increasing number have been examined by X-ray, neutron and electron diffraction techniques. The structures determined prior to mid-1970 have been reviewed by Addison and co-workers (73). The nitrate ligand has been shown to exhibit three major modes of bonding - unidentate, bidentate and bridging, as illustrated by $\text{Au}(\text{NO}_3)_4^-$ (63, 64), $\text{Tl}(\text{NO}_3)_4$ (45) and $\text{Cu}(\text{NO}_3)_2$ (61) in Figures 1.1 to 1.3 respectively. Furthermore, there are at least two types of bidentate

Table 1.1. Anhydrous Metal Nitrate and Nitrate Complexes.

<u>Compound</u>	<u>Mode of Coordination^a</u>	<u>Preparative Method^b</u>	<u>References</u>
LiNO_3	I	D	2
NaNO_3	I	A	2
KNO_3	I	A	2
RbNO_3	I	A	2
CsNO_3	I	A	2
$\text{Be}(\text{NO}_3)_2$	C	F	30
$\text{Be}_4\text{O}(\text{NO}_3)_6$	Br	G	17, 30
$\text{Mg}(\text{NO}_3)_2$	I	F	30
$\text{Ca}(\text{NO}_3)_2$	I	D	30
$\text{Sr}(\text{NO}_3)_2$	I	D	30
$\text{Ba}(\text{NO}_3)_2$	I	A	30
$\text{B}(\text{NO}_3)_4^-$	C	E	31
$\text{Al}(\text{NO}_3)_3$	C	G	26
$\text{Al}(\text{NO}_3)_4^-$	C	E,G,H	13, 14, 26
$\text{Ga}(\text{NO}_3)_4^-$	U	G	19
$\text{In}(\text{NO}_3)_3$	C	F,G	17, 32
$\text{In}(\text{NO}_3)_4^-$	C	L	33
TlNO_3	I	A	2
$\text{Tl}(\text{NO}_3)_4^-$	C	G	34

Table 1.1. (continued).

<u>Compound</u>	<u>Mode of Coordination^a</u>	<u>Preparative Method^b</u>	<u>References</u>
$\text{Sn}(\text{NO}_3)_4$	SBi	G	35, 36, 37
$\text{Sn}(\text{NO}_3)_6^{2-}$	C	K	21
$\text{Pb}(\text{NO}_3)_2$	I	A	2
$\text{SbO}(\text{NO}_3)$	C	F	38
$\text{SbO}(\text{NO}_3)_3$	U	G	39
$\text{Bi}(\text{NO}_3)_3$	C	D,F	2, 38
$\text{BiO}(\text{NO}_3)$	C	D,F	2, 38
$\text{Po}(\text{NO}_3)_4$	C	E	40
$\text{Zn}(\text{NO}_3)_2$	C	E,G	17, 41
$\text{Zn}(\text{NO}_3)_4^{2-}$	C	E	42
$\text{Cd}(\text{NO}_3)_2$	I	D,E	2, 41
$\text{Hg}(\text{NO}_3)_2$	C	F,G	17, 41
$\text{Hg}(\text{NO}_3)_4^{2-}$	C	L	43
$\text{Sc}(\text{NO}_3)_3$	C	D	2
$\text{Y}(\text{NO}_3)_3$	C	E	44
$\text{La}(\text{NO}_3)_3$	C	E	44

Table 1.1. (continued).

<u>Compound</u>	<u>Mode of Coordination^a</u>	<u>Preparative Method^b</u>	<u>References</u>
Ti(NO ₃) ₄	SB1	F,G,M	20, 36, 39, 45
TiO(NO ₃) ₂	C	T	46
Zr(NO ₃) ₄	B1	G	17
Zr(NO ₃) ₆ ²⁻	C	K	21
ZrO(NO ₃) ₂	C	F	46
Hf(NO ₃) ₄	B1	G	17
Hf(NO ₃) ₆ ²⁻	C	K	21
VO(NO ₃) ₃	B1	G	36, 39
VO ₂ (NO ₃)	C	F	47
NbO(NO ₃) ₃	C	G	2, 48
NbO ₂ (NO ₃)	C	F	49
NbO(NO ₃) ₄ ⁻	C	G	50
TaO(NO ₃) ₃	C	G	49
TaO(NO ₃) ₄ ⁻	C	G	50
Cr(NO ₃) ₃	C	J	23
CrO ₂ (NO ₃) ₂	C	G	39
MoO ₂ (NO ₃) ₂	C	G	39
WO ₂ (NO ₃) ₂	C	G	39

Table 1.1. (continued).

<u>Compound</u>	<u>Mode of Coordination^a</u>	<u>Preparative Method^b</u>	<u>References</u>
$\text{Mn}(\text{NO}_3)_2$	C	F,D	41, 51
$\text{Mn}(\text{NO}_3)_4^{2-}$	SBi	L	52, 53
$\text{ReO}_3(\text{NO}_3)$	--	-- ^d	5
$\text{Fe}(\text{NO}_3)_3$	C	E	54
$\text{Fe}(\text{NO}_3)_4^-$	SBi	F	11, 29
$\text{FeO}(\text{NO}_3)$	C	T	29
$\text{Co}(\text{NO}_3)_2$	C	F	41
$\text{Co}(\text{NO}_3)_4^{2-}$	ABi	L	52, 55
$\text{Co}(\text{NO}_3)_3$	SBi	L	18, 56
$\text{Ni}(\text{NO}_3)_2$	C	E	2
$\text{Ni}(\text{NO}_3)_4^{2-}$	C	L	52
$\text{Ni}(\text{NO}_3)_3^c$	C	T	57
$\text{Ni}(\text{NO}_3)_4^{-c}$	C	G	57
$\text{Pd}(\text{NO}_3)_2$	C	G	17
$\text{Pd}(\text{NO}_3)_4^{2-}$	C	H	5
$\text{Pd}(\text{NO}_3)_4$	C	G	58

Table 1.1. (continued).

<u>Compound</u>	<u>Mode of Coordination^a</u>	<u>Preparative Method^b</u>	<u>References</u>
$\text{Cu}(\text{NO}_3)_2$	Br	F	1, 59, 60, 61
$\text{Cu}(\text{NO}_3)_2(\text{g})$	SB1	F	62
$\text{Cu}(\text{NO}_3)_4^{2-}$	C	L	52
AgNO_3	I	A	2
$\text{Au}(\text{NO}_3)_4^-$	U	-- ^d	63, 64
$\text{Ln}(\text{NO}_3)_3$	C	E,F	44, 65
(Ln = La, Pr, Nd, Sm, Eu, Gd, Tb, Dy, Ho, Er, Tm, Yb, Lu)			
$\text{Ce}(\text{NO}_3)_6^{2-}$	SB1	A	6, 66
$\text{Th}(\text{NO}_3)_4$	C	H	67
$\text{Th}(\text{NO}_3)_6^{2-}$	SB1	H	67
$\text{ThO}(\text{NO}_3)_2$	C	T	67
$\text{Pa}(\text{NO}_3)_6^-$	C	G	50
$\text{LnO}(\text{NO}_3)$	C	T	68
(Ln = Eu, Gd, Dy, Ho, Er, Tm, Tl, Lu)			
$\text{An}(\text{NO}_3)_6^{2-}$	C	L	69, 70
(An = U, Np, Pu)			
$\text{UO}_2(\text{NO}_3)_2$	SB1	F	71
$\text{UO}_2((\text{NO}_3)_3)^-$	SB1	A	72
$\text{UO}_2(\text{NO}_4)_4^{2-}$	C	L	70

Table 1.1. (continued).

- a Mode of Coordination: I, Ionic; C, Covalent;
U, Unidentate; SBI, Symmetric Bidentate;
ABI, Asymmetric Bidentate; Br, Bridging.
- b Preparative Method: A, aqueous; D, dehydration;
E, N_2O_4 ; F, N_2O_4 /solvent mixtures; G, N_2O_5 ;
H, HNO_3 or HNO_3/N_2O_5 ; J, N_2O_5/CCl_4 ;
K, "Liquid N_2O_5 "; T, thermal decomposition;
L, Metathetical or stoichiometric addition;
M, $ClNO_3$.
- c These products are unlikely to be Ni(III) species in
view of the work reported in reference 204.
- d Preparation still to be published.

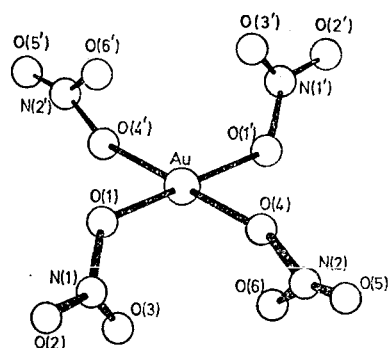


Figure 1.1. Unidentate coordination - the tetranitratoaurate(III) ion (references 63, 64).

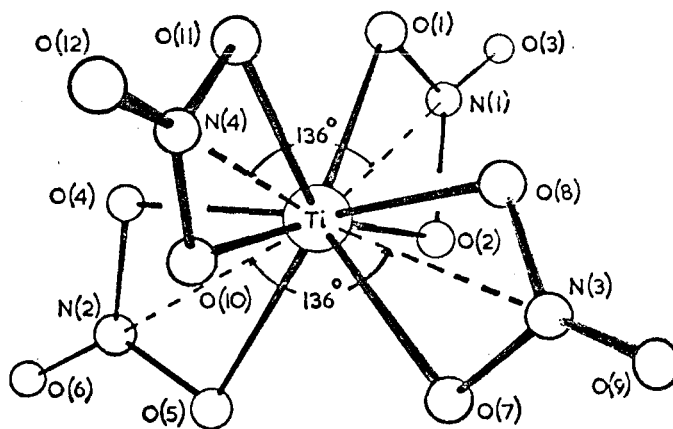


Figure 1.2. Symmetric bidentate coordination - titanium tetranitrate (reference 45).

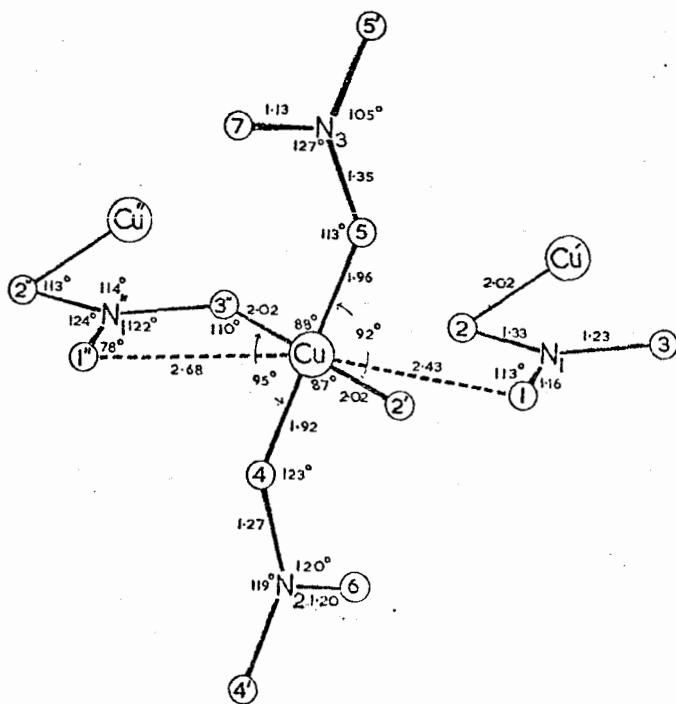


Figure 1.3. Bridging coordination - α copper nitrate (reference 61).

coordination (symmetric with less than 0.10\AA difference in M-O bond lengths, and asymmetric with a difference of 0.10 to 0.70\AA in M-O bond lengths) and numerous types of bridging coordination. The various modes of coordination, along with recent examples of each are shown in Figure 1.4.

The majority of structures determined to date have revealed symmetric bidentate coordination. This is partially due to the fact that the complexes studied were frequently chosen to support the interpretation of other physical and chemical properties (such as reactivity, volatility, spectral properties, and predicted high coordination of the metal atoms) which have become indicative of this particular mode of coordination. Furthermore, many of the compounds suspected of containing bridging nitrates, e.g., $\text{Cr}(\text{NO}_3)_3$ (23), $\text{Fe}(\text{NO}_3)_3$ (54), and the majority of the transition metal dinitrates, do not form crystals suitable for structural determinations, thus making the number of complexes containing symmetric bidentate coordination disproportionately large. Even so, Addison (73) suggests that nitrate groups do show a preference for this mode of coordination for two reasons: (i) the geometry of the nitrate groups forces the second oxygen close to the metal, and (ii) the donation of less electronic charge by two oxygen atoms is more favorable than all the

Figure 1.4. Modes of Nitrate Coordination.

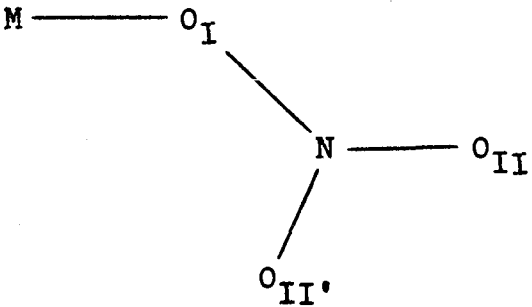
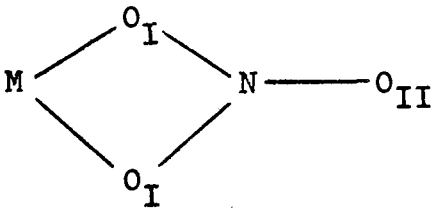
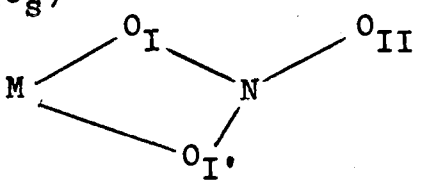
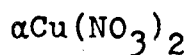
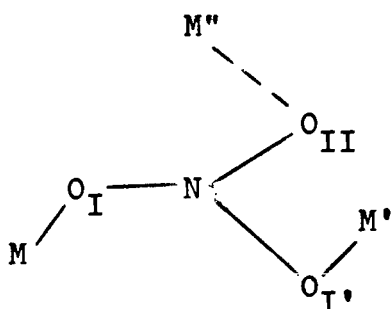
MODE (POINT GROUP SYMMETRY)	COORDINATION GEOMETRY	RECENT EXAMPLES	REFERENCES
UNIDENTATE (C_s)		$VO(NO_3)_3 \cdot MeCN$ $Mn(NO_3)_3 \cdot bipy$ $[Co(tn)_2(NO_3)_2]NO_3$ $Ni(py)(H_2O)_2(NO_3)_2$ $(PPh_2Me)_3Cu(NO_3)$ $[Cu(bipy)_2NO_3]NO_3$ $Cu(picam)_2(NO_3)_2$ $Ag(bipy)(NO_3)_2$ $Sn(CH_3)_3(NO_3)H_2O$	74 This work 75 76 77 78 79 80 81
SYMMETRIC BIDENTATE (C_{2v})		$VO(NO_3)_3 \cdot MeCN$ $Mn(NO_3)_3 \cdot bipy$ $[Ph_4As][Fe(NO_3)_4]$ $(OPPh_3)_2Ce(NO_3)_4$ $UO_2(NO_3)_2(H_2O)_2$	74 This work 11 82 83
ASYMMETRIC BIDENTATE (C_s)		$Mn(NO_3)_3 \cdot bipy$ $Cu(pic)_2(NO_3)_2$ $[Cu(py)_2(NO_3)_2]py$ $(CH_3)Sn(NO_3)_3$	This work 84 85, 86 87

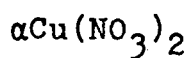
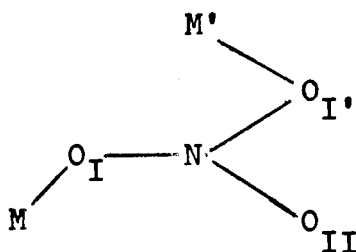
Figure 1.4. (continued).

BRIDGING
(VIA 3 O's)
(C_s)

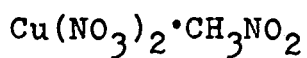


61

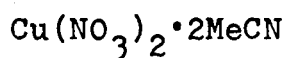
BRIDGING
(VIA 2 O's)
(C_{2v} or C_s)



61

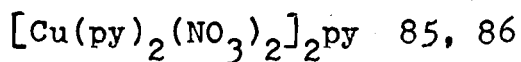
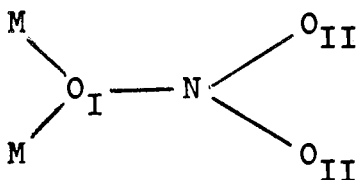


88



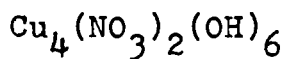
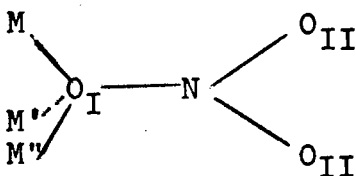
89

BRIDGING
(VIA 1 O)
(C_{2v})



85, 86

BRIDGING
(OF 3M BY 1 O)
(C_s)



90

donation from one oxygen atom, because of the electronegativity of oxygen.

Asymmetric bidentate coordination may be caused by (i) the electronic distribution in the metal being such that each oxygen atom will experience different repulsive interactions or (ii) the presence of a ligand with a strong trans-effect opposite one of the oxygens of the bidentate nitrate or (iii) steric crowding around the metal atom forcing one M-O bond to lengthen. Thus, the asymmetry in $\text{Co}(\text{NO}_3)_4^{2-}$ and $\text{Cu}(\text{apic})_2(\text{NO}_3)_2$ may be explained in terms of unsymmetric electronic distribution on the metal (55, 84), whereas the asymmetry in $(\text{CH}_3)\text{Sn}(\text{NO}_3)_3$ (87) and $\text{Mn}(\text{NO}_3)_3 \cdot \text{bipy}$ (synthesised in this work, see chapter four) may arise from steric effects. There has been no well documented example of the trans-effect causing asymmetric nitrate coordination at the present time.

Of the examples studied since Addison's review (73), almost twice as many have turned out to contain unidentate nitrate groups compared with those in which symmetric bidentate nitrate groups occur (see Figure 1.4.). Unidentate coordination may be caused by steric requirements around the metal or by the limited number of coordination sites imposed by valence considerations. Steric requirements

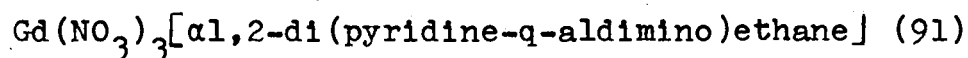
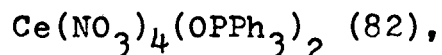
account for the unidentate nitrate coordination in $\text{VO}(\text{NO}_3)_3 \cdot \text{MeCN}$ (74) and $[\text{Co}(\text{tn})_2(\text{NO}_3)_2]\text{NO}_3$ (75), whereas in $\text{Re}(\text{CO})_5\text{NO}_3$ (73) and $\text{KAu}(\text{NO}_3)_4$ (64) each nitrate must form only one metal oxygen bond to permit the metal to achieve the expected coordination number.

Bridging coordination by nitrate groups would result in donation of charge from two oxygen atoms in a manner similar to symmetric bidentate coordination. The known examples of bridging nitrates are presented in Figure 1.4.

From the numerous structural results now available, some trends in nitrate coordination can be established; these are presented below.

- (1) The angle subtended at the metal by a bidentate nitrate group is between 55° and 70° . This imposes significant distortions in the coordination of the metals, for instance $\text{Co}(\text{NO}_3)_3$ is not octahedral, but severely distorted (56). Furthermore the small "bite" (2.1\AA) of the bidentate nitrate permits larger than usual coordination numbers; thus, numerous eight-coordinate nitrate complexes for the first row transition metals, such as $\text{Ti}(\text{NO}_3)_4$ (45), $\text{Mn}(\text{NO}_3)_4^{2-}$ (53), $\text{Fe}(\text{NO}_3)_4^-$ (11), and $\text{Co}(\text{NO}_3)_4^{2-}$ (55) and ten- and twelve-coordinate

complexes of the lanthanides, such as



and $(\text{NH}_4)_2\text{Ce}(\text{NO}_3)_6$ (66) have been reported.

- (ii) The terminal N-O(II) bond lengths in all coordination modes are less than the N-O(I) bond lengths in all structures except $(\text{PPh}_2\text{Me})_3\text{Cu}(\text{NO}_3)$ (77). Here the quoted distances are Cu-O(I), 2.206(6); N-O(I), 1.247(8); N-O(II), 1.247(8); and N-O(II'), 1.209(8)Å. Although the authors offer a rationale for this observation, its significance is in some doubt. The Cu-O distance seems exceedingly large compared to the only other structural determination of a copper(I) nitrate complex (92) in which the Cu-O distance in a bidentate nitrate group is 2.22(1)Å and a unidentate Cu-O(I) distance would be expected to be ≈ 0.2 Å shorter. Furthermore, in $(\text{PPh}_2\text{Me})_3\text{Cu}(\text{NO}_3)$ the N-O(I) bond is exceedingly short and it is possible that O(I) is incorrectly positioned. The authors do not state whether any correction for thermal motion was made, nor was there any indication of the residual peak heights in an electron density difference map to indicate the adequacy of the model they put forth. Until

such time as these details are reported, the evidence presented is still of questionable value.

- (iii) The order of metal-oxygen bond lengths is:
M-O(I) (unidentate) < M-O(I) (asymmetric bidentate) < M-O(I) (symmetric bidentate) < M-O(I') (asymmetric bidentate), for the same metal and the same oxidation state.
- (iv) The angle O(I)-N-O(I) in a symmetric bidentate nitrate group is less than 120° and the other angles around the nitrogen are greater than 120° . In a unidentate nitrate, the angle O(II)-N-O(II'), which is trans to the coordinated oxygen, is greater than 120° and the other angles less than 120° .

1.3.2. Vibrational Spectroscopy.

Other methods used to identify the mode of coordination of nitrate groups in metal nitrate compounds are based on vibrational spectroscopic techniques.

The nitrate ion has four fundamental vibrational frequencies, three of which are infrared active and three are Raman active, as summarized in Table 1.2. Coordination of the nitrate ligand, with either C_{2v} or C_s symmetry, causes the degeneracy of the E' modes to be lifted and all

six frequencies become both infrared and Raman active. Therefore, it is a simple matter to differentiate between ionic or coordinated nitrates on the basis of the number of bands, but a more complete spectral analysis is necessary to distinguish the mode of coordination.

Raman depolarization ratios offer a method of distinguishing between totally symmetric vibrational modes (A_1 modes) and antisymmetric modes (B or E modes) (93, 94). Normal coordinate analyses (95, 96) have been carried out for both symmetric bidentate (C_{2v}) and unidentate (C_s) coordination and indicate that the order of the stretching frequencies will be N-O(II) (Antisymmetric) B_1 , > N-O(II) (Symmetric) A_1 , > N-O(I) (Symmetric) A_1 , for unidentate coordination, whereas for bidentate coordination N-O(II) (Symmetric) A_1 , > N-O(I) (Antisymmetric) B_1 , > N-O(I) (Symmetric) A_1 . Thus, if the highest nitrate stretching frequency is polarized and the second highest is depolarized, the coordination is likely to be bidentate, as was observed for $Tl(NO_3)_4$, $Sn(NO_3)_4$ and $VO(NO_3)_3$ (36), whereas if the highest mode is depolarized and the second highest polarized, the coordination is likely to be unidentate as in the unidentate nitrate in $VO(NO_3)_3 \cdot MeCN$ (74).

It generally has been observed that the intensity

Table 1.2. Nitrate Vibrational Modes.

IONIC NITRATE

Mode	ν_1	ν_2	ν_3	ν_4
Species	A_1'	A_2''	E'	E'
Frequency (cm^{-1})	1050	830	1390	720
Description	Symmetric Stretch	Out of Plane Bend	Degenerate Stretch	Degenerate Bend
Activity	R	IR	R, IR	R, IR

UNIDENTATE NITRATE (C_s)

Mode	ν_2	ν_4	ν_5	ν_1	ν_6	ν_3
Species	A_1	A_2	B_1	A_1	B_1	A_1
Approximate Frequency (cm^{-1})	1020	800	1580	1300	750	730
Description	Symmetric Stretch	Out of Plane Bend	Antisym. Stretch	Symmetric Stretch	Antisym. Bend	Symmetric Bend
Activity	ALL INFRARED AND RAMAN ACTIVE					

BIDENTATE NITRATE (C_{2v})

Mode	ν_2	ν_4	ν_1	ν_5	ν_3	ν_6
Species	A_1	A_2	A_1	B_1	A_1	B_1
Approximate Frequency (cm^{-1})	1000	800	1600	1200	760	730
Description	Symmetric Stretch	Out of Plane Bend	Symmetric Stretch	Antisym. Stretch	Symmetric Bend	Antisym. Bend
Activity	ALL INFRARED AND RAMAN ACTIVE					

of a symmetric (A_1) mode in the Raman spectra of nitrates or nitrate complexes is greater than antisymmetric modes (73). Thus from the order of the stretching frequencies predicted by the normal coordinate analyses for symmetric bidentate nitrate coordination, the order of relative intensities should be strong, medium and strong, whereas for unidentate coordination the order should be medium or weak, strong and strong for the highest to the lowest stretching frequencies. This phenomenon has been rationalized in terms of the relative electron density in each N-O bond (73).

Several other methods have been suggested to obtain the mode of coordination from spectral data (3, 97, 98, 99, 100, 101). The earliest of these depended on the separation of the two highest frequencies to be characteristic of the mode of coordination, bidentate having a larger separation than unidentate coordination (3, 97). Field and Hardy (3) also thought that if one frequency was higher than 1570 cm^{-1} and the other was below 1280 cm^{-1} , this was indicative of bridging coordination. This was a gross oversimplification since it has been observed (73) that wide ranges of frequencies that often overlap are obtained for the various modes of coordination. Another oversimplified approach was to assume that the number of far infrared bands was directly dependent on the mode of nitrate coordination

(98, 99, 100).

Recently A.B.P. Lever (101) has proposed that the infrared combination frequencies for coordinated nitrates are diagnostic of the mode of coordination. These are the combination modes arising from ($\nu_2 + \nu_3$) and ($\nu_2 + \nu_6$) for coordinated nitrates and ($\nu_1 + \nu_4$) for ionic nitrates. Ionic nitrates should give rise to one combination frequency in the range 1750 to 1800 cm^{-1} . Unidentate and bidentate coordination should each result in two frequencies separated by 5 to 20 cm^{-1} and 20 to 66 cm^{-1} respectively. Bridging coordination almost invariably has one combination band in the region 1780 to 1800 cm^{-1} , but this is not diagnostic of the mode of bridging. The examples used in Lever's study support his postulates, but there are many other nitrates which do not fit his criteria. For instance, the ionic nitrates of rubidium and cesium show two bands split by 20 and 10 cm^{-1} respectively (splitting of ν_3 can clearly be seen in references 102 and 103). The ionic nitrates of magnesium and calcium have combination frequencies at 1845 and 1810 cm^{-1} respectively (104 and chapter six), which are outside the proposed range for ionic nitrates. The overtone bands are frequently too weak to be observed, thus limiting the application of this technique.

Thus it can be concluded from the foregoing discussion that only if the Raman depolarization ratios and relative intensities agree, can a reasonably certain assignment of the nature of the coordination of the nitrate be made on spectroscopic grounds alone. The compounds whose mode of coordination has been identified are indicated in Table 1.1.

1.4. Research Proposal.

By 1967 the situation was that anhydrous metal nitrates or nitrate complexes could be prepared by using appropriate non-aqueous solvent systems, and that methods were available to identify the mode of coordination of the nitrate group, but these had only been applied to a limited number of the metal nitrates. There were then two obvious approaches to extend the growing understanding of anhydrous metal nitrate systems. The first was the preparation of new nitrate compounds and the second was the determination of the modes of coordination in existing metal nitrates.

1.4.1. Preparative Chemistry.

Table 1.1 can be used as a guide to the areas most likely to be rewarding with respect to the preparation

of anhydrous metal nitrates. Anhydrous nitrates or oxy-nitrates are known for all of the 3d transition metals. The dinitrates of manganese, cobalt, nickel and copper are known, and since nitrate groups are sufficiently strong oxidants, the trinitrates of scandium, chromium and iron are known instead of the dinitrates. Titanium is oxidized to titanium(IV), giving only titanium tetranitrate, and vanadium forms only the oxy-nitrate, $\text{VO}(\text{NO}_3)_3$. For the first row transition metals Sc to Cr, the maximum oxidation state of each metal forms a nitrate or an oxy-nitrate in the following series $\text{Sc}(\text{NO}_3)_3$, $\text{Ti}(\text{NO}_3)_4$, $\text{VO}(\text{NO}_3)_3$, $\text{CrO}_2(\text{NO}_3)_2$. The next member of the series would be the heptapositive manganese compound, $\text{MnO}_3(\text{NO}_3)$. The titanium and vanadium compounds appear to be stable indefinitely at room temperature, whereas $\text{CrO}_2(\text{NO}_3)_2$ slowly decomposes (105, 106). Therefore $\text{MnO}_3(\text{NO}_3)$ would be expected to be quite unstable if it existed. The only MnO_3X compound to be definitely established is MnO_3F which is extremely unstable (107, 108). An attempt by D.J. Chapman at the University of Nottingham to prepare $\text{MnO}_3(\text{NO}_3)$ by reaction of potassium permanganate or manganese heptoxide with dinitrogen pentoxide produced a highly unstable product which could not be identified as $\text{MnO}_3(\text{NO}_3)$ with any certainty (109). Thus it was considered unwise to try to prepare new nitrate complexes of the remaining 3d transition metals in their highest possible oxidation states.

This, of course, does not preclude studies of the more unusual oxidation states such as nickel(III), or copper(III). Addison's group was examining Ni(III), but never has attempted the preparation from a known nickel(III) compound.

At the same time as this work was undertaken, Fereday succeeded in preparing cobalt(III) trinitrate (18), by overcoming the problem of the ease of formation of cobalt(II) nitrate complexes (110). Cobalt(III) trinitrate proved to be stable and monomeric with distorted octahedral coordination (56). For the first time, anhydrous nitrates had definitely been identified for two oxidation states of the same metal (18, 41). This prompted the question, "Which other metals might also form anhydrous binary nitrates in two oxidation states?" One of the possibilities in the first row transition metals was manganese(III).

No previous work on the nitrates of manganese(III) had been reported and in general compounds of manganese(III) are considerably less abundant and less well characterised than those of the neighbouring elements chromium, iron, and cobalt. The trinitrates of the latter are known (18, 23, 54), as are the tetranitrato anions of iron(III), manganese(II) and cobalt(II) (11, 29, 52, 53, 55). Both chromium and iron trinitrates have low thermal stability

and are involatile and, presumably, polymeric solids. By contrast cobalt(III) trinitrate is stable and volatile. Again, anhydrous iron(II) and chromium(II) nitrates are unknown, whereas the ease of formation of the (II) oxidation states complicates the syntheses of cobalt(III) nitrate complexes. Therefore it was felt that the preparation of manganese(III) trinitrate could be complicated by reduction of the metal or by low thermal stability of the product. On the other hand, its preparation would complete the series of trinitrates from chromium to cobalt, so that the properties of the series could be compared. Furthermore, there are few well established simple anhydrous compounds of manganese(III), and perhaps this number could be increased by the preparation of the trinitrate. Thus it was considered worthwhile to attempt the preparation of manganese(III) trinitrate. The successful preparation and properties of this compound are presented in chapter two of this thesis.

A number of other compounds and complexes have been reported which contain manganese(III) (Table 1.3.). The least thermally stable of all of these compounds is manganese(III) trichloride which decomposes above -35°C (117). However, its complexes are stable at room temperature. This increased stability of the complexes over the parent

Table 1.3. Compounds and Complexes of Manganese(III).

<u>COMPOUND</u>	<u>REFERENCE</u>	<u>COMPOUND</u>	<u>REFERENCE</u>
<u>Halides and Pseudohalides</u>			
MnF ₃	111	MnCl ₃	117
MnF ₄ ⁻	112	MnCl ₅ ²⁻	118, 119
MnF ₅ ²⁻	112, 113, 114, 115	MnCl ₆ ³⁻	120, 121
MnF ₆ ³⁻	112, 116	Mn(CN) ₆ ³⁻	122, 123
<u>Oxygen Donor Ligands and Oxides</u>			
Mn(ox) ₃ ³⁻	124, 125	Mn(OH)O	135
Mn(acac) ₃	126 - 129	Mn ₂ O ₃	136
Mn(OAc) ₃	130	Mn ₃ O ₄	137
Mn(DMSO) ₆ ³⁺	131	Mn ₂ O ₄ ²⁻	137
Mn(DMF) ₆ ³⁺	131	MnO(SO ₃ F)	138
Mn(acac)(patl) ₂	132	Mn(OPh ₃) ₃ Cl ₃	139
Mn(terpy-O ₃) ₂ ³⁺	133	Mn(pyO) ₃ Cl ₃	139
Mn(sal) ₃	134	Mn(Ph ₃ AsO) ₃ Cl ₃	139
<u>Nitrogen Donor Ligands</u>			
Mn(o-phen)Cl ₃ ·H ₂ O	140, 141	Mn(NR ₃) ₃ Cl ₃	142
Mn(bipy)Cl ₃ ·H ₂ O	140, 141	Mn(py) ₃ Cl ₃	142
[Mn(o-phen)Cl ₃] ₂	140, 141 142	Mn(acac)(patl) ₂	132
[Mn(bipy)Cl ₃] ₂	140, 141, 142	Mn(sal) ₃	134
		Mn(porph)Cl·H ₂ O	143, 144

compound is also now observed with manganese(III) trinitrate complexes, whose preparation and properties are presented in chapters three and five. The crystal structure of one of these complexes, $\text{Mn}(\text{NO}_3)_3 \cdot \text{bipy}$, has been determined and is presented in chapter four.

1.4.2. Investigation of the Coordination of Nitrates by Spectroscopic Techniques.

The possibility of determining the type of interaction of the metal and the nitrate group in a wide range of metal nitrates, both ionic and covalent was also investigated. To distinguish between symmetric and anti-symmetric vibrational modes, Raman depolarization ratios are necessary. The usual methods employed to obtain depolarization ratios are to examine orientated single crystals or to examine the sample in solution. The problems encountered in obtaining depolarization ratios for anhydrous metal nitrates are (i) the lack of suitable single crystals, (ii) the fact that Raman radiation scattered from powdered samples is always depolarized, thus preventing determination of the symmetric vibrational modes and (iii) the change in coordination that can occur upon dissolving a metal nitrate in a solvent suitable for Raman studies. At the start of this project, two authors reported the determination of

depolarization ratios by immersing powdered samples in a liquid of a similar index of refraction (145, 146). The application of this technique to inorganic solids and anhydrous nitrates in particular was undertaken but found to be of very limited use; the results are presented in chapter six.

Chapter 2

Anhydrous Manganese(III) Nitrate.

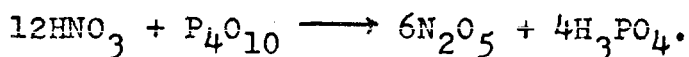
2.1. Introduction.

One of the most obvious features of the chemistry of manganese(III) is the small number of well established simple anhydrous compounds, even though a comparatively large number of manganese(III) complexes have been reported (see Table 1.3.). These are limited to the oxide, Mn_2O_3 (136); the hydroxide, $Mn(OH)O$ (135); the oxofluorosulfate, $MnO(SO_3F)$ (138); the fluoride, MnF_3 (111); and the chloride, $MnCl_3$ (117). The latter is extremely unstable, decomposing rapidly at $-35^\circ C$. Prior to this study, manganese(III) nitrate or its hydrate, and complexes of manganese(III) containing coordinated nitrates were all unknown. This chapter gives the details of the reactions which were undertaken in the attempt to produce manganese(III) trinitrate, and reports the successful preparation by reaction of manganese(III) fluoride and dinitrogen pentoxide. The physical and chemical properties are then presented.

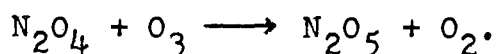
2.2. Preparation of Manganese(III) Nitrate.

2.2.1. Reaction of MnF₃ and N₂O₅.

Dinitrogen pentoxide was generated by the dehydration of red fuming nitric acid by phosphorus pentoxide according to the following equation:



The dehydration reaction was done in the presence of ozone, since dinitrogen tetroxide was present in the fuming nitric acid, and would have been the major product of the thermal decomposition of dinitrogen pentoxide. The ozone reacted with the dinitrogen tetroxide to produce additional dinitrogen pentoxide as follows:



The ozone was prepared from oxygen by a silent electric discharge and was passed into the reaction vessel at the rate of 0.75 liters per minute. The long phosphorus pentoxide connecting tube (D, Figure 2.1.) prevented moisture from passing into the collection flask and dehydrated any nitric acid vapour carried into the tube. The dinitrogen pentoxide was condensed in the collection

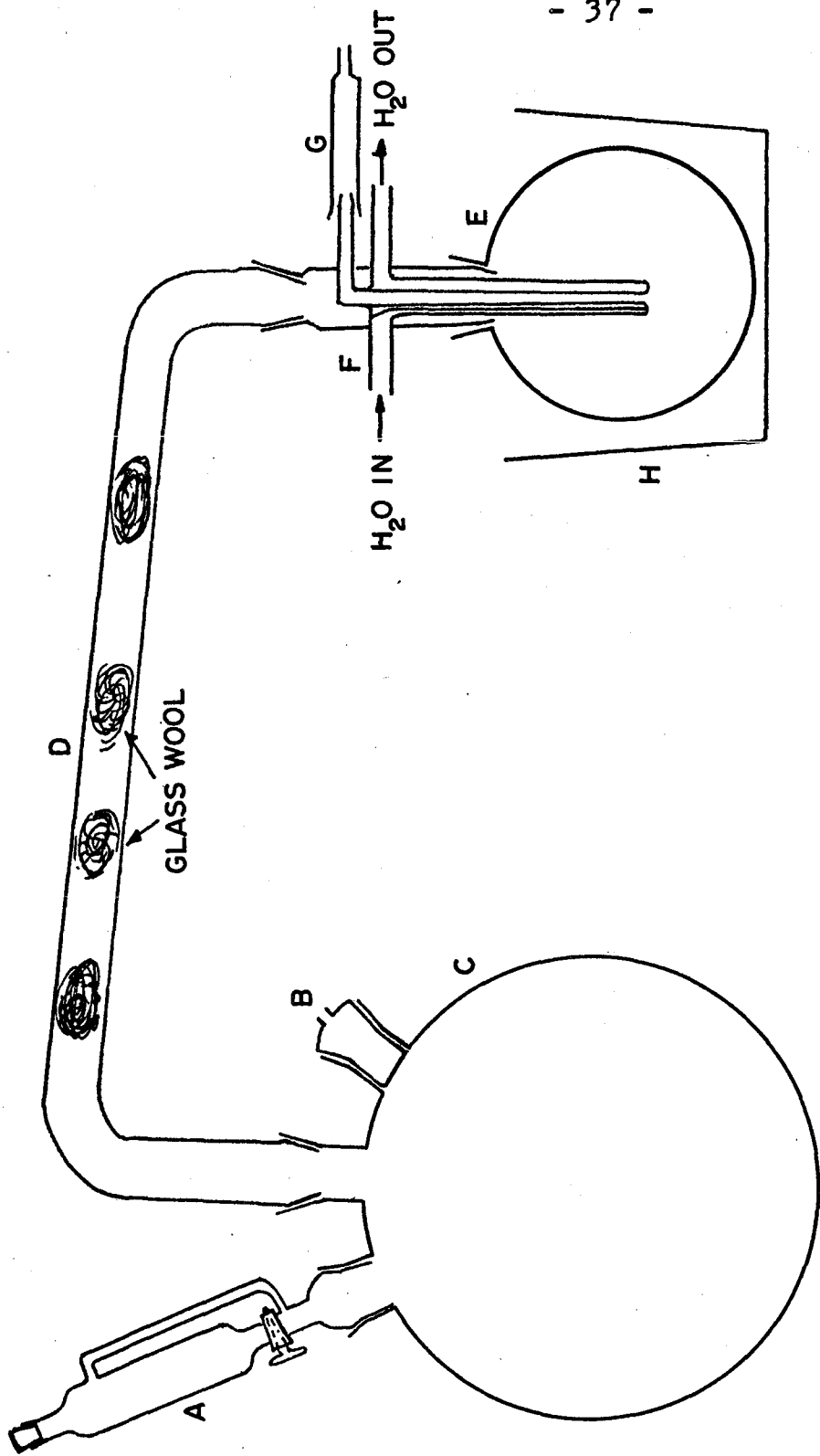
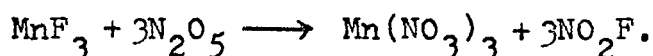


Figure 2.1. The apparatus used for the generation of dinitrogen pentoxide.
A, pressure equalizing dropping funnel; B, ozone inlet; C, dehydration vessel containing P₂O₅; D, connecting tube containing P₂O₅; E, collection flask; F, water jacketed exit tube; G, P₂O₅ guard tube; H, Methanol Bath.

flask (E) which was contained in a cold bath at -78°C . The warm water jacketed exit tube (F) was designed to prevent the dinitrogen pentoxide from condensing and blocking the neck of the collection flask or the exit tube itself. The apparatus was vented to the atmosphere by the smaller phosphorus pentoxide guard tube (G).

In a typical reaction, a large excess (20 g., 0.185 mole) of dinitrogen pentoxide was condensed onto anhydrous red manganese(III) fluoride (1.0 g., 8.9 mmole). The solids were mixed and allowed to warm to room temperature to liquify the N_2O_5 ; liquid N_2O_4 was then added and the mixture was stirred at 5°C under a dry atmosphere for three days, the flask being vented to the atmosphere by a phosphorus pentoxide guard tube. During that time a reaction took place producing a dark brown oil which was then filtered from unreacted MnF_3 . Careful removal of the volatiles (mainly N_2O_4) in vacuo at room temperature gave a dark brown hygroscopic solid. Extreme care had to be taken to avoid excess pumping on this because the eventual product, $\text{Mn}(\text{NO}_3)_3$, has low thermal stability, and evolves N_2O_4 at room temperature also. The procedure adopted was to isolate the sample from the pump as soon as all liquid had disappeared and then to continue pumping cautiously until an infrared spectrum of the product exhibited no bands assignable to

nitrogen oxides, NO^+ or NO_2^+ . Samples were sealed in glass ampoules and kept at -14°C in a refrigerator. Manipulations were carried out quickly in a dry-box, using cooled apparatus where necessary. The reaction may be represented by the following equation:



[Found: Mn, 22.5; N, 17.4%. Calculated for $\text{Mn}(\text{NO}_3)_3$: Mn, 22.8; N, 17.4%]. The same compound could be synthesized using solid N_2O_5 alone, but use of N_2O_4 as a solvent enabled the reaction to proceed more quickly and minimized evaporation of N_2O_5 .

2.2.2. Reaction of MnF_3 and AgNO_3 .

A metathetical reaction was attempted by adding a dry methanol solution of silver nitrate (4.6 g.; 27 mmoles) dropwise to the methanol solution of MnF_3 (1.0 g.; 8.9 mmoles). The reaction was attempted at both 20°C and 60°C . When the solution was concentrated by removal of methanol either in vacuo or by distillation, silver nitrate precipitated out, so no reaction had occurred.

2.2.3. Reaction of MnF_3 and N_2O_4 .

Dinitrogen tetroxide (50 ml; 0.79 mole) was added to a flask containing MnF_3 (0.43 g.; 3.8 mmoles). After three days there appeared to have been no reaction and 95% of the original MnF_3 was recovered. Therefore it is unlikely that the dinitrogen tetroxide is the reactive species in the preparation of $\text{Mn}(\text{NO}_3)_3$ (see section 2.2.1.), although it may promote the reaction of the dinitrogen pentoxide and MnF_3 , by either improving the contact between the dinitrogen pentoxide and MnF_3 over that in the solid state reaction, or by increasing the dissociation of the dinitrogen pentoxide into NO_2^+ and NO_3^- . The latter seems rather unlikely since dinitrogen tetroxide has a very low dielectric constant ($\epsilon_{20^\circ\text{C}} = 2.6$).

2.2.4. Reaction of MnO_2 and N_2O_5 or N_2O_4 .

To investigate the possibility of preparing nitrate species starting from manganese(IV), the reactions of manganese dioxide and dinitrogen pentoxide or dinitrogen tetroxide were examined. No reaction occurred between commercial MnO_2 and dinitrogen pentoxide, dinitrogen tetroxide or dinitrogen tetroxide in nitromethane, acetonitrile or carbon tetrachloride. The observed lack

of reactivity is probably due to phase changes brought about by the roasting of the commercial manganese dioxide.

Fresh manganese dioxide was prepared by reduction of KMnO_4 by MnCl_2 in aqueous solution (147). The precipitate was filtered and washed with water until free of permanganate; then it was dried in vacuo for twelve hours [Found: Mn, 60.0%; Calculated for MnO_2 : Mn, 63.3%]. The infrared spectrum indicated no water present in the sample. When dinitrogen tetroxide (10 ml; 0.157 mole) was added to the freshly precipitated MnO_2 (0.10 g.; 1.15 mmoles) and allowed to react for twenty-four hours, a grey black viscous oil containing nitric acid was produced (ir. bands at 3600, and 1700 cm^{-1}). It is likely that the nitric acid came from reaction of dinitrogen tetroxide and traces of moisture in the manganese dioxide or with moisture that may have leaked into the system during the reaction.

When dinitrogen pentoxide (20 g.; 0.185 mole) was condensed onto the fresh MnO_2 (0.10 g.; 1.15 mmoles) and warmed to room temperature, reaction occurred to give copious amounts of dinitrogen tetroxide and a dark solid which had decomposed before a manganese analysis could be attempted. Infrared bands at 1530, 1290, 1250, 1023, 1012, 975, 815, 800, 755, 748 cm^{-1} are indicative of coordinated

nitrate groups and an intense band at 900 cm^{-1} indicates that a coordinated oxo-ligand may also be present. The evolution of dinitrogen tetroxide may indicate oxidation of the manganese, so the product could be $\text{MnO}(\text{NO}_3)_3$ or $\text{MnO}_2(\text{NO}_3)_2$ or a similar product. This reaction definitely deserved more study, but as the reactions with fresh manganese dioxide were undertaken at the end of the period covered in this thesis, there was insufficient time available for further study.

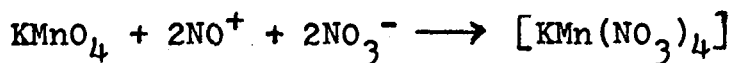
2.2.5. Reactions of K_2MnO_4 and BaMnO_4 with N_2O_4 .

The reactions of the manganese(VI) species, K_2MnO_4 and BaMnO_4 with dinitrogen tetroxide were examined to determine if manganese(VI) could be reduced to yield manganese(III) nitrate. The potassium and barium manganates were prepared by reduction of potassium permanganate in strongly basic solutions (148). [Found for K_2MnO_4 : Mn, 28.6%; Calculated for K_2MnO_4 : Mn, 30.2%. Found for BaMnO_4 : Mn, 21.0%. Calculated for BaMnO_4 : Mn, 21.4%]. Addition of dinitrogen tetroxide (20 ml; 0.315 moles) to a suspension of K_2MnO_4 (0.48 g.; 2.4 mmoles) in nitromethane, resulted in a heavy yellow precipitate of $\text{K}_2\text{Mn}(\text{NO}_3)_4$ (0.78 g.; 2.04 mmoles; 84% yield). When a similar reaction

was carried out using BaMnO_4 (0.50 g.; 1.33 mmoles) and the suspension stirred for twenty-four hours, no reaction occurred, probably due to the total lack of solubility of the BaMnO_4 .

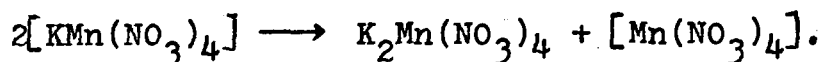
2.2.6. Reaction of KMnO_4 and N_2O_4 .

The reaction of potassium permanganate and dinitrogen tetroxide was examined to see if manganese(III) trinitrate could be obtained from it. When pure dinitrogen tetroxide or dinitrogen tetroxide in carbon tetrachloride was added to potassium permanganate and stirred, no reaction was observed, but when dinitrogen tetroxide (20 ml; 0.315 mole) was added to KMnO_4 (1.0 g.; 6.33 mmoles) in either nitromethane or acetonitrile, a precipitate of $\text{K}_2\text{Mn}(\text{NO}_3)_4$ (95 - 100% yields based on potassium, see chapter five), and a brown solution were produced. It is not a simple matter to write an equation for this reaction. A possible first step is the reduction of permanganate by the nitrosonium ion, i.e.,



since pure dinitrogen tetroxide is unable to cause the reduction and since both nitromethane and acetonitrile

promote the heterolytic dissociation of dinitrogen tetroxide (25). The tetranitratomanganate(III) anion may be unstable in solution since samples of $[\text{NO}_2^+][\text{Mn}(\text{NO}_3)_4]$ and $\text{Cs}[\text{Mn}(\text{NO}_3)_4]$ could not be recovered from solution (see chapter five). Rapid disproportionation would yield manganese(II) and manganese(IV) according to the following equation:



The manganese(IV) tetranitrate could then be reduced by nitrogen dioxide to give the solvated manganese(III) trinitrate.



Several attempts were made to obtain the anhydrous manganese(III) trinitrate from the brown solution. If the acetonitrile solution was pumped to dryness, a dark brown solid containing coordinated nitrates and acetonitrile was obtained (see chapter three for details of this compound). If the nitromethane solution was pumped to dryness a dark brown solid with between 15.0 and 18.2% manganese, and no infrared bands attributable to nitromethane were observed.

If the brown nitromethane was concentrated by removal of some of the volatiles in vacuo, and carbon tetrachloride or petroleum ether added, an oil, which was not characterized, formed. Although this reaction was not of any use in the preparation of manganese(III) trinitrate, it did provide a convenient route to the complexes of $\text{Mn}(\text{NO}_3)_3$. Large crystals of the complexes could be crystallized from the brown solution by addition of the appropriate ligands. The complexes of manganese(III) trinitrate will be discussed further in chapter three.

2.2.7. Physical Measurements.

Infrared spectra ($4000 - 350 \text{ cm}^{-1}$) were recorded on Perkin-Elmer 457 or Beckman IR-12 spectrophotometers, using silver chloride cells. The spectra were obtained as nujol and Fluorolube mulls. Reaction with nujol was observed for $\text{Mn}(\text{NO}_3)_3$ and the spectra are corrected (35, 73). A band increasing rapidly in intensity in the nujol spectra at 1680 cm^{-1} can be attributed to the formation of an alkyl nitrate. Raman spectra were recorded on a Cary 81 Raman Spectrophotometer. Electronic spectra were recorded on a Unicam S.P. 800 or a Cary 14 Spectrophotometer. Diffuse reflectance spectra were obtained using a Unicam S.P. 890 diffuse reflectance accessory. Magnetic

susceptibilities were measured at 22° or 0°C by the Faraday method using $\text{Hg}[\text{Co}(\text{NCS})_4]$ as a calibrant (149). Samples were manipulated and measurements made in a dry argon atmosphere. X-ray powder diffraction photographs were obtained by placing the powdered sample in a 0.5 mm capillary tube, and irradiating it with CuK_α radiation ($\lambda = 1.5418\text{\AA}$) in a Debye-Scherrer camera.

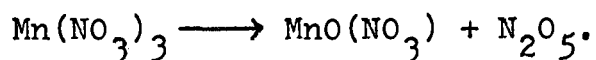
Manganese was determined by both atomic absorption spectroscopy and volumetrically following bismuthate oxidation. Nitrogen was determined by Kjeldahl's method.

2.3. Properties of Manganese(III) Trinitrate.

2.3.1. Physical Properties.

Manganese(III) nitrate, $\text{Mn}(\text{NO}_3)_3$, is stable indefinitely below -14°C in a dry atmosphere, but evolves N_2O_4 rapidly at room temperature and fumes in moist air. This makes $\text{Mn}(\text{NO}_3)_3$ the least thermally stable of any of the known first row transition metal trinitrates. Chromium(III) nitrate (23) and $\text{Fe}(\text{NO}_3)_3$ (54) decompose rapidly at 60° and 70° respectively, whereas $\text{Co}(\text{NO}_3)_3$ (18) sublimes readily in vacuo with little decomposition at 40° . Although $\text{Mn}(\text{NO}_3)_3$ is less thermally stable than other first row transition metal trinitrates, it is more stable than MnCl_3 , which decomposes to MnCl_2 and chlorine above

-35°C (117). When a stream of dry argon is passed over the $\text{Mn}(\text{NO}_3)_3$ to remove the volatile decomposition products, it was found that $\text{Mn}(\text{NO}_3)_3$ decomposes with the loss of exactly 108 M.W. units (Figure 2.2) to give a tan colored compound of formula $\text{MnO}(\text{NO}_3)$, i.e.,

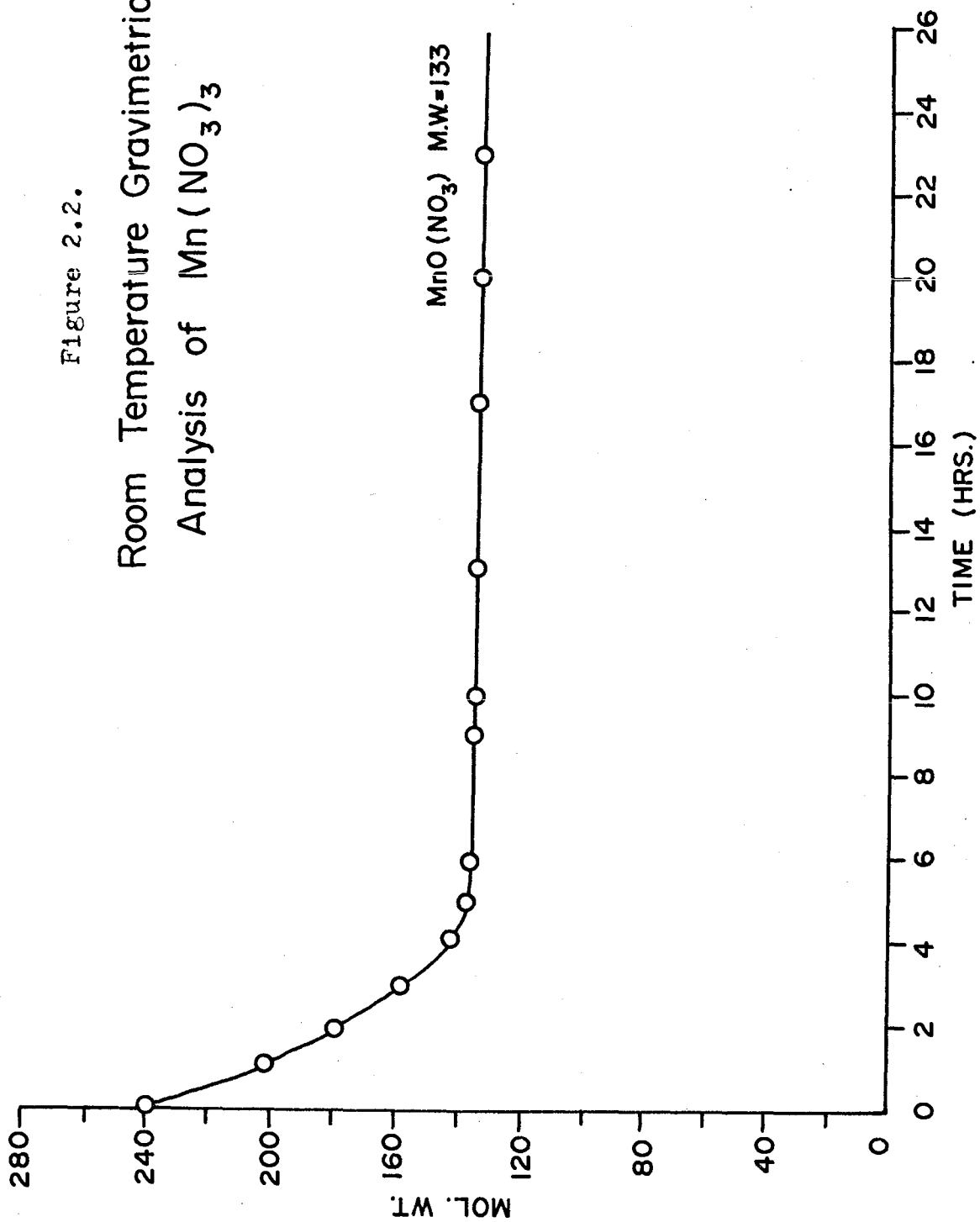


The product is stable at room temperature, in a dry atmosphere, whereas, if the decomposition takes place in a sealed tube, reduction of the manganese(III) occurred due to the dinitrogen tetroxide evolved. If liquid dinitrogen tetroxide is added to $\text{Mn}(\text{NO}_3)_3$, it slowly reduces the $\text{Mn}(\text{NO}_3)_3$ to $\text{Mn}(\text{NO}_3)_2 \cdot \text{N}_2\text{O}_4$. Fereday (150) observed similar reduction of $\text{Co}(\text{NO}_3)_3$ in contact with N_2O_4 . ($X_M^{\text{corr}} = 8670 \times 10^{-6}$ c.g.s.u. at 22°C, $\mu_{\text{eff}} = 4.52 \pm 0.05$ B.M.)

2.3.2. X-Ray Powder Patterns.

The X-ray powder patterns of $\text{Mn}(\text{NO}_3)_3$, of its decomposition product, and of the compounds $\text{Mn}(\text{NO}_3)_2$ and $\text{Mn}(\text{NO}_3)_2 \cdot \text{N}_2\text{O}_4$ are presented in Table 2.1 (d values in Å and qualitative intensities; Cu-K $_{\alpha}$ radiation, $\lambda = 1.5418\text{Å}$) as they have not been previously reported. Three points should be made about the powder patterns;

Figure 2.2.
Room Temperature Gravimetric
Analysis of $Mn(NO_3)_3$



- (i) Although the powder pattern for $\text{Mn}(\text{NO}_3)_3$ contains lines corresponding to those of MnF_3 , the starting material for the preparation of $\text{Mn}(\text{NO}_3)_3$, the relative intensities are not correct, and, furthermore, the analysis and the infrared spectrum of $\text{Mn}(\text{NO}_3)_3$ confirmed the purity of the sample.
- (ii) The $\text{Mn}(\text{NO}_3)_3$ was visibly decomposed (i.e., turning yellow) after the six hours required to achieve a reasonable exposure of the film. This is supported by the similarity of the powder patterns of $\text{Mn}(\text{NO}_3)_3$ and the decomposition products obtained by sealing $\text{Mn}(\text{NO}_3)_3$ in a tube for forty-eight hours at 21°C . Thus the powder pattern reported here must be considered to be a mixture of $\text{Mn}(\text{NO}_3)_3$ and its decomposition product. It would be necessary to have a powder camera in which the sample could be cooled, to obtain the powder pattern of pure $\text{Mn}(\text{NO}_3)_3$.
- (iii) The powder patterns of $\text{Mn}(\text{NO}_3)_2$ and $\text{Mn}(\text{NO}_3)_2 \cdot \text{N}_2\text{O}_4$ prepared from manganese metal and N_2O_4 in ethyl acetate (41), are very similar at low values of d , but sufficiently different at high values to indicate that they are not isomorphous structures.

Unfortunately powder patterns have not been reported for other anhydrous metal nitrates that form N_2O_4 adducts so it is impossible at the moment to make comparisons with the other N_2O_4 adducts (5).

2.3.3. Solubility and Electronic Spectrum.

Manganese(III) trinitrate is sparingly soluble in nitromethane, decomposes in water, acetone, acetonitrile and other polar solvents, and is insoluble in chloroform, carbon tetrachloride and benzene.

In 6M H_2SO_4 , the electronic spectrum has one band at $19,800\text{ cm}^{-1}$. Assuming octahedral coordination, this band can be assigned as the ${}^5T_{2g} \leftarrow {}^5E_g$ transition. The spectra were too weak to observe any lower energy transition which would arise from distortion from octahedral symmetry (118). Attempts to obtain the diffuse reflectance spectrum failed, as decomposition of the sample blew a hole through the grease seal between the window and the sample holder.

Table 2.1.

X-Ray Powder Patterns for Manganese Nitrate Species.

(Interplanar Spacings in Å)

<u>Mn(NO₃)₃</u>	<u>Decomp. Product</u>	<u>MnF₃</u>	<u>Mn(NO₃)₂</u>	<u>Mn(NO₃)₂·N₂O₄</u>
8.04 w				7.89 m
6.06 m			5.70 m	
5.44 m	4.89 w			4.87 m
4.71 s	4.64 m		4.54 s	
4.46 s	4.39 s			4.35 s
3.77 s	3.76 s		3.95 w	3.73 w
3.53 m	3.49 m		3.52 s	3.39 s
3.34 w	3.39 s		3.17 m	3.07 s
	3.22 m			
2.89 w	2.87 m	2.89 vs		
2.71 w	2.67 m		2.73 w	2.64 w
2.57 m	2.51 m	2.52 m	2.59 m	2.49 w
			2.47 vw	
				2.40 w
2.30 s	2.28 s		2.32 s	2.28 s
2.25 w	2.10 w		2.22 s	2.18 s
2.12 m		1.84 vs	1.92 w	2.03 s
2.03 w		1.77 m	1.75 w	1.73 m
1.96 w		1.52 w	1.70 m	1.68 m
1.84 m		1.47 m	1.56 w	1.54 w
1.74 w		1.24 s	1.47 m	1.45 m
1.67 m		1.22 w	1.29 w	1.27 w
		1.16 m	1.27 vw	1.25 vw
		1.13 m		

2.3.4. Infrared Spectrum.

The infrared spectrum of $\text{Mn}(\text{NO}_3)_3$ is pictured in figure 2.3 and is listed in table 2.2, along with those reported for $\text{Cr}(\text{NO}_3)_3$, $\text{Fe}(\text{NO}_3)_3$ and $\text{Co}(\text{NO}_3)_3$ (23, 54, 18). There are many similarities in the spectra of $\text{Cr}(\text{NO}_3)_3$, $\text{Mn}(\text{NO}_3)_3$ and $\text{Fe}(\text{NO}_3)_3$ but that of $\text{Co}(\text{NO}_3)_3$ is substantially different. Cobalt(III) trinitrate has been shown to consist of discrete molecular units, with symmetric bidentate nitrate groups resulting in an irregular octahedral coordination of the cobalt (56). Due to the difference in the spectra of $\text{Cr}(\text{NO}_3)_3$, $\text{Mn}(\text{NO}_3)_3$ and $\text{Fe}(\text{NO}_3)_3$ from that of $\text{Co}(\text{NO}_3)_3$, it is unlikely that these are similar to $\text{Co}(\text{NO}_3)_3$, but perhaps possess bridging nitrate coordination. This conclusion is further supported by the relative insolubility of $\text{Mn}(\text{NO}_3)_3$ in common solvents, which also suggests that it is a polymeric compound in which some or all of the nitrates are bridging. No Raman spectrum was obtained due to absorption of the He-Ne line; therefore the assignment in Table 2.2 is only tentative and is made on the basis of C_{2v} local symmetry with two coordinated oxygens. As has been noted in other nitrates (18, 36), there is apparently no observed absorption band corresponding to the out-of-plane bend.

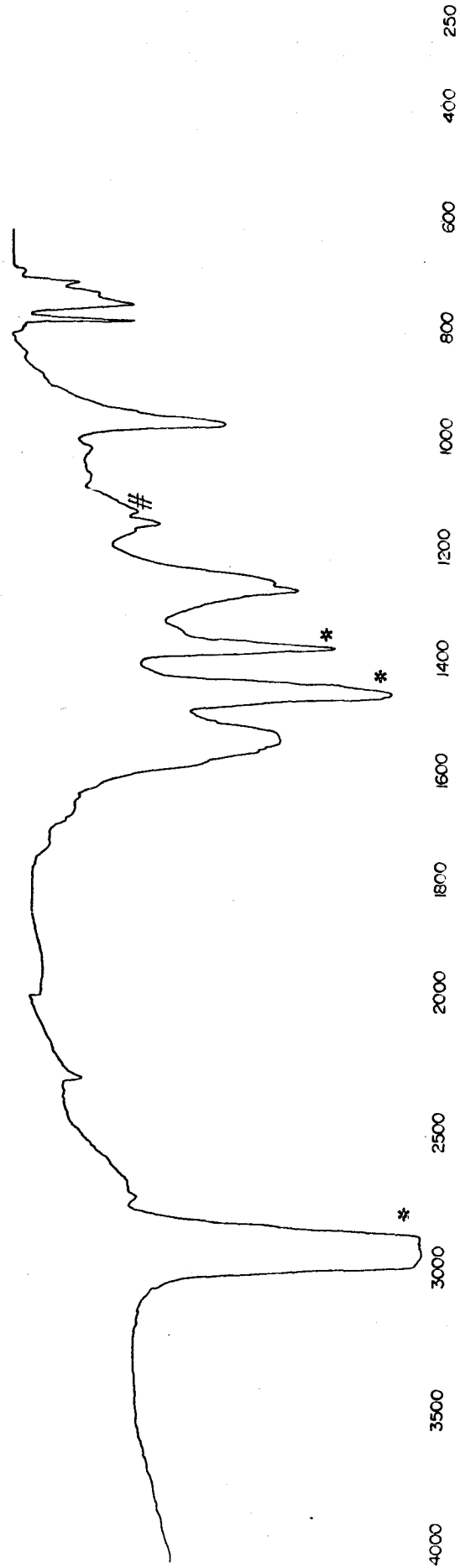


Figure 2.3. Infrared spectrum of Mn(NO₃)₃

* Nujol Bands.

Bands due to AgCl plates.

Table 2.2.

Infrared Spectra of Metal Trinitrates.

<u>Assignment</u> under C_{2v}	<u>Cr(NO₃)₃</u> (23)	<u>Mn(NO₃)₃</u>	<u>Fe(NO₃)₃</u> (54)	<u>Co(NO₃)₃</u> (18)
ν_1 ; $A_1[\nu_{NO^*}]$ (a)	1631 s (b) 1560 vs 1544 vs	1585 sh 1540 s, br	1597 s 1554 vs	1650 m 1621 s
ν_4 ; $B_1[\nu_{ASNO_2}]$	1307 sh 1283 vs 1249 vs	1270 s 1255 s	1290 vs 1252 vs	1167 s, sp 1159 s, sp
ν_2 ; $A_1[\nu_SNO_2]$	1044 s 990 s	977 s	1041 m	964 s, sp
$\nu_3 A_1[\delta_S MnO_2 N,$ ring def.] ν_5 ; $B_1[\delta ONO^*]$	782 s 727 m	794 m, sp 768 m 743 m	797 m 767 m 742 m	775 sh 764 m, sp 684 w, sp

(a) * indicates the terminal oxygen atoms

(b) vs, Very strong; s, strong; m, medium; w, weak;
sh, shoulder; sp, sharp; br, broad.

2.3.5. Magnetic Susceptibility.

For $Mn(NO_3)_3$ the molar magnetic susceptibility at 0° is $\chi_M^{corr} = 8150 \times 10^{-6}$ c.g.s.u. which gives $\mu_{eff} = 4.4 \pm 0.1$ B.M., a value which is reduced somewhat below the theoretical 'high-spin' value for the d^4 configuration. The observed and theoretical magnetic moments for $Cr(NO_3)_3$, $Mn(NO_3)_3$, $Fe(NO_3)_3$, $FeO(NO_3)$ and $Co(NO_3)_3$ are presented in Table 2.3. None of the samples with low observed magnetic moments have been examined at various temperatures to determine the nature of the interaction

in the compound. Unfortunately no variable temperature Faraday balance was available to examine $\text{Mn}(\text{NO}_3)_3$, and until this is done, it can only be assumed that the sample is magnetically non-dilute, i.e., there is some interaction between the manganese atoms in the structure.

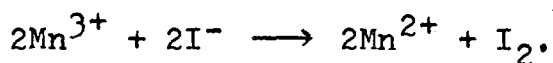
Table 2.3.

Magnetic Moments of Some Metal Nitrates.

<u>Compound</u>	<u>Observed</u> <u>μ_{eff} (B.M.)</u>	<u>Theoretical Spin Only</u> <u>μ_{eff} (B.M.)</u>
$\text{Cr}(\text{NO}_3)_3$	3.77	3.87
$\text{Mn}(\text{NO}_3)_3$	4.4	4.90
$\text{Fe}(\text{NO}_3)_3$	3.62	5.92
$\text{Co}(\text{NO}_3)_3$	1.0	0.00
$\text{FeO}(\text{NO}_3)$	3.50	5.92

2.3.6. Chemical Properties.

$\text{Mn}(\text{NO}_3)_3$ is an extremely vigorous oxidizing agent. It dissolves in water rapidly evolving oxygen, to give a yellow-brown solution with a brown precipitate, presumably representing disproportionation to $\text{Mn}(\text{II})$ and $\text{Mn}(\text{IV})$. When an ampoule of $\text{Mn}(\text{NO}_3)_3$ is broken under aqueous potassium iodide solution, the iodide is oxidized quantitatively (see Table 2.3) according to the equation:



The iodine was then determined by titration with thiosulfate, according to the equation:

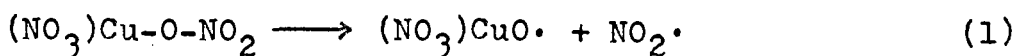


Table 2.4.

Determination of the Oxidation State of Manganese.

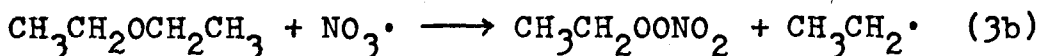
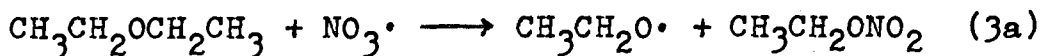
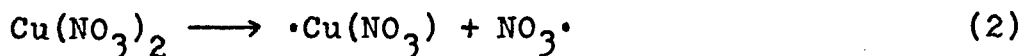
	$\text{Mn}(\text{NO}_3)_3$		$\text{S}_2\text{O}_3^{2-}$ (0.923M)		mmoles Mn	Oxidation
	<u>mg.</u>	<u>mmoles</u>	<u>ml.</u>	<u>mmoles</u>	<u>oxidized</u>	<u>State of Mn</u>
1.	28.7	0.119	1.08	1.00	1.00	2.84
2.	47.7	0.198	2.20	2.03	2.03	3.02

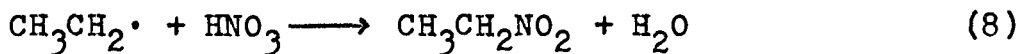
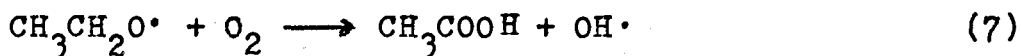
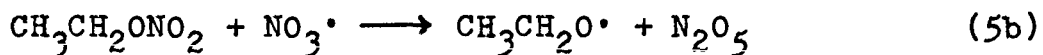
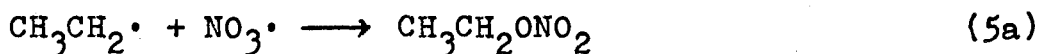
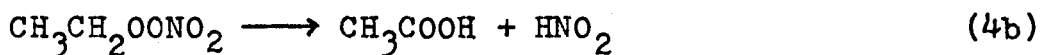
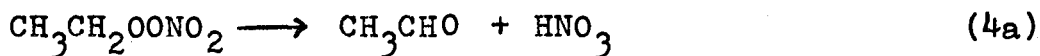
$\text{Mn}(\text{NO}_3)_3$ reacts violently with diethyl ether, and readily with hydrocarbons such as nujol. This behaviour is frequently displayed by complexes containing bidentate nitrate groups coordinated to a high oxidation state metal (20, 35, 73, 151). In 1962 Addison proposed that the reactivity of beryllium and cupric nitrates with diethyl ether could be explained by the production of the NO_2 free radical (152) in the reaction:



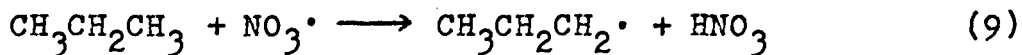
and the subsequent reaction with the diethyl ether could account for all the observed reaction products, namely N_2O_4 , CH_3CHO , NO_3^- , NO_2^- , OH^- , acetate, nitroalkanes and alkylnitrates. The only major drawback was the extreme chemical reactivity of the metal nitrates, which was much greater than was observed for $NO_2\cdot$ radicals prepared from N_2O_4 ; that is, metal nitrates react violently or explosively with diethyl ether but mixtures of N_2O_4 and ether are stable (152). This indicated that the species responsible for the oxidation of organic compounds by anhydrous metal nitrates could be the nitrate radical and NOT the NO_2 radical (151). It has been shown that the nitrate radical is one of the most reactive free radicals known in aqueous solution, only the $OH\cdot$ and $HSO_4\cdot$ radicals being more reactive (153, 154).

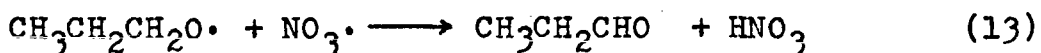
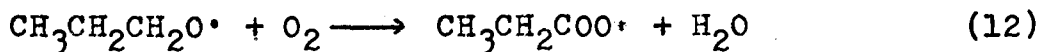
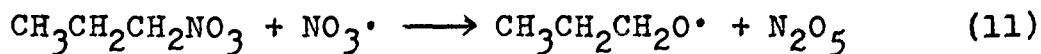
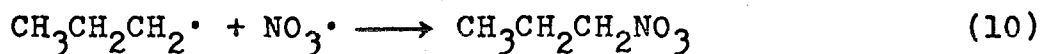
The reaction scheme below involving NO_3 radicals can also explain the observed products.





The production of the per-nitrate in reaction 3b could be the cause of the explosive reaction in this type of system. A much simpler reaction scheme can account for the rapid production of alkylnitrate followed by formation of carboxylic acid and nitroalkane in the reaction of anhydrous metal nitrates with aliphatic hydrocarbons (20, 35), and is presented below.





It must be remembered that there is no substantial proof for these mechanisms, but if they are correct, several criteria are imposed on the metal nitrates. These, and the weaknesses of them are presented below.

- (1) The metal nitrate must have a lower oxidation state available. This is obviously the case for $\text{Sn}(\text{NO}_3)_4$, $\text{Ti}(\text{NO}_3)_4$, $\text{Cu}(\text{NO}_3)_2$, and $\text{Mn}(\text{NO}_3)_3$. In the case of $\text{Be}(\text{NO}_3)_2$, the radical produced is more likely to be the NO_2 radical, as beryllium has no lower oxidation state, but does produce NO_2^- in aqueous solution (30).
- (11) Reactivity should only occur with metal nitrates coordinated through two oxygen atoms. Addison proposes that only "strongly coordinated symmetric bidentate nitrate-groups" show this reactivity (73, 151). This is obviously not the case if it

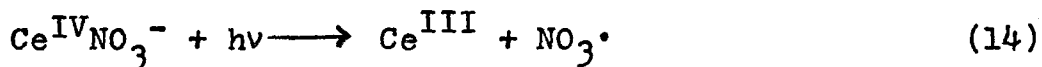
is assumed that ether and hydrocarbons react with the solid $\text{Cu}(\text{NO}_3)_2$ which contains both bridging and asymmetric bidentate nitrates (61) and not with $\text{Cu}(\text{NO}_3)_2$ in solution which may be monomeric and contain symmetric bidentate nitrates as does the vapor (62). Other nitrates such as $\text{Cr}(\text{NO}_3)_3$ (23), and $\text{Mn}(\text{NO}_3)_3$ which probably contain bridging nitrate groups and $\text{Ga}(\text{NO}_3)_4^-$ which supposedly contains unidentate nitrate groups (19) also show this reactivity. The $\text{Ga}(\text{NO}_3)_4^-$ probably is similar to the $\text{Tl}(\text{NO}_3)_4^-$ (34) and hence contains bidentate nitrates also. (This could easily be one of the cases where too much reliance was placed on the relative intensities of the N-O stretching frequencies in the Raman spectrum, without accompanying depolarization or crystal structure studies (see section 1.3.2.)).

(iii) A lowering of the number of coordinated oxygen atoms should result in the loss of chemical reactivity. This is the case for $\text{Sn}(\text{NO}_3)_4 \cdot 2\text{py}$ (35) and $\text{Mn}(\text{NO}_3)_3\text{L}$ (L = bipy, o-phen, or $2\text{Ph}_3\text{PO}$ see chapter three) which show no reactivity towards ether.

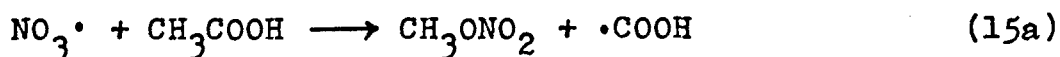
(iv) Bidentate nitrates should not pass through a

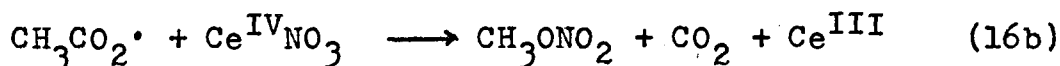
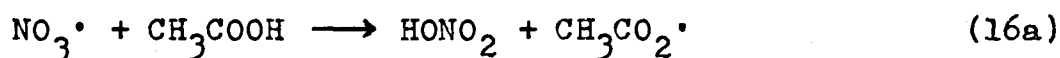
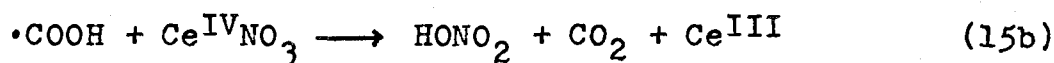
unidentate intermediate stage, i.e., both M-O bonds must be broken simultaneously; thus a metal-nitrate three centre bond would be an attractive possibility. This requirement is extremely difficult to rationalize with the number of bridging nitrates that undergo this type of reactivity i.e., $\text{Cu}(\text{NO}_3)_2$, $\text{Cr}(\text{NO}_3)_3$, $\text{Mn}(\text{NO}_3)_3$, etc.

A study by T.W. Martin (155) is also significant to the discussion of the reactivity of metal nitrates and the postulate that this reactivity arises from the production of nitrate radicals. Martin, in a study of the reactivity of $\text{Ce}(\text{NO}_3)_6^{2-}$ and glacial acetic acid demonstrated that NO_3^\cdot radical was not a major reactive intermediate in their system. He showed that if a primary reaction process was the production of nitrate radicals according to equation 14,

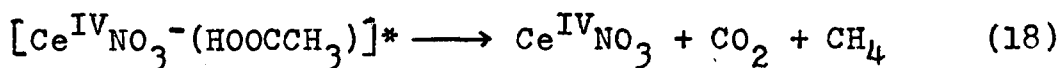
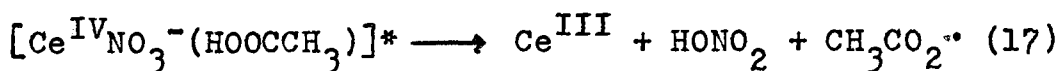


and this was to produce CO_2 , which was one of the major reaction products, then the nitrate radical must react according to either reactions 15, or 16.





Thus both possible reaction pathways produce two Ce^{III} species for each CO_2 , whereas in all the steady state experiments the quantum yield of CO_2 was greater than that of Ce^{III} , nor could the reaction yields of the other products be explained using nitrate radicals as intermediates. Thus the production of nitrate radical does not appear to play an important role in the $\text{Ce}(\text{NO}_3)_6^{2-}$ acetic acid system. The active species in this case appears to be the excited complex $[\text{Ce}^{\text{IV}}\text{NO}_3^-(\text{HOOCCH}_3)]^*$ which decomposes according to the equations 17 and 18.



Thus the reaction of other metal nitrates may involve a reactive solvated intermediate, rather than the production

of free nitrate radicals. This would be consistent with the observed reactivity of bridging nitrate systems as well as symmetric bidentate systems. The reactions of anhydrous metal nitrates with organic species is the area in nitrate chemistry that has received little concentrated effort to date and yet should be one of the most rewarding areas of study.

Reactions with a number of donor ligands have been studied and yield complexes which are presented in the following chapter.

Chapter 3.

Complexes of Manganese(III) Trinitrate.

3.1. Introduction.

Numerous complexes of manganese(III) have been reported with nitrogen or oxygen ligands and with the halogens. The complexes with nitrogen bases included such ligands as the porphyrins (143, 144), bipyridyl and o-phenanthroline (140, 142) and primary, secondary and tertiary amines (142). The complexes with oxygen donor ligands included such ligands as oxalato (124, 125) acetylacetonato (126 - 127) acetato (130), dimethylsulphoxide and dimethylformamide (131) and the oxides of pyridine, phosphine, arsine and 2,2',2''-terpyridine (133, 139). Complexes which include mixed nitrogen and oxygen donor ligands are the tris-salicylaldimino (134) and acetylacetonatobis-(N-phenylaminotroponiminato) manganese(III) (132) complexes. The halo or pseudohalo complexes which are known are the tetrafluoro- (112), the pentachloro- and fluoro- (112 - 115, 119), the hexachloro-, fluoro- and cyano- (116, 120 - 123) manganates(III). None of these complexes have nitrate ligands or anions incorporated in them; therefore the reactions described in this chapter were undertaken to investigate the preparation of manganese(III)

nitrate complexes and to determine if the nitrate complexes would exhibit increased stability with respect to the parent nitrate, as is the situation with manganese(III) trichloride complexes (117, 142).

3.2. Trinitrato-2,2'-bipyridylmanganese(III).

3.2.1. Preparation.

Addition of 2,2'-bipyridyl to a nitromethane solution of $\text{Mn}(\text{NO}_3)_3$ at 5°C in a 1:1 mole ratio gave a low yield ($\approx 20\%$) of dark crystals. An alternative preparative route was found that permitted manganese(III) trinitrate to be prepared in situ and, upon addition of the ligand, the complexes crystallized in much better yields. Potassium permanganate (1.0 g., 6.4. μmoles), when stirred with N_2O_4 (20 ml, 0.31 mole) in nitromethane or acetonitrile (20 ml) for two hours produced a yellow precipitate of $\text{K}_2[\text{Mn}(\text{NO}_3)_4]$, which will be discussed in detail with the other tetranitratomanganate anions in chapter five, and a dark "brown solution" which contained manganese, nitrate, dinitrogen tetroxide and nitromethane. There was no reaction between potassium permanganate and pure dinitrogen tetroxide which suggests that the organic solvents are necessary to promote the reaction (see section 2.2.7 for a possible reaction scheme). Solid 2,2'-bipyridyl (0.32 g., 2.0 μmoles)

was added to a freshly filtered portion of the "brown solution" in nitromethane calculated to contain 2.0 mmoles of manganese. Within 24 hours at 5°C large crystals of $\text{Mn}(\text{NO}_3)_3 \cdot \text{bipy}$ crystallized from the mixture in good yield ($\approx 80\%$). The compounds prepared by each method were shown to be identical by elemental analysis and i.r. spectroscopy. [Found: Mn, 13.8; C, 30.0; H, 2.08; N, 17.5%. $\text{Mn}(\text{NO}_3)_3 \cdot \text{C}_{10}\text{H}_8\text{N}_2$ requires Mn, 13.8; C, 30.2; H, 2.03; N, 17.6%].

3.2.2. Physical Measurements.

Physical measurements were made as described in section 2.2.7. C, H and N analyses were performed by the Simon Fraser University micro-analytical laboratory.

3.2.3. Discussion.

In view of the numerous possibilities for the molecular structure of this complex, bearing in mind the various coordinating modes open to the nitrate group, the crystal structure of this complex was determined, and is reported in the following chapter. The complex is molecular and monomeric. The manganese atom has an approximate pentagonal bipyramidal coordination environment, with the four oxygen atoms of one symmetric and one asymmetric

bidentate nitrate group and one bipyridyl nitrogen atom defining the equatorial plane. The remaining bipyridyl nitrogen atom, and the oxygen atom of a unidentate nitrate group are at the apices (Figure 4.1.).

The infrared spectrum (Table 3 and Figure 3.1) indicates the absence of nitrate ions and the presence of coordinated bipyridyl, but without the complementary Raman spectrum it is difficult to assign the i.r. spectrum with confidence in terms of discrete vibrations associated with unidentate and bidentate nitrate groups. Several attempts were made to observe the combination frequencies in the $1700 - 1900 \text{ cm}^{-1}$ regions to aid the assignment (see section 1.3.2) but these were found to be too weak to locate with certainty. On the basis of the generalization that where a bidentate and a unidentate nitrate group are coordinated to the same or similar metal atoms in comparable oxidation states the separation of the two highest nitrate fundamental stretching frequencies will be greater for the bidentate group than for the unidentate group (73, 74), the bands at 1518 and 1265 cm^{-1} are tentatively assigned to bidentate nitrate vibrations, and those at 1500 and 1285 cm^{-1} to the unidentate nitrate vibrations. Despite the inequivalence of the three nitrate groups in the molecule, only a single band is observable in the third and lowest fundamental

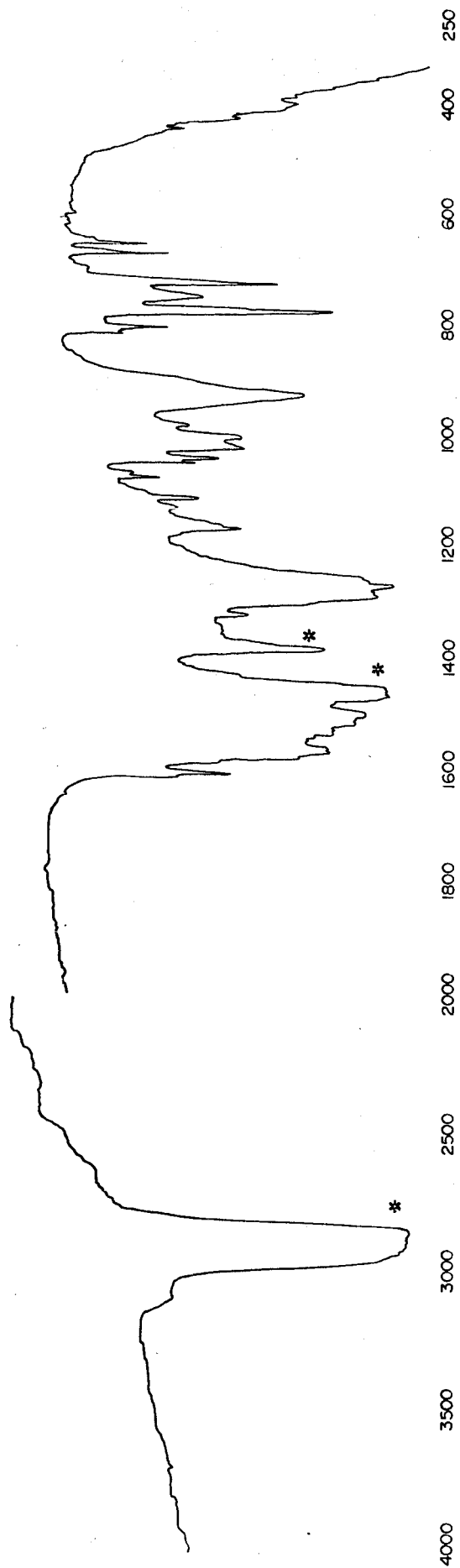


Figure 3.1. Infrared spectrum of $\text{Mn}(\text{NO}_3)_3 \cdot \text{bipy}$
* Nujol Bands.

Table 3.1.

Infrared Spectra of Some complexes of $\text{Mn}(\text{NO}_3)_3^a$ (cm^{-1}).

$\text{Mn}(\text{NO}_3)_3 \cdot \text{bipy}$	$\text{Mn}(\text{NO}_3)_3 \cdot \text{o-phen}$	$\text{Mn}(\text{NO}_3)_3 \cdot 2\text{Ph}_3\text{PO}$	$\text{Mn}(\text{NO}_3)_3 \cdot x\text{MeCN}$
1518 s	1555 sh	1552 sh	1555 s, br
1500 s	1535 s, br ^b	1520 s, br	
1285 s	1243 s	1265 s	1270 s, br
1265 s	1230 sh		
	1210 s		
923 s	948 m	968 s	972 s
		953 sh	
802 m	800 w	798 m, sp	791 m
		787 m, sp	
747 m	752 m	c	c

a Only the nitrate absorptions are listed.

b May be partially overlapped by a band due to o-phen

c This region of the spectrum is obscured by ligand bands.

nitrate stretching region and is at an extremely low position, 923 cm^{-1} . This is close to the lowest value so far reported for this band, at 920 cm^{-1} in the unidentate nitrate complex $\text{K}[\text{Au}(\text{NO}_3)_4]$ (73).

$\text{Mn}(\text{NO}_3)_3 \cdot \text{bipy}$ is a high spin complex having $\chi_M^{\text{corr}} = 10,530 \times 10^{-6}$ c.g.s.u. at 22°C , $\mu_{\text{eff}} = 5.0 \pm 0.1$ B.M. The room temperature diffuse-reflectance spectrum of a powdered sample shows a band at 19.7 kcm^{-1} assigned to a d-d transition. No complexes containing a greater proportion of bipyridyl could be obtained even upon increasing the excess of ligand up to threefold. Thus the complexes of 1:1.5 stoichiometry formed with $\text{Co}(\text{NO}_3)_3$ (18) and InX_3 ($X = \text{Cl}, \text{Br}, \text{I}, \text{NCS}$) (156, 157), are apparently not formed in the case of $\text{Mn}(\text{NO}_3)_3$, under these conditions. There have been two reports of anhydrous manganese(III) bipyridyl complexes (140, 142) for which, due to the low magnetic moments (140, 141), the stoichiometry has been postulated to be the bimolecular species $[\text{Mn}(\text{bipy})\text{Cl}_3]_2$ with bridging chloro ligands. This is not the case in $\text{Mn}(\text{NO}_3)_3 \cdot \text{bipy}$, however.

For the comparison with other manganese(III) complexes, the X-ray powder pattern of $\text{Mn}(\text{NO}_3)_3 \cdot \text{bipy}$ is reported in Table 3.2. The compound is soluble in methanol,

Table 3.2.

X-Ray Powder Patterns for Several Mn(III) Complexes.

(Interplanar spacings in Å)

$\text{Mn}(\text{NO}_3)_3 \cdot \text{bipy}$	$\text{Mn}(\text{NO}_3)_3 \cdot \text{ophen}$	$\text{Mn}(\text{NO}_3)_3 \cdot 2\text{OPPh}_3$
		10.35 m
9.83 m	8.52 w	9.18 s
7.03 s	7.73 w	8.16 m
	6.98 s, br	
6.51 m	6.07 w	6.48 m
5.57 m		
5.28 w	5.31 s	5.29 w
5.01 w	5.01 w, br	5.02 vw
		4.93 w
4.54 s	4.48 m	4.60 s
4.18 w	4.14 w	4.10 s, br
3.95 w		3.93 w
3.79 s	3.75 w	
3.72 m		
3.49 m	3.46 m	
3.43 s	3.33 w	3.41 w
3.20 w	3.23 w	3.27 w
	3.09 w	3.08 vw
2.86 m	2.94 w	2.93 w
2.76 m	2.78 vw	2.78 w
	2.65 m	
	2.49 m	
	2.42 w	
2.32 w	2.30 m	
2.23 w	2.20 w	
2.14 w, br		
2.06 w		

and sparingly soluble in acetone to give a yellow solution, and decomposes in water to give a yellow-brown solution. It is insoluble in benzene, carbon tetrachloride, ethyl acetate and nitromethane.

3.3. Trinitrato-o-phenanthroline manganese(III).

This brick red crystalline complex was prepared by the same two methods used for the bipyridyl complex. [Found: Mn, 12.8; C, 34.3; H, 1.87; N, 16.2% $\text{Mn}(\text{NO}_3)_3 \cdot \text{C}_{12}\text{H}_8\text{N}_2$ requires Mn, 13.0; C, 34.2; H, 1.91; N, 16.6%].

The stoichiometry of this compound suggests that this complex could have a similar molecular structure to that of the bipyridyl complex. The infrared spectrum (Table 3.1 and Figure 3.2) is similar, where bands can be discerned from o-phenanthroline absorption, but there are small shifts in band positions. A comparison of the X-ray powder patterns (Table 3.2) of the bipyridyl and o-phenanthroline complexes indicates that they are not isomorphous, although the patterns are quite similar at low angles. The difference in structure could be imposed on the o-phenanthroline complex by the rigidity of the ligand (158), whereas the bipyridyl ligand is able to rotate about the carbon-carbon bond and has a dihedral angle of 5.1° between

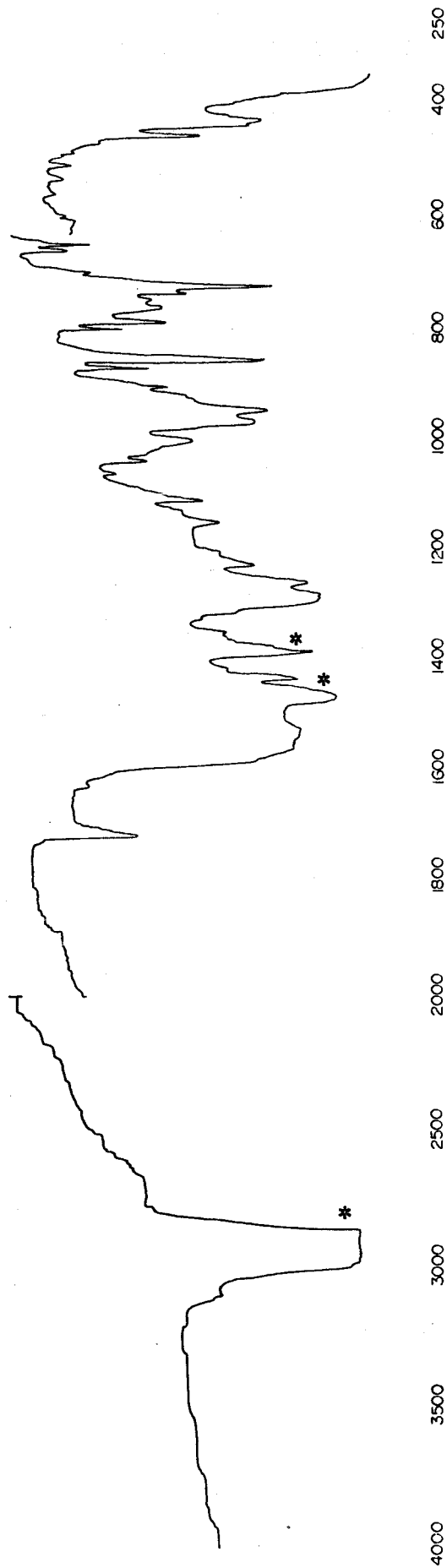


Figure 3.2. Infrared spectrum of $Mn(NO_3)_3 \cdot 0.5\text{-phen}$
* Nujol Bands.

the two rings in the complex. The o-phenanthroline planarity might permit slight shifts in the nitrate groups which may affect the coordination of the manganese and/or the packing of the molecules in the unit cell. Thus it would be interesting to determine the crystal structure of the o-phenanthroline complex so that the effects of the more rigid ligand could be examined. At the present time, no definite conclusion as to the molecular structure of the o-phenanthroline complex can be drawn. Magnetic measurements give $X_M^{\text{corr}} = 10,830 \times 10^{-6}$ c.g.s.u.; $\mu_{\text{eff}} = 5.0 \pm 0.1$ B.M. at 22°C. $\text{Mn}(\text{NO}_3)_3 \cdot \text{o-phen}$ shows solubility properties similar to those of the bipyridyl complex.

3.4. Trinitratomanganese(III)·bistriphenylphosphineoxide.

Addition of triphenylphosphine oxide (1.28 g., 4.6 mmoles) to the "brown solution" in nitromethane (2:1 mole ratio) yielded dark red crystals of $\text{Mn}(\text{NO}_3)_3 \cdot 2\text{Ph}_3\text{PO}$.

[Found: Mn, 6.9; C, 53.3; H, 3.65; N, 5.1.

$\text{Mn}(\text{NO}_3)_3 \cdot \text{C}_{36}\text{H}_{30}\text{P}_2\text{O}_2$ requires Mn, 6.9; C, 54.2; H, 3.77; N, 5.3%].

Triphenylphosphine oxide was chosen as an oxygen donor ligand as it was unlikely to reduce the manganese(III) or to react with the reagents in the "brown solution".

Triphenylphosphine oxide forms the high-spin complex $\text{Mn}(\text{NO}_3)_3(\text{Ph}_3\text{PO})_2$ having $X_M^{\text{corr}} = 10,150 \times 10^{-6}$ c.g.s.u. and $\mu_{\text{eff}} = 4.9 \pm 0.1$ B.M. The infrared spectrum shows the nitrate bands listed in Table 3.1 as well as bands typical of complexed Ph_3PO (e.g., $\nu(\text{P}=\text{O})$ 1150 cm^{-1} (159)). The infrared spectrum is shown in Figure 3.3. The X-ray powder pattern of the complex is shown in Table 3.2, but the structure of this complex is not known. The complex dissolves in benzene and acetonitrile to give yellow solutions and is insoluble in carbon tetrachloride, nitromethane and water. Attempts to measure the ^{31}P N.M.R. of saturated solutions at 35°C in C_6H_6 were unsuccessful due to insufficient solubility.

3.5. Trinitratomanganese(III)·acetonitrile.

Acetonitrile was used instead of nitromethane as the solvent in producing the "brown solution". Evaporation of this solution in vacuo gave a dark brown solid containing both $\text{Mn}(\text{NO}_3)_3$ and coordinated acetonitrile. Although reproducible analyses could not be obtained, a composition between $\text{Mn}(\text{NO}_3)_3 \cdot 1.5\text{CH}_3\text{CN}$ and $\text{Mn}(\text{NO}_3)_3 \cdot 2.0\text{MeCN}$ based on manganese, carbon and hydrogen, was indicated by the results presented in Table 3.3. The nitrogen analysis was low and

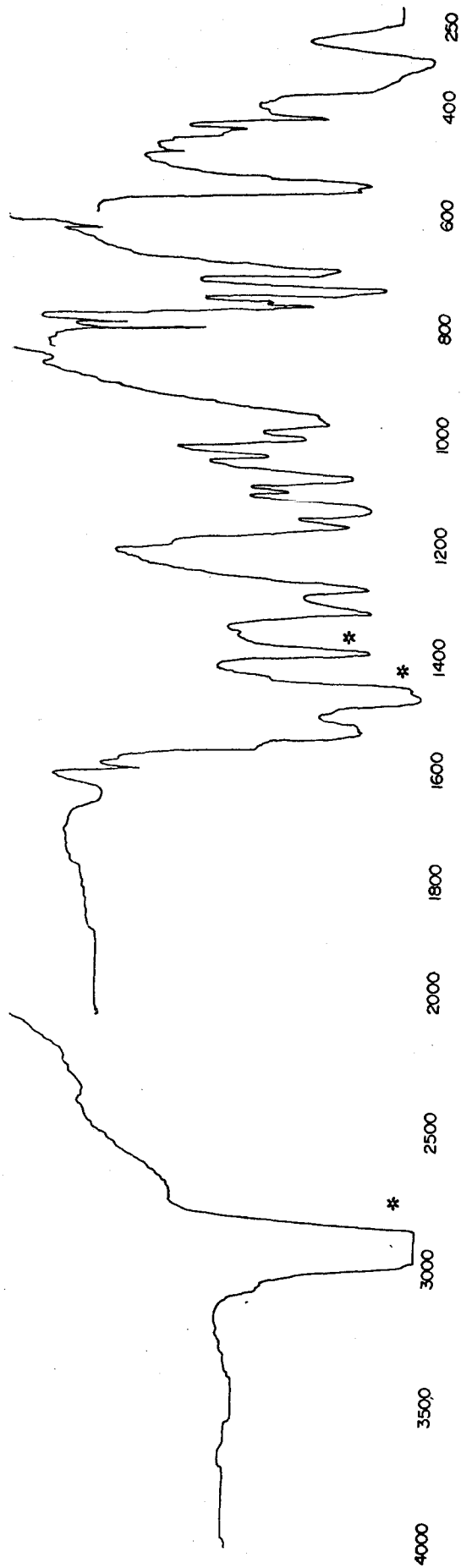


Figure 3.3. Infrared spectrum of $Mn(NO_3)_3 \cdot 20PFh_3$
* Nujol Bands.

not consistent in all samples which may be due to incomplete degradation of the sample upon combustion.

Table 3.3.

Analyses of $Mn(NO_3)_3 \cdot xMeCN$.

<u>Theoretical</u>	Mn	C	H	N
$Mn(NO_3)_3 \cdot 1.5MeCN$	18.20	11.95	1.49	20.84
$Mn(NO_3)_3 \cdot 2.0MeCN$	17.05	14.84	1.86	21.70
<u>Observed</u> (with hours and temperature under vacuum).				
1. (16 Hrs., 20°C)	17.75	12.35	1.59	15.53
2. (48 Hrs., 80°C)	17.30	14.30	1.59	14.44
3. (8 Hrs., 20°C)		12.79	1.74	16.37

The acetonitrile complex shows infrared bands (Table 3.1 and Figure 3.4) typical of coordinated nitrate groups and coordinated acetonitrile ($\nu(C\equiv N)$ 2291 cm^{-1}). A strong band also occurs at 415 cm^{-1} which is absent from the spectra of the other complexes and therefore is presumably not due to a Mn-O mode; it may be the Mn-N stretch of the coordinated acetonitrile, though such modes have been difficult to assign with certainty (74). For this compound $\chi_M^{corr} = 11,400 \times 10^{-6}$ c.g.s.u. $\mu_{eff} = 5.2$ B.M. assuming the formula contains two molecules of CH_3CN .

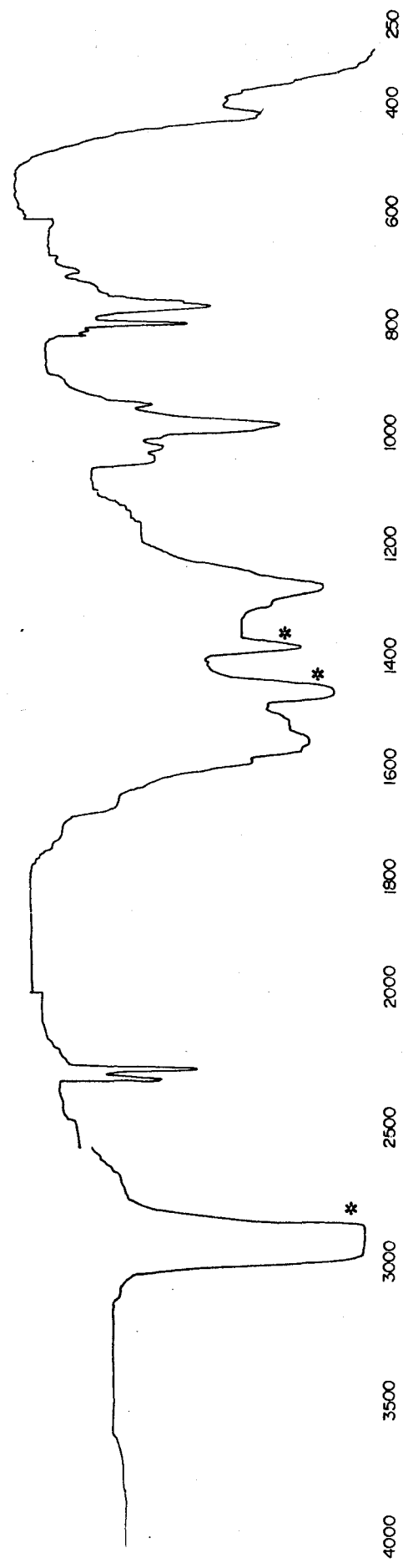


Figure 3.4. Infrared spectrum of $Mn(NO_3)_3 \cdot xMeCN$
* Nujol Bands.

3.6. Reaction of Manganese(III) Trinitrate with Pyridine.

When pyridine was added to the "brown solution" (2:1 mole ratio) a violent reaction took place and the solution became an intense dark green - the color of the complex $N_2O_4 \cdot 2py$ (25, 160). When the solution was concentrated and cooled, it turned orange, but no crystals were obtained. When the solvent was removed in vacuo an orange gum was obtained. If this gum was stirred for two hours in acetone, an orange powder resulted which would not oxidize iodide and was thus likely to contain manganese(II). Infrared bands at 823 m, sp; 1350 s, br and 1750 m cm^{-1} indicate the presence of ionic nitrate groups and although the 601 cm^{-1} band of pyridine does not shift, the band at 1578 cm^{-1} shifts to approximately 1600 cm^{-1} and broadens, so it seems likely that the pyridine is coordinated. The lack of a strong band in the 1200 - 1265 cm^{-1} region indicates that the coordinated species is not pyridine-N-oxide which could have been produced from reaction of pyridine and dinitrogen tetroxide. Analyses (Mn, 16.7; C, 40.82; H, 3.03; N, 19.89%) did not conform to any simple combination of manganese, pyridine, pyridine-N-oxide and nitrate; thus, the composition of this material is not known.

3.7. Reaction of Manganese(III) Trinitrate with Triphenylphosphine.

When triphenylphosphine was added to the "brown solution" (1:1 mole ratio) a violent reaction took place. When the solution was pumped to dryness, a brown, intractable gum was obtained, which could not be ground or smeared to obtain an infrared spectrum. When this gum was stirred with iodide, it was unable to oxidize the iodide, indicating reduction of the manganese had occurred during the reaction. No further attempts were made to characterize it.

3.8. Discussion.

The number of addition complexes with manganese(III) trinitrate is not large due to three factors. First, the thermal instability and the lack of suitable solvent for $\text{Mn}(\text{NO}_3)_3$ negates any attempt to prepare complexes directly in an appreciable yield. Second, the preparation of complexes from $\text{Mn}(\text{NO}_3)_3$ in situ limits the number of ligands to those that will not react with the other reagents present. Finally, the recovery of complexes from the "brown solution" seems frequently to yield only viscous gums. Even so, complexes containing nitrogen and oxygen donor ligands have

been prepared and are more stable than the parent nitrate.

In the brown nitromethane solution, pyridine and triphenylphosphine were able to reduce manganese(III) trinitrate. However, manganese(III) trichloride is not reduced by pyridine so that the complexes $\text{MnCl}_3 \cdot \text{py}$ and $\text{MnCl}_3 \cdot 3\text{py}$ have been synthesized (142). With cobalt(III) trinitrate, triphenylphosphine was oxidized, but with pyridine a stable cobalt(III) complex, $\text{Co}(\text{NO}_3)_3 \cdot 2\text{py}$, is isolated from CCl_4 solution (18). In view of these reactions, it would appear likely that a stable pyridine complex of manganese(III) trinitrate could perhaps be prepared by stirring pyridine in carbon tetrachloride with manganese(III) trinitrate at -30°C .

Chapter 4

The Crystal and Molecular Structure of Trinitrato-2,2'-bipyridylmanganese(III)

4.1. Introduction.

In the preceding chapter the syntheses of 1:1 high spin complexes of manganese(III) nitrate with bidentate nitrogen bases such as 2,2'-bipyridyl and o-phenanthroline were reported. The solid state structure of such compounds is of interest in view of the diversity of possibilities which exist for the coordination environment of the manganese and for the mode of nitrate ligand coordination. There have been few structural determinations of high spin manganese(III) compounds, the only examples being $(bipH_2)MnCl_5$ (119), $(NH_4)_2MnF_5$ (161), $K_2Mn(SO_4)F_3$ (162), MnF_3 (111), Mn_2O_3 (136), $ZnMn_2O_4$ (137), Mn_3O_4 (137), $Mn(acac)_3$ (118, 163), $Mn(acac)(pati)_2$ (132) and $(bipy)_2MnO_2Mn(bipy)_2$ (164). Although the manganese in $MnCl_5^{2-}$ (119) is pentacoordinate, all the other examples exhibit octahedral coordinated manganese(III), with bridging ligands where necessary to complete the coordination sphere.

The nitrate group is capable of considerable versatility as a ligand toward metal ions (5, 73) and

frequently acts as a bidentate ligand thereby inducing rather high coordination numbers. Thus, eight coordinate nitrato complexes of 3d metals have been established for a range of oxidation states, e.g., $\text{Mn}(\text{NO}_3)_4^{2-}$ (53), $\text{Fe}(\text{NO}_3)_4^-$ (11) and $\text{Tl}(\text{NO}_3)_4$ (45). If all of the nitrate groups were to be bidentate in $\text{Mn}(\text{NO}_3)_3 \cdot \text{bipy}$, an eight coordinate molecular complex could result in this case also; however the steric requirements of the bipyridyl might hinder this arrangement due to the larger bite of the bipyridyl which is $\approx 2.6\text{\AA}$ compared to that of the nitrate which is 2.1\AA . Conversely, wholly unidentate nitrate coordination could yield a pentacoordinate species. Between these extremes there exist numerous structural possibilities which might arise from a combination of unidentate, bidentate or bridging coordination. One alternative is ruled out on infrared spectral evidence; the structure cannot contain uncoordinated nitrate ions. Finally the possibility of octahedrally coordinated manganese(III) occurring has its own special interest regarding the possible mechanism for the removal of the degeneracy of the ground state in the d^4 configuration (Jahn-Teller effect). In tris-(acetylacetonato) manganese(III) this occurs by angular distortion (118, 163) while in acetylacetonato-bis-(N-phenylaminotroponiminato) manganese(III) and in tetrakis(bipyridyl)- μ -dioxo-dimanganese(III, IV) there are unequal bond lengths (132, 164).

For a variety of reasons, therefore, it was considered that the X-ray crystal structure determination of $\text{Mn}(\text{NO}_3)_3 \cdot \text{bipy}$ would be of interest.

4.2. Determination of the Structure.

4.2.1. Crystal Mounting.

Crystals of trinitrato-2,2'-bipyridyl-manganese(III) were grown by the method previously outlined in chapter three. Numerous crystals were sealed under an inert atmosphere in 0.3 or 0.5 mm. Lindeman glass capillaries in a dry box. These, upon examination under a microscope, appeared dark red to reflected light and dark green to transmitted light.

An approximately cube shaped crystal (0.05 cm.) was considered too large for intensity data collection but was used for preliminary photographs. A smaller crystal, a parallelepiped of 0.28 x 0.24 x 0.18 mm. dimensions was used for a Weissenberg photograph and the data collection.

4.2.2. Photographs.

Precession photographs of the $h\ 0\ l$ and $0\ k\ l$ zones and zero and first level Weissenberg photographs indicated the presence of a mirror plane and the systematic absences $h\ 0\ l$, $l = 2n + 1$ and $0\ k\ 0$, $k = 2n + 1$. This

allowed the space group to be unambiguously assigned as the monoclinic group $P2_1/c$. The approximate unit cell dimensions were $a = 7.29$, $b = 18.04$, $c = 11.72\text{\AA}$ and $\beta = 107^\circ 55'$. The unit cell volume calculated from the formula $V = a b c \sin \beta$, is 1469\AA^3 .

The number of molecules per unit cell (n) was calculated, using the cell dimensions determined from the photographs. The density (ρ) is given by the formula

$$\rho = \frac{(M)(n)}{(N)(V)} \tag{1}$$
$$= 0.448 n$$

where M is the gram formula weight (397.15g.), N is Avogadro's number (6.02×10^{23}) and V is the unit cell volume ($1.469 \times 10^{-21} \text{ cm}^3$). The actual density of two crystals was measured by flotation, using CCl_4 ($\rho = 1.59 \text{ g. cm}^3$) and CH_2I_2 ($\rho = 3.33 \text{ g. cm}^{-3}$). The crystal was placed in CCl_4 (1.00 cm^3) and CH_2I_2 added dropwise from a micro-syringe until the crystal achieved zero buoyancy: the density of the crystal then being identical with that of the liquid. The results are presented in Table 4.1. The average density is $1.82 (\pm 0.05) \text{ g. cm}^{-3}$. Therefore

there must be four formula units per unit cell to achieve the observed density.

Table 4.1.

Density of $\text{Mn}(\text{NO}_3)_3 \cdot \text{bipy}$.

<u>Crystal</u>	<u>Vol.</u> <u>CCl_4 (cm³)</u>	<u>Vol.</u> <u>CH_2I_2 (cm³)</u>	<u>Total Vol.</u> <u>(cm³)</u>	<u>Total Wt.</u> <u>(g.)</u>	<u>Density</u> <u>(g. cm⁻³)</u>
1	1.00	0.13	1.13	2.04	1.80
2	1.00	0.14	1.16	2.12	1.83

4.2.3. Data Collection.

The crystal was mounted on a Picker FACS-1 computer controlled four circle diffractometer, and optically aligned to position the crystal precisely at the intercepts of the ϕ , χ and 2θ circles (ω is coincident with 2θ and hence the crystal was centered in ω also). To detect a reflection, the reciprocal lattice point must be brought into contact with the sphere of reflection in the same plane as the source, crystal and detector. This was achieved by setting the 2θ value for one reflection with $\chi = 0^\circ$ and ϕ was driven until the reflection was located. (This reflection was $0\ 1\ 8, 2\theta = 29.78, \omega = 0.0, \chi = 356.17, \phi = 355.33^\circ$.) A second reflection (with $\phi \approx 90^\circ$ away from the first reflection) was then aligned by setting the 2θ angle and driving χ . (This

reflection was 0 12 1, $2\theta = 27.57$, $\omega = 0.0$, $\chi = 354.55$ and $\phi = 277.21^\circ$.) The orientation matrix was then obtained from the two reflections and the unit cell dimensions. Eighteen strong reflections (from the photographs) were used to obtain cell dimensions by a least squares procedure.

Following the data collection, dimensions were redetermined from accurate measurement of twenty-three of the strongest reflections having $2\theta > 30^\circ$ with Mo-K $_{\alpha 1}$ radiation ($\lambda = 0.70926\text{\AA}$) with a 1.0° take off angle.

Reflection intensities for the unique set of data (one-quarter of the limiting sphere of reflection with a $2\theta \leq 45^\circ$, for a monoclinic crystal) were collected by peak-top counting using niobium filtered Mo-K $_{\alpha}$ ($\lambda = 0.7107\text{\AA}$) radiation, and a scintillation counter with pulse height analysis. The take-off angle was 3.5° . Each reflection with $2\theta < 45^\circ$ was measured for twenty seconds with two background counts of ten seconds each taken 2.0° apart plus allowance for dispersion. Every hour, two standard reflections were measured; their variation was $\pm 5\%$ over the entire data collection. The inner set of data ($2\theta \leq 30^\circ$) had initially been collected by the ($2\theta - \theta$) scan technique, but as the peaks were broad and flat, it was felt that the peak-top

counting technique was more accurate for the weak intensities which comprised the bulk of the data.

4.2.4. Solution of the Structure.

A brief description of all of the programs utilized in this section appears in Appendix A. The raw intensity data was converted into observed structure factors, F . The net intensities were corrected for Lorentz and polarization effects; absorption was neglected since it was estimated that it would introduce a maximum error of $\pm 1\%$. A reflection was considered unobserved if the net count was less than 3.0σ , $\sigma = (\text{total count} + \text{background})^{\frac{1}{2}}$. 1914 reflections were measured of which 1119 were regarded as observed.

An examination of the unsharpened three dimensional Patterson function based on the data in the range $2\theta \leq 30^\circ$ allowed the determination of the position of the manganese since in the space group P_{2_1}/C the four equivalent positions $x, y, z; \bar{x}, \bar{y}, \bar{z}; x, \frac{1}{2} - y, \frac{1}{2} + z;$ and $\bar{x}, \frac{1}{2} + y, \frac{1}{2} - z$ are related in the section of the unit cell examined by three vectors $2x, 2y, 2z; 0, \frac{1}{2} + 2y, \frac{1}{2};$ and $2x, \frac{1}{2}, \frac{1}{2} + 2z$. There were only three strong vectors meeting these requirements which indicated the manganese position to be approximately $x = 0.056, y = 0.141,$ and $z = 0.276$. Six other peaks were

located within 2.5\AA of the manganese. Structure factors $|F_c|$ were calculated from the atomic coordinates and assumed temperature factors. A full matrix least squares refinement was done on the set of data in the range $2\theta \leq 30^\circ$ and the residual index, $R = \sum (|F_o| - |F_c|) / |F_o|$, was 58.3%. After three cycles of refinement on the seven atoms, varying the scale, the positional parameters and isotropic thermal parameters, R reduced to 38.8%. An electron density Fourier synthesis on the data permitted all non-hydrogen atoms to be found and refinement of all atomic coordinates and isotropic temperature factors gave $R = 13.2\%$. An examination of bond lengths and angles indicated that the unidentate nitrate was not properly defined. Shifting the terminal oxygen atoms, O(12) and O(13), to positions indicated by an electron density difference map, and which also gave chemically reasonable angles about N, reduced R to 8.5%. The three distinct modes of nitrate coordination were clearly visible at this point. Inclusion of the remaining data in the range $45^\circ \geq 2\theta > 30^\circ$ and refinement gave $R = 11.6\%$. Further refinement including anisotropic motion of the manganese and N(1), O(12), and O(13) of the unidentate nitrate group reduced R to 8.8%. At this stage all the hydrogen atoms were visible in an electron density difference map; including these at the calculated positions ($d(C-H) = 0.98\text{\AA}$ (165)) in

further refinement of the non-hydrogen atoms reduced R to 8.3%. At no time were the positions or temperature factors of the hydrogen atoms refined, although their positions were periodically re-determined as the carbon atom positions were refined. Allowance of anisotropic temperature factors for all oxygen atoms, and full matrix least squares refinement of all positional and thermal parameters for non-hydrogen atoms gave R = 6.7%.

An electron density difference map indicated that the principal discrepancies at this stage were in the region of the unidentate nitrate group, notably the uncoordinated oxygen atoms; therefore it was decided to examine this region in detail. Refinement of all positional and thermal parameters except those for N(1), O(11), O(12) and O(13) gave R = 18.6%. A set of structure factors was then created and used as input in the various Fourier syntheses that follow. In retrospect, it would have been better to use structure factors generated without further parameter refinement, as refinement may result in unrealistic shifts in other light atom parameters.

Three approaches were then attempted. First Mn, N(I), O(11), O(12) and O(13) were given anisotropic thermal parameters and refinement resulted in $R = 7.0\%$. By comparison, refinement as isotropic atoms gave only $R = 8.3\%$. Since the temperature factors were large for O(12) and O(13) and there were large peaks in the difference map associated with these atoms, it was felt that whole atoms may not have been capable of describing the unidentate nitrate. Furthermore, the unidentate nitrates may have been disordered with a fraction of them occupying each of two different positions; a second approach was therefore attempted. This approach was to describe each of the terminal oxygen atoms as a pair of "half atoms" positioned approximately 0.9\AA apart, near the larger peaks on the difference map associated with O(12) and O(13). Refinement of this arrangement resulted in $R = 7.1\%$, but the half atoms arising from O(13) would not refine to any unique set of positions, so this approach was not satisfactory. Even if only O(12) was replaced with half atoms no improvement was observed. For the third model, the occupancy or multiplicity of the "fractional atoms" were varied from 0.50 for each of to 0.80 and 0.20 as an attempt to match the differences in peak height on the difference map, but refinement of this model only produced $R = 7.6\%$. Thus there was no significant improvement in agreement when the unidentate nitrate group

was defined by employing fractional atoms for one or both of the terminal oxygens, and so all further refinement included these as anisotropic atoms only.

Final refinement of all positional and anisotropic thermal parameters with the reflections weighted as described below gave a final R = 5.9%. This improvement was somewhat surprising as the major features in an electron density map (peaks and troughs up to $\epsilon = 0.7(2) e^{-/\text{\AA}^3}$, which is approximately 20% of the broad peak observed for O(1)) were still in the region of unidentate nitrate, but the high correlation coefficients (≈ 0.3) between the x and z parameters of the uncoordinated oxygen atoms of this group may provide an explanation for this.

The weight given to each reflection should be a measure of its reliability and is thus equal to the reciprocal of the square of the standard deviation (equation 2).

$$W_1 = \frac{1}{\sigma_1^2} \quad (2)$$

The weighting function used in this case was $\sigma = A^{\frac{1}{2}}$ for $B \leq F_0 \leq C$, $\sigma = (AB/F_0)^{\frac{1}{2}}$ for $F_0 < B$ and $\sigma = (AB/F_0)^{\frac{1}{2}}$ for $F_0 > C$. A was chosen such that the error of fit was equal

to unity, B and C were chosen to give constant values of $W\Delta^2/n$ over 4.48. The final error of fit was 1.048.

In the structure factor calculations, the atomic scattering factors for Mn, O, N, and C were taken from reference 166 and those for H from reference 165 and Mn was corrected for anomalous dispersion (167). The final atomic coordinates and temperature factors are listed in Table 4.2 and the structure factors are listed in Table 4.3.

Table 4.2.

Final Fractional Coordinates and Thermal Parameters.^{a,b}

ATOM	x	y	z	U ^c
Mn	0.0636(2)	0.1447(1)	0.2780(1)	
O11	-0.1395(12)	0.1517(6)	0.1332(7)	
O12	-0.2578(23)	0.1442(9)	-0.0590(9)	
O13	-0.0810(28)	0.0659(11)	0.0346(14)	
N1	-0.1579(19)	0.1272(8)	0.0310(11)	
O21	-0.0835(11)	0.0669(4)	0.3502(7)	
O22	-0.1789(12)	0.1771(5)	0.3653(8)	
O23	-0.3086(13)	0.0847(5)	0.4303(8)	
N2	-0.1962(15)	0.1104(6)	0.3845(8)	
O31	0.2103(13)	0.0392(4)	0.2604(7)	
O32	0.2935(13)	0.1384(5)	0.1969(7)	
O33	0.4286(13)	0.0369(5)	0.1721(7)	
N3	0.3162(14)	0.0698(5)	0.2088(8)	
N4	0.2596(11)	0.1567(4)	0.4410(6)	
N5	0.1080(11)	0.2592(4)	0.2814(7)	
C1	0.3256(15)	0.1002(5)	0.5165(9)	
C2	0.4611(16)	0.1115(7)	0.6287(10)	
C3	0.5302(16)	0.1808(7)	0.6614(10)	
C4	0.4645(15)	0.2393(6)	0.5838(9)	
C5	0.3284(14)	0.2268(5)	0.4738(9)	
C6	0.2376(14)	0.2845(5)	0.3842(8)	
C7	0.2757(16)	0.3588(6)	0.4030(9)	
C8	0.1755(21)	0.4083(6)	0.3141(11)	
C9	0.0477(18)	0.3824(6)	0.2112(11)	
C10	0.0160(16)	0.3070(6)	0.1960(9)	
H1	0.279	0.050	0.492	61
H2	0.507	0.069	0.684	73
H3	0.624	0.188	0.741	73
H4	0.514	0.289	0.608	66
H5	0.371	0.377	0.477	73
H6	0.196	0.461	0.325	67
H7	-0.020	0.417	0.146	73
H8	-0.078	0.288	0.120	67

Table 4.2 (continued)

ATOM	U ₁₁	U ₂₂	U ₃₃	U ₁₂	U ₁₃	U ₂₃
Mn	49(1)	42(1)	44(1)	1(1)	11(1)	1(1)
O11	95(7)	116(8)	52(5)	8(6)	8(4)	-17(5)
O12	231(15)	208(15)	47(6)	70(3)	-14(8)	27(8)
O13	238(20)	198(16)	140(13)	28(15)	-14(12)	-61(12)
N1	107(9)	106(10)	61(8)	42(5)	14(7)	3(7)
O21	67(5)	56(5)	77(5)	-5(4)	28(4)	-11(4)
O22	87(7)	48(5)	112(7)	-2(4)	36(5)	10(5)
O23	81(6)	115(8)	87(6)	-21(6)	50(5)	7(5)
N2	69(7)	60(6)	46(5)	-2(5)	16(5)	1(5)
O31	97(7)	72(5)	85(6)	23(5)	58(5)	-7(5)
O32	118(7)	53(5)	86(6)	16(5)	53(5)	10(5)
O33	94(6)	96(7)	76(6)	37(5)	42(5)	5(5)
N3	63(6)	58(6)	55(6)	12(5)	20(5)	-3(5)
N4	52(5)	37(5)	39(4)	2(4)	18(4)	9(4)
N5	51(5)	46(5)	37(4)	10(4)	13(4)	6(4)
C1	53(6)	43(6)	51(6)	5(5)	16(5)	12(5)
C2	48(7)	77(8)	55(7)	16(6)	20(6)	24(6)
C3	52(7)	90(9)	45(7)	2(7)	15(5)	-2(6)
C4	62(7)	60(7)	40(6)	-1(6)	5(6)	-1(5)
C5	54(6)	41(6)	42(6)	3(5)	22(5)	6(4)
C6	53(6)	42(6)	38(6)	5(5)	20(5)	6(5)
C7	83(8)	46(6)	57(6)	-7(6)	27(6)	-4(6)
C8	118(11)	39(6)	64(8)	5(7)	44(8)	2(6)
C9	77(8)	54(7)	61(8)	13(6)	27(6)	24(6)
C10	69(8)	53(6)	46(6)	2(6)	14(6)	17(5)

a For the expression $\exp(-2\pi^2 (a^2 h^2 U_{11} + b^2 k^2 U_{22} + c^2 l^2 U_{33} + 2a*b*hkU_{12} + 2a*c*hlU_{13} + 2b*c*klU_{23}))$.

b e.s.d.'s in the least significant figures are given in parentheses in this and subsequent tables.

c U_{ij} are in 10³Å²

Table 4.3.

Table of Observed and Calculated Structure

Factors ($20 \times \underline{F}$ absolute) for $\text{Mn}(\text{NO}_3)_3 \cdot \text{bipy}$.

M L OBS CALC

**** K = 0 ****

Table with 4 columns: M, L, OBS, CALC. Contains numerical data for K=0.

**** K = 1 ****

Table with 4 columns: M, L, OBS, CALC. Contains numerical data for K=1.

**** K = 3 ****

Table with 4 columns: M, L, OBS, CALC. Contains numerical data for K=3.

**** K = 5 ****

Table with 4 columns: M, L, OBS, CALC. Contains numerical data for K=5.

**** K = 7 ****

Table with 4 columns: M, L, OBS, CALC. Contains numerical data for K=7.

**** K = 9 ****

Table with 4 columns: M, L, OBS, CALC. Contains numerical data for K=9.

**** K = 11 ****

Table with 4 columns: M, L, OBS, CALC. Contains numerical data for K=11.

**** K = 14 ****

Table with 4 columns: M, L, OBS, CALC. Contains numerical data for K=14.

**** K = 15 ****

Table with 4 columns: M, L, OBS, CALC. Contains numerical data for K=15.

**** K = 12 ****

Table with 4 columns: M, L, OBS, CALC. Contains numerical data for K=12.

**** K = 10 ****

Table with 4 columns: M, L, OBS, CALC. Contains numerical data for K=10.

**** K = 8 ****

Table with 4 columns: M, L, OBS, CALC. Contains numerical data for K=8.

**** K = 6 ****

Table with 4 columns: M, L, OBS, CALC. Contains numerical data for K=6.

**** K = 4 ****

Table with 4 columns: M, L, OBS, CALC. Contains numerical data for K=4.

**** K = 2 ****

Table with 4 columns: M, L, OBS, CALC. Contains numerical data for K=2.

**** K = 13 ****

Table with 4 columns: M, L, OBS, CALC. Contains numerical data for K=13.

**** K = 17 ****

Table with 4 columns: M, L, OBS, CALC. Contains numerical data for K=17.

**** K = 1 ****

Table with 4 columns: M, L, OBS, CALC. Contains numerical data for K=1.

**** K = 0 ****

Table with 4 columns: M, L, OBS, CALC. Contains numerical data for K=0.

Large table on the right side of the page, containing numerical data for various K values.

3 1 245 269	-4 9 -604 -8	-3 6 197 -187	-3 3 163 158	-4 1 365 334	**** k = 9 ****	-5 3 266 273	-2 1 -65 -24
0 2 -67 -54	-5 9 -66 -91	-4 6 -61 41	-4 3 319 293	-1 2 282 260		-6 3 132 139	-3 1 -68 -100
1 2 132 128	-6 9 143 138	-5 6 -67 74	-5 3 -59 -35	-6 1 296 250	-2 1 162 -141	-4 1 106 126	-4 -68 -87
2 2 -63 51	-7 10 311 325	-6 6 229 -226	-6 3 173 112	-7 2 -70 42	-3 1 64 61	-4 2 206 213	-5 1 -69 -97
3 2 -86 2	-8 10 215 240	-7 7 836 -649	-1 4 -51 44	-2 2 232 228	-4 1 181 -167	-3 4 237 -242	-2 2 384 -371
0 3 -67 48	-9 10 -66 166	-2 7 310 -323	-2 4 -53 41	-3 2 -56 -110	-5 1 126 -129	-5 4 189 -206	-2 2 281 -256
1 3 147 -162	-4 10 119 119	-3 7 154 166	-3 4 218 -200	-4 2 -59 114	-6 1 121 -118	-5 4 -87 -65	-3 2 181 -200
2 3 164 -163	-5 10 -67 84	-4 7 109 148	-4 5 288 -275	-5 2 -65 32	-7 2 193 -209	-6 4 -71 -64	-4 3 129 89
0 4 -67 -10	-6 10 152 -150	-5 7 244 260	-5 4 200 -216	-6 2 -70 -57	-8 2 275 -275	-2 5 -63 -47	-1 3 -63 -15
1 5 199 181	-11 11 -71 32	-6 7 -75 136	-6 4 171 -163	-7 2 -71 -56	-3 2 214 -219	-3 5 -63 -27	-2 3 220 208
2 5 201 167	-12 11 -70 64	-7 8 -63 239	-7 4 176 -147	-1 3 -51 -14	-4 2 146 -145	-4 5 232 -231	-3 -66 22
	-13 11 -66 55	-8 9 -67 196	-1 5 255 243	-2 3 454 -479	-5 2 288 -281	-5 5 115 -112	-4 3 -65 -1
	-14 11 217 275	-9 10 337 -177	-2 6 124 145	-3 4 222 -246	-6 3 197 -172	-6 5 111 -133	-5 3 -71 76
	-15 11 -68 -35	-10 11 -68 -35	-3 8 -59 30	-4 3 284 -292	-1 3 102 -86	-1 6 159 -144	-1 4 -66 -25
**** k = 13 ****	-12 12 265 -200	-4 8 -61 18	-4 5 -58 -35	-5 3 151 -176	-2 3 259 271	-2 6 -62 56	-2 4 350 341
0 0 153 -167	-2 12 100 -120	-5 8 -64 -34	-5 5 172 -174	-6 3 -72 -109	-3 3 201 213	-3 6 168 161	-4 4 -67 25
1 0 128 -153	-3 12 155 -150	-6 8 -71 -90	-6 5 -69 -56	-7 3 147 -116	-4 3 298 303	-4 6 -68 36	-5 4 -67 79
2 0 106 -116	-4 12 145 -141	-7 8 -73 86	-7 5 -70 -16	-8 1 98 -79	-5 3 -66 32	-5 6 -67 51	-6 4 -67 79
0 1 141 126		-1 9 481 479	-1 6 143 -155	-2 4 328 346	-6 3 -68 39	-6 6 -72 94	-1 5 -65 22
1 1 -69 41		-2 9 322 342	-2 6 333 -358	-3 4 242 -226	-1 4 187 -182	-2 7 243 -248	-2 5 172 186
2 1 107 115		-3 9 -63 55	-3 6 -59 31	-4 4 205 -194	-2 4 -58 -34	-3 7 205 193	-4 5 126 -131
0 2 262 243		-4 9 191 -194	-4 6 130 130	-5 5 103 112	-3 4 58 -34	-4 7 -64 -31	-5 5 -68 37
1 2 130 149		-5 9 125 -110	-5 6 247 244	-6 4 -64 -29	-4 4 220 224	-5 7 -64 -31	-6 5 -69 -53
2 2 -64 -32		-6 9 -71 -45	-6 6 216 205	-7 4 -74 91	-5 4 262 270	-6 7 -63 15	-1 6 -68 70
0 3 137 -145		-1 10 170 178	-7 6 189 175	-1 5 210 -207	-6 4 162 151	-1 8 275 273	-2 6 136 -143
1 3 118 -106		-2 10 -69 102	-2 7 -59 50	-2 5 135 -139	-5 5 112 -103	-2 1 122 141	-3 4 264 -262
0 4 119 -138		-3 10 -67 66	-3 8 189 187	-3 6 -60 60	-3 5 -60 60	-3 8 -65 3	-4 6 264 -262
		-4 1 167 111	-2 10 -69 102	-2 7 -59 50	-2 5 135 -139	-2 8 -66 29	-1 7 -67 -2
		-5 1 182 154	-3 10 -67 66	-3 8 189 187	-3 7 -62 69	-4 8 -69 -23	-2 7 -69 -42
		-6 1 182 154	-4 10 -68 80	-4 9 189 187	-4 8 -69 23	-5 9 -69 23	-3 7 -69 -100
		-7 1 154 150	-5 10 -67 77	-5 7 -64 80	-5 5 353 364	-4 5 160 -164	-2 4 276 276
**** k = 19 ****		-1 2 1158 1156	-6 10 136 -137	-6 5 -61 19	-1 9 128 109	-2 9 247 217	-4 7 -67 67
1 0 159 164		-2 2 380 360	-1 11 -65 -51	-2 7 -68 -20	-2 7 127 118	-3 9 269 56	-1 8 -72 76
0 0 -65 -84		-3 2 336 315	-2 11 125 -86	-3 8 189 187	-4 10 189 187	-4 9 -69 -17	-2 8 286 293
1 1 -66 8		-4 2 336 315	-3 11 196 -193	-1 8 388 394	-2 6 190 -194	-2 6 102 80	-3 8 170 184
0 2 -68 -25		-5 2 -59 10	-4 11 120 -110	-2 8 279 300	-3 6 133 -130	-2 10 111 -101	-3 8 170 184
		-6 2 123 -101	-5 11 -69 117	-3 8 133 -130	-4 6 -62 89	-1 10 177 -185	
		-7 2 -70 -53	-1 12 -68 40	-4 8 179 -179	-5 6 113 -113	-2 10 170 -184	
		-8 3 1085 -1092	-2 12 -68 40	-5 8 209 -228	-6 6 70 -72	-3 10 172 -67	
		-9 3 887 832	-3 12 173 -165	-6 6 -67 -58	-7 6 -72 -100	-1 7 -63 -3	**** k = 15 ****
		-10 3 887 832	-4 12 110 -101	-7 8 169 -166	-1 7 510 516	-2 7 -64 43	
		-11 3 335 335	-1 9 141 146	-2 7 240 246	-2 7 240 246	-3 7 -64 -20	-1 1 -65 3
		-12 3 -59 7	-2 9 -65 -61	-3 7 181 -199	-4 7 181 -199	-4 7 -66 63	-2 1 -68 -60
		-13 3 162 -153	-4 9 129 120	-5 7 178 -191	-6 7 178 -191	-5 7 118 103	-3 1 277 287
		-14 3 162 -153	-5 9 -44 28	-6 7 194 -204	-1 8 255 -272	-1 8 -61 -42	-2 2 -68 -11
		-15 3 497 -506	-2 1 -44 12	-7 7 163 -176	-2 8 -66 -18	-2 9 152 -166	-3 2 -71 -116
		-16 3 497 -506	-3 1 -52 -38	-8 8 105 90	-3 8 -66 -18	-3 9 152 -166	-4 2 -65 -34
		-17 3 293 304	-4 3 933 -877	-9 8 -64 -21	-4 8 -67 41	-4 10 152 -166	-5 2 -65 -34
		-18 3 293 304	-5 4 600 20	-10 8 -64 -21	-5 8 -67 41	-5 11 152 -166	-6 3 -65 -34
		-19 3 293 304	-6 5 600 20	-11 8 -64 -21	-6 8 -67 41	-6 12 152 -166	-7 4 -65 -34
		-20 3 293 304	-7 6 600 20	-12 8 -64 -21	-7 8 -67 41	-7 13 152 -166	-8 5 -65 -34
		-21 3 293 304	-8 7 600 20	-13 8 -64 -21	-8 8 -67 41	-8 14 152 -166	-9 6 -65 -34
		-22 3 293 304	-9 8 600 20	-14 8 -64 -21	-9 8 -67 41	-9 15 152 -166	-10 7 -65 -34
		-23 3 293 304	-10 9 600 20	-15 8 -64 -21	-10 8 -67 41	-10 16 152 -166	-11 8 -65 -34
		-24 3 293 304	-11 10 600 20	-16 8 -64 -21	-11 8 -67 41	-11 17 152 -166	-12 9 -65 -34
		-25 3 293 304	-12 11 600 20	-17 8 -64 -21	-12 8 -67 41	-12 18 152 -166	-13 10 -65 -34
		-26 3 293 304	-13 12 600 20	-18 8 -64 -21	-13 8 -67 41	-13 19 152 -166	-14 11 -65 -34
		-27 3 293 304	-14 13 600 20	-19 8 -64 -21	-14 8 -67 41	-14 20 152 -166	-15 12 -65 -34
		-28 3 293 304	-15 14 600 20	-20 8 -64 -21	-15 8 -67 41	-15 21 152 -166	-16 13 -65 -34
		-29 3 293 304	-16 15 600 20	-21 8 -64 -21	-16 8 -67 41	-16 22 152 -166	-17 14 -65 -34
		-30 3 293 304	-17 16 600 20	-22 8 -64 -21	-17 8 -67 41	-17 23 152 -166	-18 15 -65 -34
		-31 3 293 304	-18 17 600 20	-23 8 -64 -21	-18 8 -67 41	-18 24 152 -166	-19 16 -65 -34
		-32 3 293 304	-19 18 600 20	-24 8 -64 -21	-19 8 -67 41	-19 25 152 -166	-20 17 -65 -34
		-33 3 293 304	-20 19 600 20	-25 8 -64 -21	-20 8 -67 41	-20 26 152 -166	-21 18 -65 -34
		-34 3 293 304	-21 20 600 20	-26 8 -64 -21	-21 8 -67 41	-21 27 152 -166	-22 19 -65 -34
		-35 3 293 304	-22 21 600 20	-27 8 -64 -21	-22 8 -67 41	-22 28 152 -166	-23 20 -65 -34
		-36 3 293 304	-23 22 600 20	-28 8 -64 -21	-23 8 -67 41	-23 29 152 -166	-24 21 -65 -34
		-37 3 293 304	-24 23 600 20	-29 8 -64 -21	-24 8 -67 41	-24 30 152 -166	-25 22 -65 -34
		-38 3 293 304	-25 24 600 20	-30 8 -64 -21	-25 8 -67 41	-25 31 152 -166	-26 23 -65 -34
		-39 3 293 304	-26 25 600 20	-31 8 -64 -21	-26 8 -67 41	-26 32 152 -166	-27 24 -65 -34
		-40 3 293 304	-27 26 600 20	-32 8 -64 -21	-27 8 -67 41	-27 33 152 -166	-28 25 -65 -34
		-41 3 293 304	-28 27 600 20	-33 8 -64 -21	-28 8 -67 41	-28 34 152 -166	-29 26 -65 -34
		-42 3 293 304	-29 28 600 20	-34 8 -64 -21	-29 8 -67 41	-29 35 152 -166	-30 27 -65 -34
		-43 3 293 304	-30 29 600 20	-35 8 -64 -21	-30 8 -67 41	-30 36 152 -166	-31 28 -65 -34
		-44 3 293 304	-31 30 600 20	-36 8 -64 -21	-31 8 -67 41	-31 37 152 -166	-32 29 -65 -34
		-45 3 293 304	-32 31 600 20	-37 8 -64 -21	-32 8 -67 41	-32 38 152 -166	-33 30 -65 -34
		-46 3 293 304	-33 32 600 20	-38 8 -64 -21	-33 8 -67 41	-33 39 152 -166	-34 31 -65 -34
		-47 3 293 304	-34 33 600 20	-39 8 -64 -21	-34 8 -67 41	-34 40 152 -166	-35 32 -65 -34
		-48 3 293 304	-35 34 600 20	-40 8 -64 -21	-35 8 -67 41	-35 41 152 -166	-36 33 -65 -34
		-49 3 293 304	-36 35 600 20	-41 8 -64 -21	-36 8 -67 41	-36 42 152 -166	-37 34 -65 -34
		-50 3 293 304	-37 36 600 20	-42 8 -64 -21	-37 8 -67 41	-37 43 152 -166	-38 35 -65 -34
		-51 3 293 304	-38 37 600 20	-43 8 -64 -21	-38 8 -67 41	-38 44 152 -166	-39 36 -65 -34
		-52 3 293 304	-39 38 600 20	-44 8 -64 -21	-39 8 -67 41	-39 45 152 -166	-40 37 -65 -34
		-53 3 293 304	-40 39 600 20	-45 8 -64 -21	-40 8 -67 41	-40 46 152 -166	-41 38 -65 -34
		-54 3 293 304	-41 40 600 20	-46 8 -64 -21	-41 8 -67 41	-41 47 152 -166	-42 39 -65 -34
		-55 3 293 304	-42 41 600 20	-47 8 -64 -21	-42 8 -67 41	-42 48 152 -166	-43 40 -65 -34
		-56 3 293 304	-43 42 600 20	-48 8 -64 -21	-43 8 -67 41	-43 49 152 -166	-44 41 -65 -34
		-57 3 293 304	-44 43 600 20	-49 8 -64 -21	-44 8 -67 41	-44 50 152 -166	-45 42 -65 -34
		-58 3 293 304	-45 44 600 20	-50 8 -64 -21	-45 8 -67 41	-45 51 152 -166	-46 43 -65 -34
		-59 3 293 304	-46 45 600 20	-51 8 -64 -21	-46 8 -67 41	-46 52 152 -166	-47 44 -65 -34
		-60 3 293 304	-47 46 600 20	-52 8 -64 -21	-47 8 -67 41	-47 53 152 -166	-48 45 -65 -34
		-61 3 293 304	-48 47 600 20	-53 8 -64 -21	-48 8 -67 41	-48 54 152 -166	-49 46 -65 -34
		-62 3 293 304	-49 48 600 20	-54 8 -64 -21	-49 8 -67 41	-49 55 152 -166	-50 47 -65 -34
		-63 3 293 304	-50 49 600 20	-55 8 -64 -21	-50 8 -67 41	-50 56 152 -166	-51 48 -65 -34
		-64 3 293 304	-51 50 600 20	-56 8 -64 -21	-51 8 -67 41	-51 57 152 -166	-52 49 -65 -34
		-65 3 293 304	-52 51 600 20	-57 8 -64 -21	-52 8 -67 41	-52 58 152 -166	-53 50 -65 -34
		-66 3 293 304	-53 52 600 20	-58 8 -64 -21	-53 8 -67 41	-53 59 152 -166	-54 51 -65 -34
		-67 3 293 304	-54 53 600 20	-59 8 -64 -21	-54 8 -67 41	-54 60 152 -166	-55 52 -65 -34
		-68 3 293 304	-55 54 600 20	-60 8 -64 -21	-55 8 -67 41	-55 61 152 -166	-56 53 -65 -34
		-69 3 293 304	-56 55 600 20	-61 8 -64 -21	-56 8 -67 41	-56 62 152 -166	-57 54 -65 -34
		-70 3 293 304	-57 56 600 20	-62 8 -64 -21	-57		

4.3. Results and Discussion.

4.3.1. $\text{Mn}(\text{NO}_3)_3 \cdot \text{bipy}$ Crystal Data.

$\text{Mn}(\text{NO}_3)_3 \cdot \text{bipy}$, $M = 397.15$, Monoclinic, $P2_1/c$,
 $a = 7.311(3)$, $b = 18.022(7)$, $c = 11.704(4)\text{\AA}$, $\beta = 108.73(3)^\circ$,
 $V = 1461\text{\AA}^3$, $\rho_o = 1.82(5) \text{ g. cm}^{-3}$ (flotation), $\rho_c = 1.81 \text{ g. cm}^{-3}$,
 $z = 4$, $\mu = 10.6 \text{ cm}^{-1}$, $\text{Mo-K}\alpha_1 = 0.70926\text{\AA}$, $T = 20^\circ\text{C}$.

4.3.2. Description of the Structure.

The interatomic distances and angles are listed in Table 4.4, along with the estimated standard deviations. Mean planes through appropriate groups of atoms are presented in Table 4.5.

$\text{Mn}(\text{NO}_3)_3 \cdot \text{bipy}$ is a molecular monomeric seven coordinate complex. The molecular configuration (Figure 4.1) is that of an irregular pentagonal bipyramid. The equatorial "plane" consists of N(5) of the bipyridyl group and the four oxygen atoms O(21), O(22), O(31), and O(32) of two bidentate nitrate groups. The apical atoms are N(4) of the bipyridyl group and O(11), the coordinated atom of a unidentate nitrate group. The manganese is displaced out of the plane by 0.13\AA towards O(11). The pentagon is slightly distorted as would be anticipated in view of the shorter distances between the coordinating oxygens within

Table 4.4.

Interatomic Distances (Å) and Angles (Deg)

(a) Interatomic Bonded Contracts

Mn	-0(11)	1.864(8)	1.896(8) ^a	N(4)-C(1)	1.333(11)
	-0(21)	2.102(8)	2.112(8)	-C(5)	1.368(12)
	-0(22)	2.386(9)	2.400(9)	N(5)-C(6)	1.350(11)
	-0(31)	2.225(8)	2.237(8)	-C(10)	1.327(12)
	-0(32)	2.183(8)	2.201(8)	C(1)-C(2)	1.383(15)
	-N(4)	1.997(7)	1.993(7)	C(2)-C(3)	1.355(15)
	-N(5)	2.088(8)	2.086(8)	C(3)-C(4)	1.374(15)
N(1)	-0(11)	1.241(13)		C(4)-C(5)	1.370(13)
	-0(12)	1.115(14)	1.233(17)	C(5)-C(6)	1.474(12)
	-0(13)	1.234(18)	1.332(18)	C(6)-C(7)	1.371(14)
N(2)	-0(21)	1.291(12)		C(7)-C(8)	1.387(15)
	-0(22)	1.237(11)		C(8)-C(9)	1.349(16)
	-0(23)	1.209(11)		C(9)-C(10)	1.379(15)
N(3)	-0(31)	1.253(11)			
	-0(32)	1.248(11)			
	-0(33)	1.200(11)			

Table 4.4 (continued)

(b) Interatomic Angles (Deg)

O(11)-Mn-O(21)	92.8(4)	C(1)-N(4)-C(5)	119.8(8)
-O(22)	83.6(4)	Mn -N(4)-C(1)	123. (7)
-O(31)	103.9(4)	Mn -N(4)-C(5)	117.1(6)
-O(32)	96.2(4)	Mn -N(5)-C(6)	114.2(6)
-N(4)	168.3(4)	Mn -N(5)-C(10)	126.1(7)
-N(5)	91.4(4)	C(6)-N(5)-C(10)	119.6(8)
O(21)-Mn-O(22)	56.3(3)	Mn -O(11)-N(1)	131.3(8)
-O(31)	78.0(3)	Mn -O(21)-N(2)	100.4(6)
-N(4)	89.5(3)	Mn -O(22)-N(2)	88.4(7)
O(22)-Mn-N(4)	88.2(3)	Mn -O(31)-N(3)	93.4(6)
-N(5)	83.2(3)	Mn -O(32)-N(3)	95.5(6)
O(31)-Mn-O(32)	56.9(3)	N(4)-C(1)-C(2)	120.9(10)
-N(4)	87.8(3)	C(1)-C(2)-C(3)	119.5(9)
O(32)-Mn-N(4)	90.2(3)	C(2)-C(3)-C(4)	120.1(10)
-N(5)	85.6(3)	C(3)-C(4)-C(5)	119.3(10)
N(4) -Mn-N(5)	79.3(3)	C(4)-C(5)-C(6)	125.3(9)
O(11)-N(1)-O(12)	130.3(14)	C(5)-C(6)-C(7)	123.6(9)
-O(13)	112.2(14)	C(6)-C(7)-C(8)	118.5(10)
O(12)-N(1)-O(13)	115.6(15)	C(7)-C(8)-C(9)	119.6(10)
O(21)-N(2)-O(22)	114.9(10)	C(8)-C(9)-C(10)	119.7(10)
-O(23)	119.9(10)	C(9)-C(10)-N(5)	121.2(10)
O(22)-N(2)-O(23)	125.2(11)		
O(31)-N(3)-O(32)	114.2(9)		
-O(33)	123.7(10)		
O(32)-N(3)-O(33)	122.1(10)		

Table 4.4 (continued)

(c) Selected Intramolecular Nonbonded Contacts

Mn-0(13)	3.05(1)	0(21)-0(22)	2.13(2)
-N(1)	2.84(1)	-0(23)	2.16(2)
-N(2)	2.66(1)	-0(31)	2.71(3)
-N(3)	2.62(1)	-N(4)	2.89(3)
0(11)-0(12)	2.14(3)	-C(1)	3.06(4)
-0(13)	2.06(3)	0(22)-0(23)	2.17(2)
-0(21)	2.88(3)	-N(4)	3.06(3)
-0(22)	2.86(3)	-N(5)	2.98(3)
-0(31)	3.23(4)	0(31)-0(32)	2.09(2)
-0(32)	3.02(3)	-0(33)	2.16(2)
-N(5)	2.83(3)	-N(4)	2.93(3)
-C(10)	3.02(3)	0(32)-0(33)	2.14(2)
0(12)-0(13)	1.99(2)	-N(4)	2.96(3)
0(13)-0(31)	2.85(3)	-N(5)	2.90(3)
-0(32)	3.08(3)	N(4)-N(5)	2.61(3)
		C(4)-C(7)	3.03(4)

(d) Intermolecular Contacts Shorter than 3.5^oÅ

0(11)-C(4)	3.39(4)(2) ^b	0(23)-C(1)	3.40(3)(4) ^b
0(12)-0(22)	3.44(4)(2)	0(31)-C(9)	3.47(3)(3)
-C(7)	3.30(3)(2)	0(32)-C(4)	3.04(3)(2)
0(13)-0(13)	2.88(5)(4)	-C(7)	3.40(3)(2)
-0(33)	3.43(5)(4)	0(33)-C(2)	3.47(3)(4)
0(21)-C(8)	3.39(3)(3)	C(2)-C(8)	3.48(3)(2)
-C(9)	3.43(3)(3)	-C(9)	3.46(3)(2)
		C(3)-C(10)	3.45(3)(2)

a After correction for thermal motion.

b Figures in this column refer to the following symmetry transformations with respect to atoms in column two:

(1) x,y,z; (2) x, $\frac{1}{2}$ -y, $\frac{1}{2}$ +z; (3) 1-x, $\frac{1}{2}$ +y, $\frac{1}{2}$ -z;

(4) 1-x, 1-y, 1-z.

Mean Planes as $Ax + By + Cz + D = 0^c$

Plane	Atoms in the Plane with their deviations(Å)	A	B	C	D	χ^2	Dist. of Mn from Plane (Å)
1.	N(1) 0(11) 0(12) 0(13) (0.069)(-0.010)(-0.029)(-0.035)	0.8544	0.5132	-0.0819	0.006	25.9 ^a	0.596
2.	N(2) 0(21) 0(22) 0(23) (-0.007)(0.001)(0.002)(0.002)	-0.4249	-0.0923	-0.9015	2.778	0.64	0.032
3.	N(3) 0(31) 0(32) 0(33) (-0.003)(0.001)(0.001)(0.001)	-0.4507	-0.1313	-0.8830	2.892	0.13	0.090
4.	N(4) C(1) C(2) C(3) (-0.002)(0.007)(-0.006)(-0.003)	0.9030	-0.1581	-0.3975	2.171	1.09	0.010
5.	C(4) C(5) (0.007)(-0.003) N(5) C(6) C(7) C(8) (-0.004)(-0.001)(0.010)(-0.10)	0.9060	-0.0709	-0.4172	1.872	1.89	0.124
6.	C(9) C(10) (-0.001)(0.009) N(5) 0(21) 0(22) 0(31) (-0.092)(-0.008)(0.082)(-0.094)	-0.4057	-0.0288	-0.9135	2.788	580 ^a	0.133
7.	0(32) (0.149) N(5) 0(21) 0(22) 0(31) ^b (-0.012)(-0.027)(0.031)(0.018)	-0.3605	-0.0261	-0.9324	2.932	28.7 ^a	0.194

a As noted in the text, these atoms are not coplanar.

b 0(32) is 0.317 Å out of the plane.

c Where the coordinates are orthogonalized, i.e., $a = a$, $b = b$ and c is normal to the ab plane.

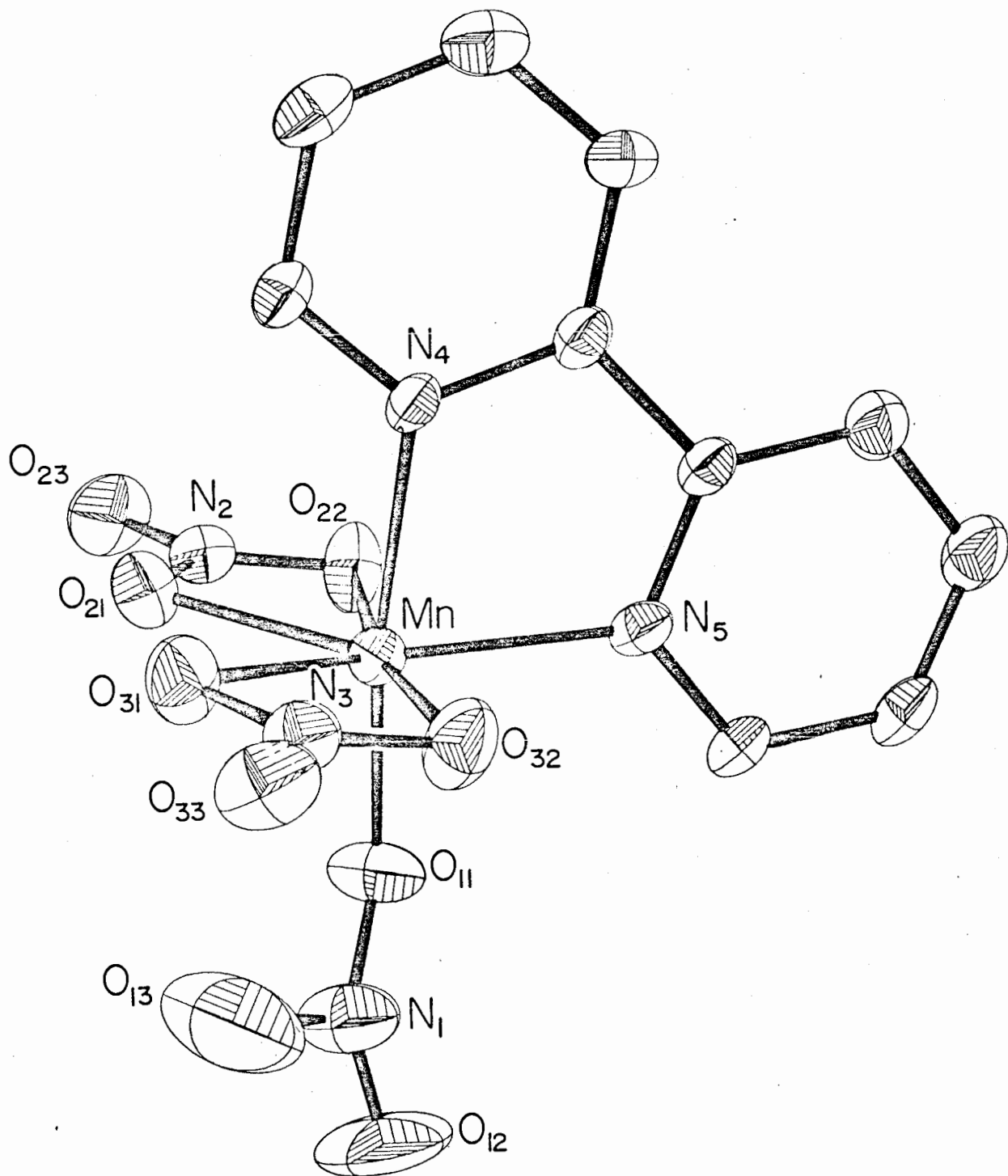


Figure 4.1 The molecular configuration of $\text{Mn}(\text{NO}_3)_3 \cdot \text{bipy}$.

each bidentate nitrate group compared to the non-bonded contacts between nitrate and bipyridyl groups; thus O(21)-O(22) and O(31)-O(32) are 2.13(2) and 2.09(2)Å whereas O(21)···O(31) = 2.71(3)Å and O(22)···N(5) and O(32)···N(5) are 2.98(3) and 2.90(3)Å respectively. As can be seen from Table 4.5, plane 7, the main distortion in the equatorial "plane" is a large out-of-plane displacement of atom O(32) towards O(11), the four remaining atoms N(5), O(21) and O(32) being almost coplanar.

Each of the two bidentate nitrate groups and the two heterocyclic rings of the bipyridyl group are planar (Table 4.5), with a dihedral angle of 5.1° between the pyridine rings. The unidentate nitrate group shows the largest departure from statistical planarity ($\chi^2 = 25.9$), but as the unidentate nitrate shows no unusual chemical or spectral properties (see chapter 3) the non-planarity may be due to the inadequacies of the model used. The molecular packing is shown in Figure 4.2.

4.3.3. Discussion of the Structure.

The observed seven coordinate environment of manganese(III) was rather unexpected. Whilst seven coordinate compounds of 3d metals are known, they do not occur commonly (168), and this is the first established instance of this geometry occurring for Mn(III). Also

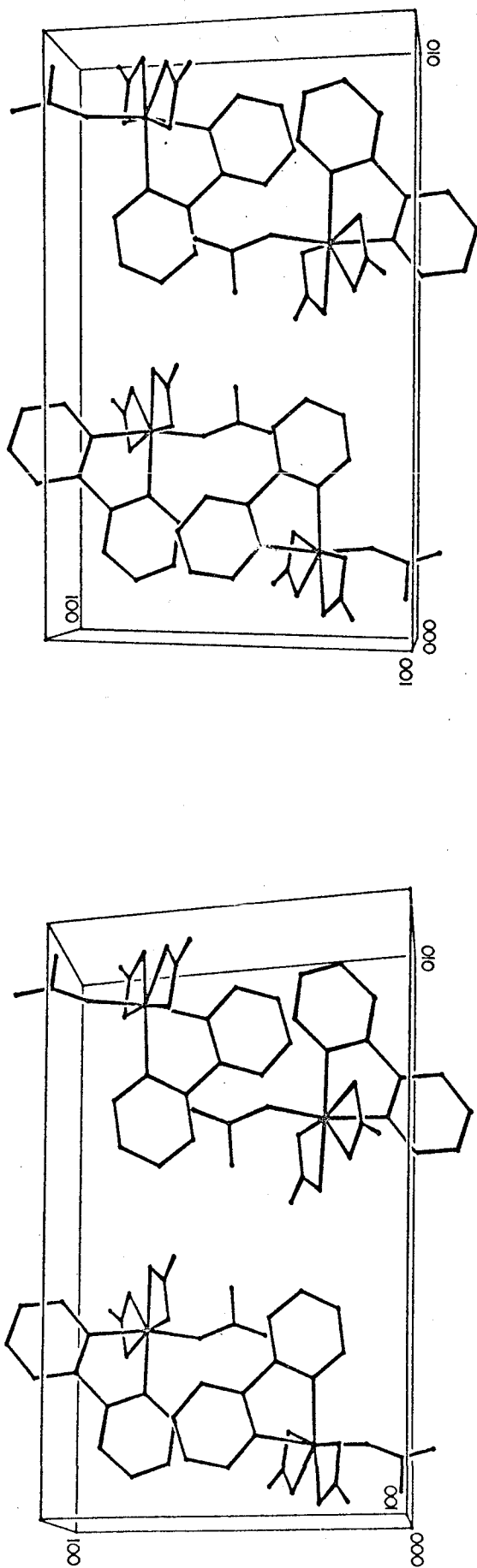


Figure 4.2. A stereoscopic view showing the molecular packing.

intriguing is the observation that the two bidentate nitrate groups are quite dissimilar, one being symmetrically, the other unsymmetrically bonded to manganese. Thus the structure contains three dissimilarly coordinated nitrate groups, the first time this has been reported.

An explanation for this structure probably lies in the different stereochemical requirements of nitrate and bipyridyl ligands, and for comparison we can view the complex as formally derived from $\text{Mn}(\text{NO}_3)_4^-$ by replacement of NO_3^- by bipyridyl with subsequent shifts in nitrate coordination. By comparison with $\text{Mn}(\text{NO}_3)_4^{2-}$ (53) and $\text{Fe}(\text{NO}_3)_4^-$ (11) we may assume the $\text{Mn}(\text{NO}_3)_4^-$ ion to be eight coordinate involving four bidentate nitrate groups, each subtending an angle of about 60° at the manganese. Replacement of a nitrate group by bipyridyl which subtends a larger interbond angle of $\approx 80^\circ$ at manganese presumably introduces steric crowding which is relieved by one nitrate group having to adopt the unidentate configuration. It is more difficult to judge whether the coordination difference between the two remaining bidentate nitrate groups is also merely a consequence of crowding or whether it originates, at least partially, in the electronic configuration of the manganese atom, which is non-spherically symmetrical high spin d^4 . Unlike the more "regular" tetranitrato

complexes for which the possibility of electronically induced distortions have been discussed (73), the inequivalence of the residual ligands in this complex (i.e., bipyridyl and the unidentate nitrate) may well be the main reason for the apparent differences in the bidentate nitrates. It may be noted, however, (a) that the long Mn-O(22) bond is not trans to a bipyridyl nitrogen, and (b) that of the five equatorial atoms, O(32) is displaced the greatest distance (0.15Å) from the mean plane, whereas the weaker coordinated O(22) is only 0.08Å out of the plane. It may well be that both nitrates are potentially symmetric but that O(22) cannot relieve crowding by a large out-of-plane displacement and has to do so by additional lengthening of the Mn-O(22) bond. This is consistent with the non-bonded contacts from O(22) and O(32) to the apical atoms O(11) and N(4) shown in Table 4.4(c). The distances and angles to N(4) are similar but O(11) is angled towards O(22) and is closer to it than to O(32). The effect of a dissimilar ligand in seven coordinate complexes is well illustrated in $\text{CH}_3\text{Sn}(\text{NO}_3)_3$ where all the nitrates are unsymmetrically bidentate (87), a dramatic change from four symmetric bidentate nitrates in the structure of $\text{Sn}(\text{NO}_3)_4$ (37). By contrast, the bidentate nitrate groups in the seven coordinate molecule

$\text{VO}(\text{NO}_3)_3\text{CH}_3\text{CN}$ (74) are symmetric, despite the dissimilar nature of the remaining ligands.

An alternative view of the manganese coordination arises if the bidentate nitrates are considered to occupy only one coordination site (45, 55, 169 - 171). On this basis the coordination would be trigonal bipyramidal. The angles in the equatorial plane would then be approximately $\text{N}(5)\text{MnN}(3) = 114^\circ$, $\text{N}(5)\text{MnN}(2) = 111^\circ$ and $\text{N}(2)\text{MnN}(3) = 134^\circ$, which indicate greater repulsion in the equatorial plane between the two nitrate ligands than between the nitrates and the bipyridyl ligand. With this model, however, it is much more difficult to usefully discuss the differences in the bidentate nitrate coordination since a three centre bond must be postulated to each bidentate nitrate.

The compound $\text{VO}(\text{NO}_3)_3\text{CH}_3\text{CN}$ (74) offers the only other example in which the dimensions of bidentate and unidentate nitrate groups may be compared within the same molecule, and similarities with the present structure are evident. The unidentate nitrate groups are coordinated with almost identical metal oxygen bond lengths which are significantly shorter than those to the bidentate nitrate groups.

The dimensions within the unidentate and bidentate

nitrate groups are according to expectations (section 1.3.1). The unidentate group is the least well defined feature of the structure, due to its rather large thermal motion, but the long manganese-oxygen contact to the nearest uncoordinated oxygen atom O(13), 3.05(1)Å, shows that there is no question as to the unidentate character of this nitrate group. The apparently large departure from planarity probably reflects positional inaccuracies of the uncoordinated oxygen atoms arising from both high correlation between parameters and large thermal motion.

There have been only a relatively few accurate structural determinations of compounds containing unidentate nitrates; the bond lengths of these are presented in Table 4.6.

In Table 4.6, it is obvious that all the N(1)-O(11) bond lengths are longer than N(1)-O(12) or N(1)-O(13) except for Cu(PPh₂Me)(NO₃) (77). Carty postulated that charge delocalization must occur throughout the nitrate ligand due to the low oxidation state of the metal and the strong σ donor ability of the other ligands. It would be necessary to know the size and direction of the anisotropic thermal parameters and whether the thermal motion has been corrected for in the bond lengths before

Table 4.6.

Interatomic Distances in Unidentate Nitrates.

<u>Compound</u>	<u>N(1)-O(11)^a</u>	<u>N(1)-O(12)</u>	<u>N(1)-O(13)</u>	<u>Ref.</u>
VO(NO ₃) ₃ ·CH ₃ CN	1.45(3)	1.19(3)	1.24(3)	74
Mn(NO ₃) ₃ ·bipy	1.241(13) ^b	1.115(14)	1.234(18)	
Ni(py) ₂ (NO ₃) ₂ (H ₂ O) ₂	1.267(3)	1.232(4)	1.258(3)	76
Ni(NO ₃) ₂ (H ₂ O) ₄ ^I	1.293(12)	1.213(12)	1.244(12)	8
II	1.304(12)	1.236(12)	1.264(12)	
[Co(tn) ₂ (NO ₃) ₂] ₂ NO ₃	1.336(12)	1.190(14)	1.223(13)	75
Cu(picam)(NO ₃) ₂	1.275(14)	1.195(17)	1.231(14)	79
Cu(pyNO) ₂ (NO ₃) ₂ ^I	1.316(9)	1.222(9)	1.227(10)	172
II	1.304(8)	1.221(8)	1.234(9)	
Cu(dach) ₂ (NO ₃) ₂ · $\frac{1}{2}$ H ₂ O	1.258(11)	1.214(13)	1.222(13)	173
Cu(PPh ₂ Me) ₃ NO ₃	1.166(8)	1.209(8)	1.247(8)	77
Ag(bipy)(NO ₃) ₂ ^I	1.325(22)	1.192(23)	1.200(22)	80
II	1.336(21)	1.221(21)	1.238(21)	
K[Au(NO ₃) ₄] ^I	1.34(2)	1.14(3)	1.24(3)	63
II	1.39(3)	1.20(2)	1.22(3)	
Sn(CH ₃) ₃ (NO ₃)H ₂ O	1.33(2)	1.18(2)	1.26(2)	81

a O(11) is the coordinated oxygen.

b Bond lengths are not corrected for thermal motion.

any sound argument could be based on the structure of $\text{Cu}(\text{PPh}_2\text{Me})_3(\text{NO}_3)$.

The molecular packing illustrated in Figure 4.2 is somewhat unexpected. The shortest intermolecular contact is $\text{O}(13)\cdots\text{O}(13) = 2.88(5)\text{\AA}$ (see Table 4.4), equal to the sum of the covalent radii. This is contrary to the anticipated "head - to - tail" packing to be expected if molecular dipolar forces dominate, and indicates that the polarity of the molecule is not the major packing force. Van der Waal's attraction is thus likely to be the determining factor.

Chapter 5.

Tetranitratomanganates.

5.1. Introduction.

Since the recent reviews of nitrate complexes and structures (5, 73), the tetranitrato anions of gallium, thallium and aluminum have been reported (19, 34, 13, 14) and the structure of $[\text{Ph}_4\text{As}][\text{Fe}(\text{NO}_3)_4]$ has been determined (11). Until the present work, tetranitrato complexes were known for each metal in one oxidation state only. Thus $\text{M}(\text{NO}_3)_4^{2-}$ was formed by manganese, cobalt, nickel and copper; $\text{M}(\text{NO}_3)_4^-$ was formed by iron, aluminum, gallium and thallium; and the neutral species $\text{M}(\text{NO}_3)_4$, was formed by titanium and tin.

Previously, tetranitratomanganate(II) had been reported with large bulky cations such as $(\text{AsPh}_4)^+$ and $(\text{AsPh}_3\text{Me})^+$ (52, 53), but not with alkali metal cations. The only other transition metal tetranitrato anions that have been widely studied are those with iron and cobalt which had been prepared with a wide range of cations such as $(\text{R}_4\text{N})^+$, $(\text{AsPh}_3\text{Me})^+$, Cs^+ , Na^+ and K^+ (11, 52, 110). Furthermore, manganese and cobalt are the only metals to form both neutral di- and trinitrates. Attempts at

preparing tetranitratocobaltate(III) species always resulted in reduction of cobalt and formation of tetranitratocobalt(II) (110). The work presented in this chapter describes the preparation of alkali metal tetranitratomanganates(II) and nitronium and cesium tetranitratomanganates(III).

5.2. Tetranitratomanganates(II).

5.2.1. Potassium Tetranitratomanganate(II).

When the reaction of potassium permanganate and dinitrogen tetroxide in nitromethane or acetonitrile was carried out as described in section 2.2.6, potassium tetranitratomanganate(II) was obtained as a yellow crystalline product in 95 - 100% yield, based on potassium. [Found: K, 20.0; Mn, 14.9; N, 14.5%. Calculated for $K_2Mn(NO_3)_4$: K, 20.5; Mn, 14.4; N, 14.7%]. Carbon and hydrogen analysis and i.r. spectroscopy confirmed the absence of solvent in the precipitate. The oxidation state was confirmed by magnetic susceptibility measurements and the inability of the product to oxidize iodide.

5.2.2. Sodium Tetranitratomanganate(II).

A similar reaction using $NaMnO_4$ gave a pale

yellow precipitate of $\text{Na}_2\text{Mn}(\text{NO}_3)_4$, [Found: Na, 13.1; Mn, 15.9%. Calculated for $\text{Na}_2\text{Mn}(\text{NO}_3)_4$: Na, 13.2; Mn, 15.7%].

5.2.3. Discussion.

Both the above compounds have a magnetic susceptibility of $\chi_M^{\text{corr}} = 15,400 \times 10^{-6}$ c.g.s.u; $\mu_{\text{eff}} = 6.0 \pm 0.1$ B.M., as is expected for high spin d^5 species. The structure of $[\text{Ph}_4\text{As}]_2[\text{Mn}(\text{NO}_3)_4]$ has been determined (53) and shows that the anion exhibits approximately D_{2d} symmetry, with all the nitrates coordinating as bidentate ligands. The infrared and Raman spectra of the sodium and potassium salts are presented in Table 5.1, along with that obtained by Straub et. al. (52) for $[\text{Ph}_3\text{CH}_3\text{As}]_2[\text{Mn}(\text{NO}_3)_4]$. The assignments given in the table refer to the C_{2v} local symmetry of the bidentate nitrate groups; splitting of the main regions of absorption observed in some cases may be due to coupling of nitrate vibrations under the full molecular symmetry (18, 36) or to crystal site-symmetry splitting. The infrared spectra are shown in figures 5.1 and 5.2 to illustrate the similarity in band positions and the splitting of the 1040 and 810 cm^{-1} bands that occurs in the sodium salt. The symmetric stretching frequency is split into at least two bands, and the

Table 5.1.

Infrared and Raman Spectra of $\text{Na}_2\text{Mn}(\text{NO}_3)_4$ and $\text{K}_2\text{Mn}(\text{NO}_3)_3$ (cm^{-1}).

Assignment ^a	$\text{Na}_2\text{Mn}(\text{NO}_3)_4$		$\text{K}_2\text{Mn}(\text{NO}_3)_4$		$[\text{Mn}(\text{NO}_3)_4^{2-}]^b$
	Ir.	Raman	Ir.	Raman	
	2270 w		2270 w		
$\nu_1: A_1[\nu(\text{NO}^*)]$	1490 s	1505 w	1480 s, br	1485 s	1463
$\nu_4: B_1[\nu_{\text{AS}}(\text{NO}_2)]$	1280 s, br	1335 w 1290 w	1290 s, br	1290 s 1225 w	1283
$\nu_2: A_1[\nu_{\text{S}}(\text{NO}_2)]$	1041 sh 1036 sp	1052 vs 1043 m, sh	1048 sp 1044 sp	1046 vs	1028
$\nu_6: B_2[\pi(\text{NO}_2^*)]$	820 m 812 m 807 m		831 m 813 sp		813
$\nu_3: A_1[\delta_{\text{S}}\text{MnO}_2\text{N},$ ring def]	765 sh 750 s, sp	744 m	755 m 748 sh	750 m	
$\nu_5: B_1[\delta\text{ONO}^*]$		719 m	710 w	708 m	

a Assuming local C_{2v} symmetry of individual bidentate NO_3 groups.

b Taken from reference (52).

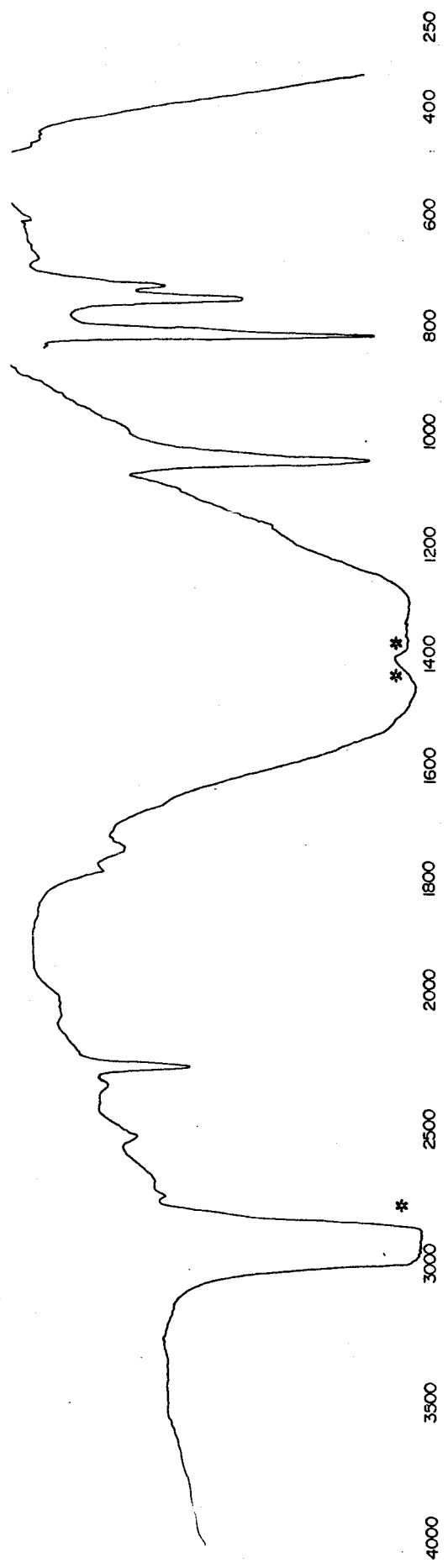


Figure 5.1. Infrared spectrum of $K_2Mn(NO_3)_4$
* Nujol Bands.

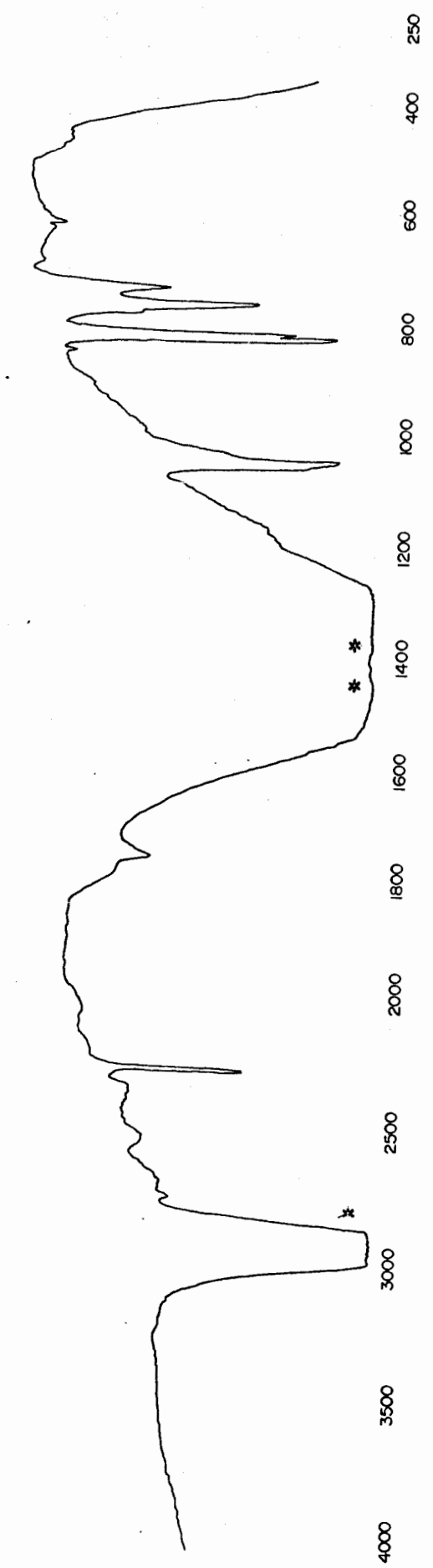


Figure 5.2. Infrared spectrum of $\text{Na}_2\text{Mn}(\text{NO}_3)_4$
* Nujol Bands.

810 cm^{-1} region has three bands. R.J. Fereday observed a similar change in the spectra of potassium and sodium tetranitratocobaltate(II) (110) and this may be attributed to a change in crystal structure on going to the smaller cation. The compounds are soluble in water but are either insoluble or decompose with precipitation of the alkali metal nitrate in most solvents studied. Thus, where solution does occur, partial dissociation of the complex anion to give solvated $\text{Mn}(\text{NO}_3)_2$ and NO_3^- takes place, as observed by Fereday (150) for alkali metal nitrate cobaltates(II).

5.3. Tetranitratomanganates(III).

5.3.1. Nitronium Tetranitratomanganate(III).

When a reaction of manganese(III) trifluoride and excess dinitrogen pentoxide was carried out as described in section 2.2.1 and the filtrate was cooled in liquid nitrogen, evacuated and the nitrogen bath removed so that the volatiles sublimed in vacuo, a residue of the brown hygroscopic nitronium salt $[\text{NO}_2]^+[\text{Mn}(\text{NO}_3)_4]^-$ remained. [Found: Mn, 15.8; N, 20.2%. Calculated for $[\text{NO}_2]^+[\text{Mn}(\text{NO}_3)_4]^-$: Mn, 15.7; N, 20.1%.] Hydrolysis, followed by ceric sulphate titration indicated the absence of nitrite, precluding

formulation as an N_2O_4 adduct or nitrosonium salt. Storage of this salt at room temperature for one week showed no observable evolution of nitrogen oxides.

The oxidation state of the metal was confirmed by the consumption of one equivalent of KI on titration in aqueous solution, and by the formation of a characteristic red solution ($\nu_{\max} \approx 19.7 \text{ kcm}^{-1}$) in 6M H_2SO_4 .

5.3.2. Cesium Tetranitratomanganate(III).

A large excess of dinitrogen pentoxide (20 g., 0.185 moles) was condensed onto a mixture of anhydrous manganese(III) trifluoride (0.75 g.; 6.7 mmoles) and cesium chloride (1.13 g.; 6.7 mmoles). The solids were mixed and warmed to room temperature, whereupon a reaction took place yielding a brown oil which was filtered from unreacted starting materials by warming the flask and filter to melt all the dinitrogen pentoxide. Removal of the volatiles in vacuo gave dark brown $Cs[Mn(NO_3)_4]$. [Found: Mn, 12.3%; $CsMn(NO_3)_4$ requires Mn, 12.6%].

5.3.3. Reaction of Cs_2MnCl_5 and N_2O_5 .

This reaction was undertaken to determine if a pentanitratomanganate(III) anion, which would be analogous

to $\text{Al}(\text{NO}_3)_5^{2-}$ (14) could be prepared. Excess dinitrogen pentoxide (12 gm.; 0.111 moles) was condensed onto anhydrous Cs_2MnCl_5 (0.20 gm., 0.402 mmoles), which had been prepared by reduction of CsMnO_4 by MnCl_2 in 5 M HCl in the presence of CsCl. The solids were mixed and warmed to liquify the dinitrogen pentoxide, whereupon a reaction took place to give a brown oil. The volatiles were removed in vacuo yielding a mixture of brown and white solids. The infrared spectrum (Table 5.2), and the X-ray powder pattern (Table 5.3) indicated the presence of CsNO_3 and $\text{CsMn}(\text{NO}_3)_4$.

5.3.4. Discussion.

The structure of the compound obtained by reaction between N_2O_5 and MnF_3 and subsequent removal of the volatile materials by sublimation is $[\text{NO}_2]^+[\text{Mn}(\text{NO}_3)_4]^-$. This formulation, rather than as a nitrosonium salt, N_2O_4 adduct, or N_2O_5 adduct, is based on the analyses and the following observations: (a) bands occur in the i.r. spectrum at 2380 and 2358 cm^{-1} [$\nu_3(\text{NO}_2^+)$] and 560 cm^{-1} [$\nu_2(\text{NO}_2^+)$] (Figure 5.3); (b) no bands attributable to N_2O_4 , N_2O_5 , NO^+ , or ionic nitrate were observed, and (c) the remaining i.r. bands are characteristic of coordinated nitrates (Table 5.2) and are generally similar to those of $\text{CsMn}(\text{NO}_3)_4$. The only difference in the infrared spectra of these two

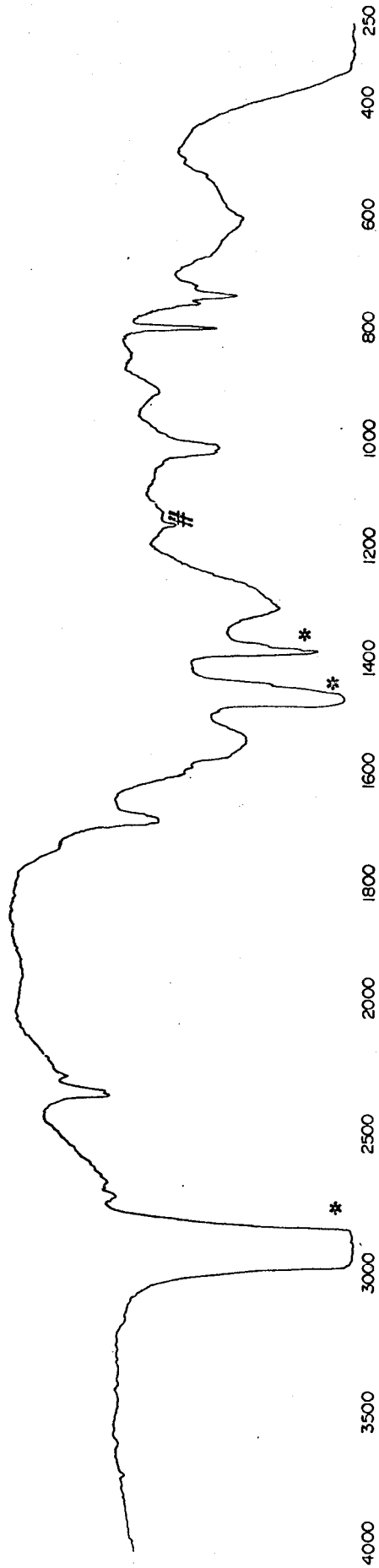


Figure 5.3. Infrared spectrum of $[\text{NO}_2^+][\text{Mn}(\text{NO}_3)_4^-]$

* Nujol Bands.

Bands due to AgCl plates.

Table 5.2. Infrared Spectra of the Tetranitratomanganate(III) Anions.

Assignment	$\text{NO}_2^+[\text{Mn}(\text{NO}_3)_4]^-$	$\text{Cs}^+[\text{Mn}(\text{NO}_3)_4]^-$	$\text{Cs}^+[\text{Mn}(\text{NO}_3)_4]^- + \text{CsNO}_3$
$\nu_3: [\text{NO}_2^+]$	2380 m 2356 m		
$\nu_1: \text{A}_1[\nu(\text{NO}^*)]$	1565 sh 1532 s, br	1550 s 1520 s, br 1480 s, br	1550 s, br 1529 s, br 1480 s, br
$\nu_3: \text{E}^*[\text{NO}_3^-]$			1350 - 1380 s, br
$\nu_4: \text{B}_1[\nu_{\text{AS}}(\text{NO}_2)]$	1298 s, br 1270 sh	1305 s 1280 s	1270 s, br
$\nu_2: \text{A}_1[\nu_{\text{S}}(\text{NO}_2)]$	1020 s 1010 s	955 s	960 s, br
$\nu_2: \text{A}_2[\text{NO}_3^-]$	912 w		837 m, sp
$\nu_6: \text{B}_2[\pi\text{O}_2\text{NO}^*]$	797 m, sp	795 m, sp	794 m, sp
$+\nu_3: \text{A}_1[\text{ring def.}]$	755 m	759 m	760 m
$+\nu_5: \text{B}_1[\delta\text{ONO}^*]$	740 m	732 m	725 sh
$\nu_2[\text{NO}_2^+]$	560 br		
$[\nu \text{ Mn-O}]$		415 m	428 sh 410 m

Table 5.3.

X-Ray Powder Photographs of Tetranitratomanganate(III) Anions.

<u>NO₂⁺[Mn(NO₃)₄⁻]</u>	<u>Cs⁺[Mn(NO₃)₄⁻]</u>	<u>Cs⁺[Mn(NO₃)₄⁻] + CsNO₃</u>	<u>CsNO₃</u>
7.30 w			
6.60 s			
5.82 s	5.72m	5.74 w	
4.79 m	4.87 m	4.85 s	
4.68 w			
4.34 s	4.49 s	4.44 s	4.46 m
4.01 w	4.10 m	4.09 m	
3.62 s	3.85 w	3.81 w	
3.37 m	3.49 s	3.48 m	
3.16 w	3.19 s	3.14 s	3.15 vs
2.86 w	2.90 vw	3.00 vw	3.00 vw
2.74 w	2.79 w	2.73 w	
2.62 m	2.64 w	2.57 w	2.58 w
2.38 vw		2.49 vw	2.48 vw
2.31 w	2.26 w	2.40 w	
2.17 w		2.23 m	2.23 m
2.10 w	2.10 w		
2.05 w			
1.96 w		1.99 m	2.00 m
1.78 w		1.82 w	1.83 w
		1.59 vw	1.58 vw
		1.49 w	1.49 w
		1.41 vw	1.41 vw

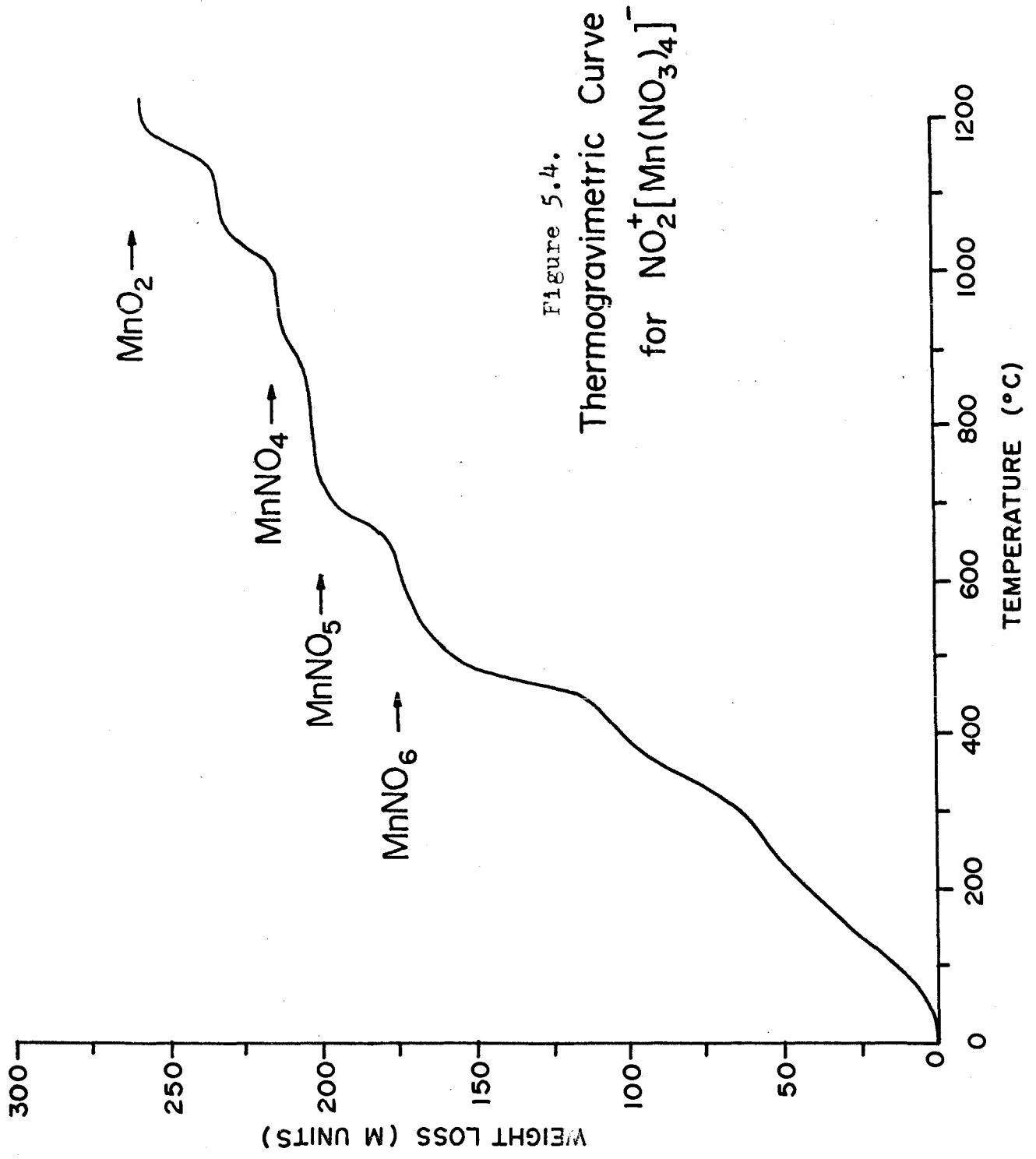
compounds is the position of the $\nu_2(A_1)$ stretching frequency. In the cesium salt it is quite low, at 940 cm^{-1} , whereas in the nitronium salt it is at 1010 cm^{-1} . The mode occurs at 1005 cm^{-1} in $\text{CsFe}(\text{NO}_3)_4$ (174); this is 36 cm^{-1} below that of $\text{Fe}(\text{NO}_3)_3$ (1041 cm^{-1}). The shift is 37 cm^{-1} from $\text{Mn}(\text{NO}_3)_3$ (977 cm^{-1}) to $\text{Cs}^+[\text{Mn}(\text{NO}_3)_4]$. The X-ray powder photographs of these species indicate that they are not isomorphous.

Tetranitrato anions are known for a wide range of metals (5, 11, 19, 34, 52, 53) but this is the first instance where the tetranitrato anion exists for two oxidation states of the same metal (52, 53). The manganese(II) analogue $[\text{Mn}(\text{NO}_3)_4]^{2-}$ (53) and the neighboring iron(III) complex ion $[\text{Fe}(\text{NO}_3)_4]^-$ (11) have both been shown by X-ray crystallography to be eight coordinate D_{2d} complexes containing four bidentate nitrate groups. The structure of $[\text{Mn}(\text{NO}_3)_4]^-$ is probably similar, though it might be expected to contain asymmetric bidentate nitrate groups on account of the non-spherical d-electron configuration (73).

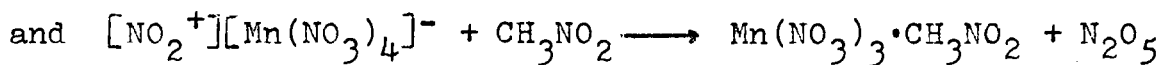
Both the cesium and nitronium salts are thermally more stable than $\text{Mn}(\text{NO}_3)_3$ and show no evolution of nitrogen oxides at room temperature within one week. Thermal decomposition commences at 55° and 60°C for the cesium and nitronium salts respectively, and does not yield $\text{Mn}(\text{NO}_3)_3$,

since their decomposition temperature is above that of the tri-nitrate itself. Similar enhanced thermal stability over that of the parent nitrate is also observed for $\text{Cr}(\text{NO}_3)_3 \cdot 2\text{N}_2\text{O}_4$ (4), $[\text{NO}]^+[\text{Fe}(\text{NO}_3)_4]^-$ and $[\text{NO}_2]^+[\text{Fe}(\text{NO}_3)_4]^-$ (29). The first point in the thermogravimetric curve, Figure 5.4, where there is a sharp decrease in decomposition rate occurs at approximately 600°C and at a mass loss which corresponds approximately to the composition MnNO_6 . No analysis of this material was attempted. While the material may be a polymeric nitrate species it is extremely unlikely that it is the molecular oxide nitrate $\text{MnO}_3(\text{NO}_3)$. Compounds MnO_3X (e.g., $\text{X} = \text{F}$) are molecular and unstable and few examples are known; attempts by Chapman to prepare the species $\text{MnO}_3(\text{NO}_3)$ by reaction of KMnO_4 or Mn_2O_7 with N_2O_5 produced a highly unstable product which eluded identification as $\text{MnO}_3(\text{NO}_3)$ with certainty (109). Similarly the other breaks in the curve are likely to be polymeric species.

The molar susceptibility of $\text{Cs}^+[\text{Mn}(\text{NO}_3)_4]^-$ and $[\text{NO}_2]^+[\text{Mn}(\text{NO}_3)_4]^-$ is $\chi_M^{\text{corr}} = 9950$ and 9960×10^{-6} c.g.s.u. respectively at 22°C ; $\mu_{\text{eff}} = 4.9 \pm 0.1$ B.M. This value is identical with the calculated spin only value of 4.90 B.M. corresponding to Mn^{3+} with four unpaired electrons. $\text{Cs}^+[\text{Mn}(\text{NO}_3)_4]^-$ is soluble in nitromethane to give a brown solution and the NO_2^+ salt gives a green solution. Both



give brown solutions in acetonitrile and ethyl acetate. Decomposition occurs in water and acetone. They are insoluble in benzene and carbon tetrachloride. The molar conductivity of a saturated ($2 \times 10^{-4} \text{M}$) nitromethane solution of $[\text{NO}_2^+][\text{Mn}(\text{NO}_3)_4]^-$ is exceedingly low (16.9 $\text{ohm}^{-1} \text{cm}^2$). A low value was also observed for $[\text{NO}_2^+][\text{Fe}(\text{NO}_3)_4]^-$ and explained in terms of a proposed solution equilibrium with non-electrolytes such as $\text{Fe}(\text{NO}_3)_3 \cdot \text{N}_2\text{O}_5$ or its dissociated and solvated components (29). Thus, dissociation and reactions of the type



may account for the low molar conductivity.

Chapter 6.

Raman Spectra of Anhydrous Metal Nitrates.

6.1. Introduction.

Section 1.3.2. outlined the usefulness of depolarization ratios (ρ) of Raman active frequencies in the determination of the mode of nitrate coordination. Briefly summarized, if the highest nitrate stretching frequency is polarized and the next highest is depolarized, the nitrate is coordinated as a symmetric bidentate ligand, whereas if the highest nitrate stretching frequency is depolarized and the next highest is polarized, then the nitrate is coordinated as a unidentate ligand.

The usual methods of obtaining depolarization ratios, namely single crystal or solution spectra, are not always applicable for inorganic nitrates due to the difficulty of obtaining single crystals, or sufficiently concentrated solutions of the more reactive nitrates. Furthermore, the species in solution may not be the same as in the solid. Unfortunately the Raman emission from powdered crystalline solids is almost always depolarized as a result of the multiple reflections and refractions which both the polarized incident radiation and the Raman emitted

light suffer at crystal surfaces within the sample. Two authors (145, 146) have recently described instances in which the measurement of depolarization ratios on powdered solids was made possible by immersing the solid in a liquid of similar refractive index (η). An investigation of this technique was undertaken to determine whether it could be successfully utilized to give information concerning the mode of coordination of the nitrate group in powdered solids. The work described in this chapter therefore is concerned with (a) studies on the immersion technique just mentioned and (b) the determination of the solid phase Raman spectra of several anhydrous nitrates.

Prior to this investigation, B.J. Bulkin (145) utilized benzophenone to demonstrate that immersion of the powder in a liquid with an identical refractive index (i.e., within 0.01 units) resulted in true depolarization ratios for that substance. D.F. Shriver (146) showed that Raman depolarization ratios could be obtained from species adsorbed on ion exchange resins and that the match of refractive index of immersion liquid and solid need only be within about 0.04 units. The results presented later show that the match of refractive index in some instances is very critical indeed.

6.2. Experimental Technique.

Barium nitrate was used as the sample in developing the experimental technique since it has a single refractive index ($\eta = 1.572$) and a strong, polarized band ($\rho \approx 0.0$) at 1047 cm^{-1} (175). Details of the development of the experimental technique to obtain depolarization ratios of powdered solids on the Cary 81 Raman Spectrophotometer are presented in this section.

6.2.1. Sample Mounting and Calibration.

Samples were illuminated with He-Ne laser radiation $\lambda = 6328\text{\AA}$. Considerable experimentation with various viewing modes and immersion media was required before satisfactory spectra could be obtained.

Since all previous work on this technique (145, 146) had been done on Spex instruments utilizing 90° viewing, it was necessary to experiment with sample holders and mounting on the Cary 81 Raman Spectrometer. After examining the 1047 cm^{-1} band in $\text{Ba}(\text{NO}_3)_2$ in both round and flat end sample tubes with both 90° and 180° viewing it was found that a melting point tube with a round end produced the highest intensity and best depolarization ratios.

The consistency of the sample was varied in the different tubes, and a thick paste was found to give the most intense Raman scattering and lowest depolarization ratios for the solids in all cases.

The sample tube was calibrated for further work by placing a volume of CCl_4 equal to the sample volume in the tube and holding it in position with the glass plunger, and then obtaining the apparent depolarization ratios for the 459 ($\rho_T = 0.00$; $\rho_{\text{obs}} = 0.080$) and 314 cm^{-1} ($\rho_T = 0.75$; $\rho_{\text{obs}} = 0.85$) bands and plotting these in the usual manner (176, 177).

6.2.2. Immersion Media.

The liquids that are suitable as immersion liquids must meet three criteria. First, the mixed liquids must provide a sufficient range of refractive indices so that if the refractive index of the solid is unknown, it may be determined by observing changes in depolarization ratio with refractive index. Second, the immersion media must not have Raman active modes close to bands in the solids. Finally the liquids must not react with or dissolve the sample. For example, quinoline ($\eta = 1.6245$) is known to complex with Co(II), Ni(II), Cu(II) and Zn(II) nitrates (178)

and thus is unsuitable as an immersion liquid for transition metal nitrates.

To obtain the full range of refractive indices, mixtures of solvents with a high and a low refractive index were utilized. The liquids and their refractive indices that were used were: diiodomethane (1.7559), iodonaphthalene (1.6946), iodobenzene (1.6215) and diethyl ether (1.3495). The Raman spectra of these liquids are reported in Table 6.1. Diiodomethane and ether mixtures were the most useful as they have fewer bands close to nitrate bands. The exact refractive index of each solution was measured on a standard Abbé refractometer.

6.3. Results.

6.3.1. Barium Nitrate.

Barium nitrate was chosen to evaluate this technique since it has a single refractive index and its Raman spectrum is fairly simple, consisting of the following three Raman active nitrate bands: 733 cm^{-1} (E'), 1047 cm^{-1} (A'_1) and 1367 cm^{-1} (E') (175). The totally symmetric mode (A'_1) is expected to yield a polarized band with a depolarization ratio (ρ) close to zero, while the E' modes should be depolarized with $\rho = 0.75$, when plane

Table 6.1.

Reference Spectra of Immersion Liquids.

<u>(C₂H₅)₂O^a</u>		<u>CH₂I₂^b</u>		<u>C₆H₅I^c</u>		<u>C₁₀H₇I</u>	
cm ⁻¹	(ρ)	cm ⁻¹	(ρ)	cm ⁻¹	(ρ)	cm ⁻¹	(ρ)
439 s	0.2	121 vs	0.25	168 m	0.70	116 w	0.75
830 w	0.2	486 vs	0.08	221 vw	0.75	153 m	0.75
842 w	0.75	573 w	0.75	267 vs	0.24	185 vw	----
1152 m	0.2	1112 vw	----	613 w	0.75	229 vw	----
1272 w	0.75	1137 vw	0.75	655 m	0.06	252 s	0.23
1452 s,br	0.75	1356 m	0.26	998 vs	0.08	406 vw	----
4465 s,br	0.75	1432 vw	----	1015 vw	----	512 m	0.72
2724 vw	----	2968 s	0.04	1060 w	0.06	582 s	0.03
2806 m	0.1	3035 w	0.75	1159 vw	0.75	643 m	0.01
2855 vs,br	0.1			1177 vw	0.01	787 m	0.02
2898 w	----			1473 vw	0.01	789 m	0.01
2935 vs,br	0.1			1574 vw	0.75	947 w	0.15
2975 s	0.75			2900 w,br	----	1024 m	0.01
				3061 vw	0.05	1058 m	0.10
				3145 w	0.01	1134 vw	0.01
						1145 vw	0.75
						1163 vw	0.75
						1250 vw	0.75
						1338 w	0.08
						1363 vw	0.10
						1432 m	0.45
						1545 w	0.08
						1558 m	0.75
						2900 vw,br	----
						3058 m	----

a Reference 187.

b References 188, 189.

c References 190, 191.

polarized incident radiation is used (93, 94). Spectra recorded using the powdered sample alone showed negligible difference in intensities of the bands with respect to the orientation of the plane of polarization of the incident radiation (see Figure 6.1).

The relationship between apparent depolarization ratio and refractive index was investigated by immersing samples in mixtures of CH_2I_2 and ether and obtaining the depolarization ratios of the 733 and 1047 cm^{-1} nitrate bands. The results are summarized in Table 6.2.

The polarized 1047 cm^{-1} band showed the largest effect, as illustrated in Figure 6.2, the apparent depolarization ratio dropping rapidly to a minimum of $\rho = 0.023$ at the true refractive index of the solid, $\eta = 1.572$. The plot of ρ versus η for the depolarized 733 cm^{-1} band (Figure 6.3) is much more erratic and less symmetrical. Nevertheless, the same general trend is observed and the curve minimized again at $\eta = 1.572$, at the expected value of $\rho = 0.75$. An examination of the 1367 cm^{-1} band gave a value of $\rho = 0.70$ at $\eta = 1.572$, the error being due to the overlap with a polarized CH_2I_2 band at 1356 cm^{-1} (Table 6.1).

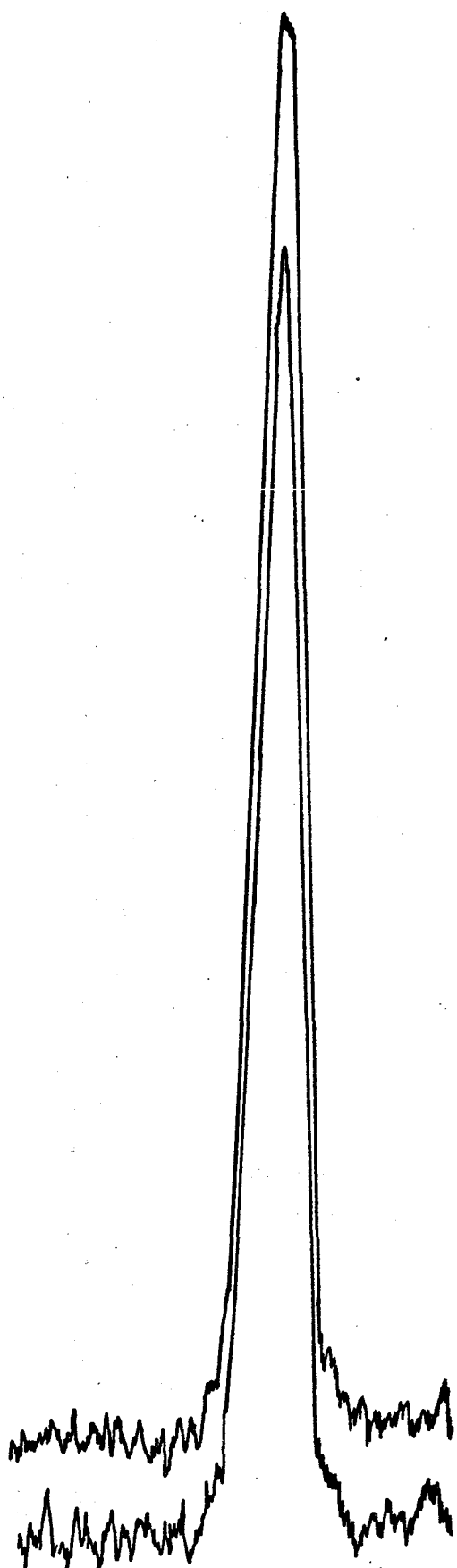


Figure 6.1(a) - 1047 cm^{-1}
band of powdered $\text{Ba}(\text{NO}_3)_2$.

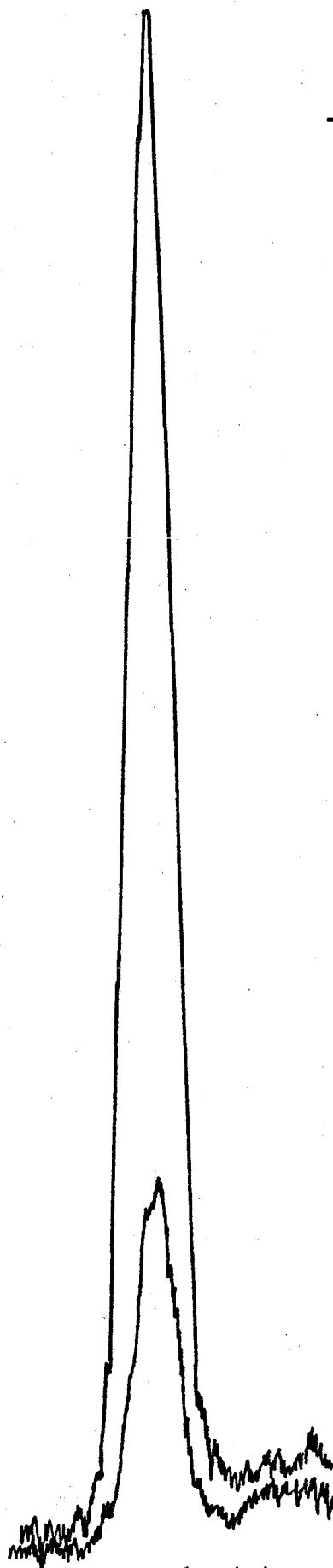


Figure 6.1(b) - 1047 cm^{-1}
band of powdered $\text{Ba}(\text{NO}_3)_2$
immersed in liquid of
 $\eta = 1.572$.

Table 6.2.

Variation of Apparent Depolarization Ratio (ρ)
for $\text{Ba}(\text{NO}_3)_2$ with Refractive Index (η) of Liquid Phase.

<u>η</u>	<u>733 cm^{-1}</u>	<u>1047 cm^{-1}</u>
1.349	0.84	0.835
1.486	0.82	0.343
1.499	0.79	0.305
1.505	0.82	0.235
1.519	0.82	0.208
1.540	0.81	0.180
1.548	0.78	0.087
1.561	0.78	0.045
1.572	0.75	0.023
1.583	0.76	0.025
1.605	0.77	0.073
1.639	----	0.230
1.647	0.77	0.285
1.675	0.79	0.325
1.707	0.82	0.360
1.756	0.84	0.390

Figure 6.2.

Variation of apparent depolarization ratio (ρ) for the 1047 cm^{-1} band of $\text{Ba}(\text{NO}_3)_2$ with refractive index (η) of the liquid.

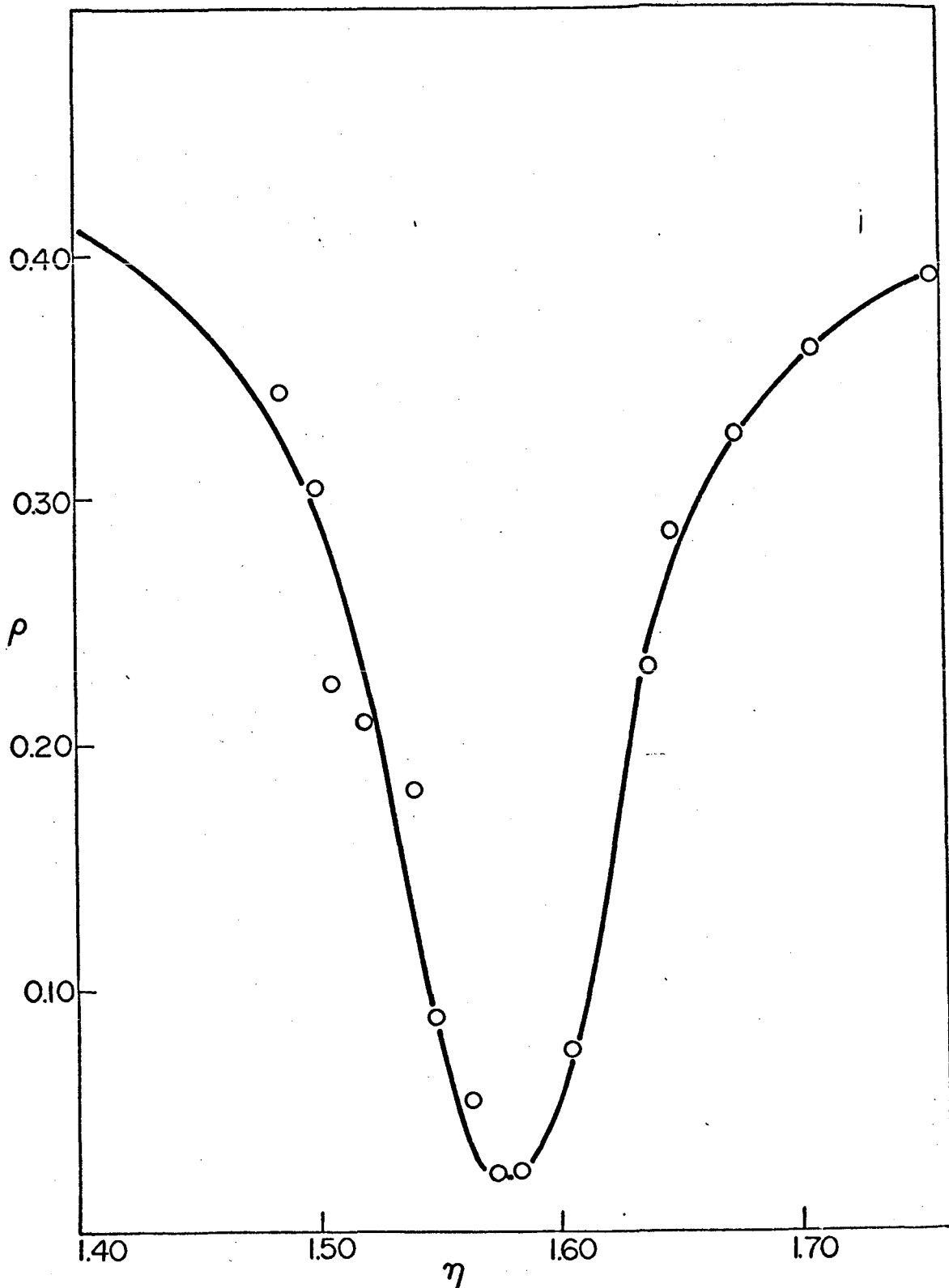
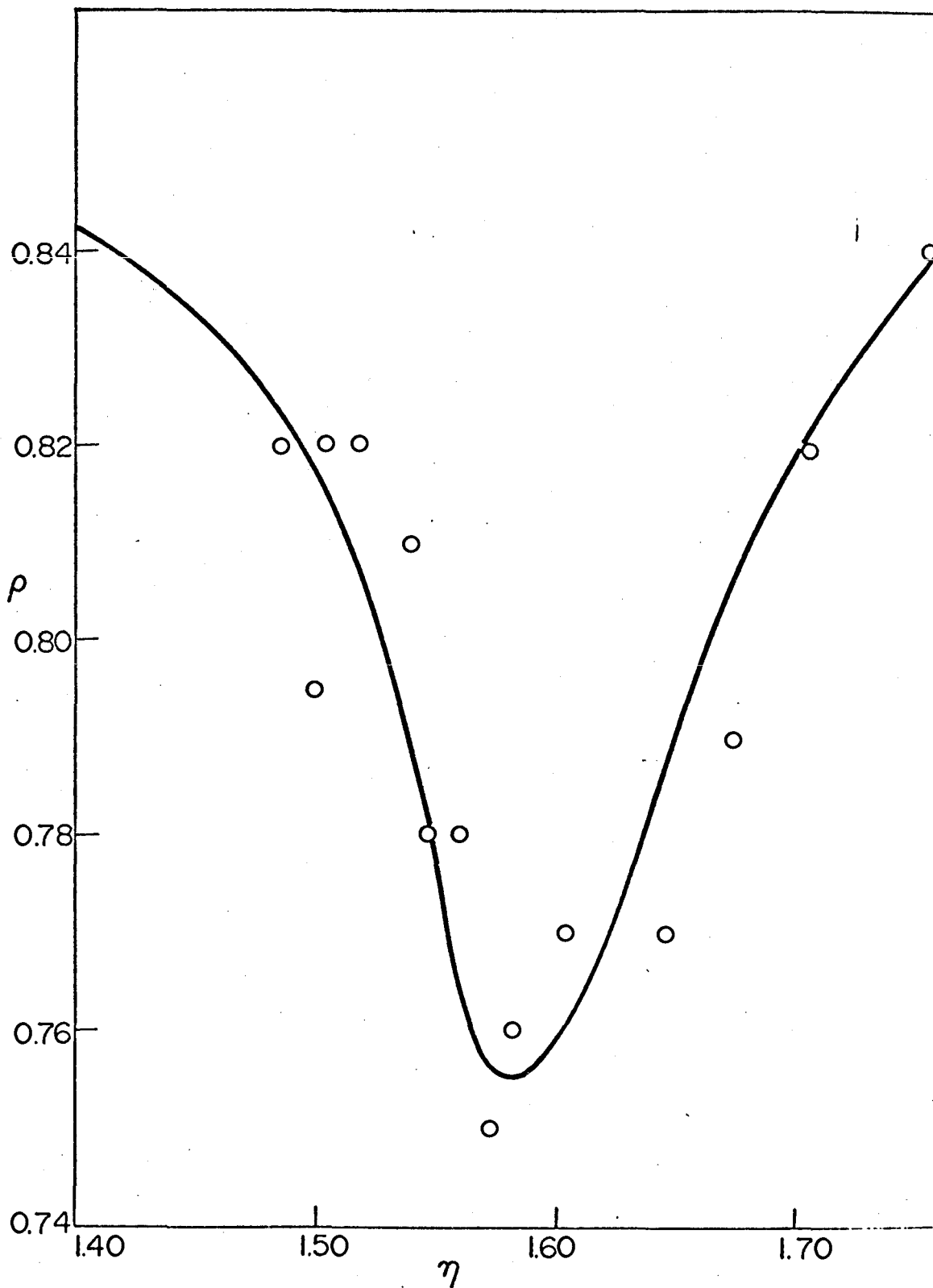


Figure 6.3.

Variation of apparent depolarization ratio (ρ) for the 733 cm^{-1} band of $\text{Ba}(\text{NO}_3)_2$ with refractive index (η) of the liquid.



6.3.2. Sodium Sulfate.

The depolarization ratios of a powdered isotropic solid have been obtained by the immersion technique. Sodium sulfate was chosen to investigate the applicability of this technique to anisotropic solids, since it has three refractive indices which lie close together (1.464, 1.474 and 1.485). Furthermore, the totally symmetric components of the bands arising from site splitting could perhaps be identified as they had not been previously (179).

The free sulfate ion has T_d symmetry (180) and four Raman active frequencies: 451(E), 613(T_2), 981(A_1) and 1104(T_2) cm^{-1} . In sodium sulfate, the symmetry is lowered sufficiently to split all the modes into their non-degenerate components (Table 6.3) so that the Raman spectrum of Na_2SO_4 consists of nine bands in the sulfate ion region. The totally symmetric (A_1) mode was expected to be totally polarized with ρ close to zero, so this band was used to study the variation of the apparent depolarization ratio as a function of the refractive index of the liquid to determine the most favorable refractive index at which to examine the other bands. The results are presented in Table 6.4. The plot of ρ versus η for this band, shown in Figure 6.4, displayed an effect which was quite different from that displayed by any of the nitrate bands in $\text{Ba}(\text{NO}_3)_2$.

Table 6.3.

Raman Active $\text{SO}_4^{=}$ Modes in Na_2SO_4

<u>Free $\text{SO}_4^{=}$</u> <u>(cm^{-1})</u>	<u>Orthorhombic Na_2SO_4</u> <u>(cm^{-1})</u>	
451 (E)	451	(A ₁) [*] (A ₂)
	466	
613 (T ₂)	622	
	634	(A ₁) (B ₁) (B ₂)
	648	
981 (A ₁)	993	(A ₁)
1104 (T ₂)	1103	
	1133	(A ₁) (A ₁) (A ₂)
	1154	

* Assignments based on lowering of symmetry to C_{2v} (179).

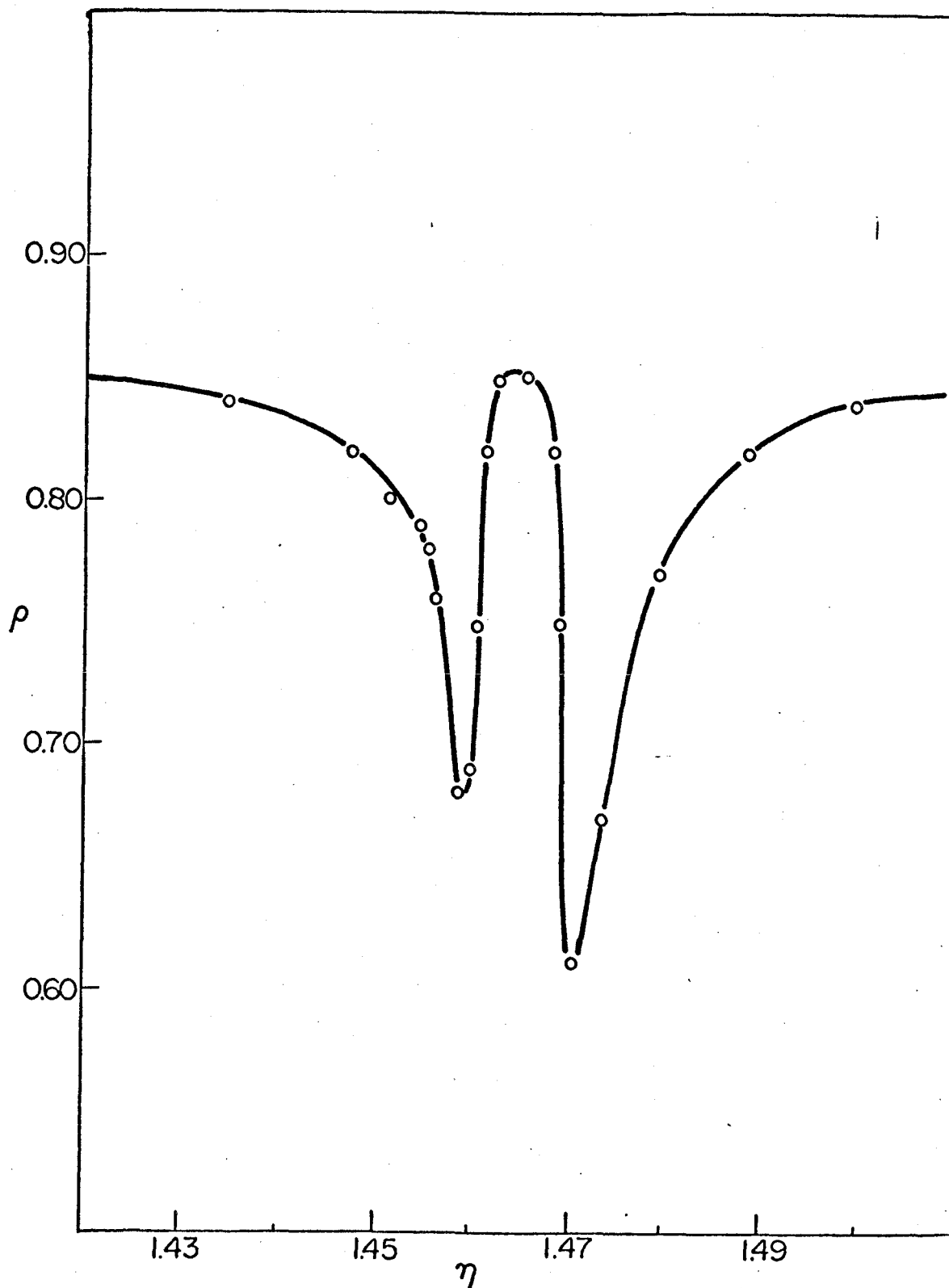
Table 6.4.

Variation of Apparent Depolarization Ratio for the A₁ Mode
of Na₂SO₄ with Refractive Index of the Liquid Phase.

1.435	.84
1.448	.82
1.452	.80
1.455	.79
1.456	.78
1.457	.76
1.459	.68
1.460	.69
1.461	.75
1.462	.82
1.463	.85
1.466	.85
1.469	.82
1.470	.75
1.471	.61
1.474	.67
1.480	.77
1.489	.82
1.506	.84

Figure 6.4.

Variation of apparent depolarization ratio (ρ) for the 993 cm^{-1} band of Na_2SO_4 with refractive index (η) of the liquid.



Rather than reaching a distinct minimum at each of the three refractive indices of Na_2SO_4 , only two minima were observed. The band at no time appeared to be strongly polarized, and this was thought to be the result of birefringent effects in the anisotropic solid. To substantiate this, a single crystal of anhydrous sodium sulphate, grown from hot (80°C) aqueous solution in the form of a pyramidal plate (height 0.5 mm., base 2.2 x 2.2 mm.) was viewed in the 180° mode with incident and scattered radiation propagated normal to the base. With the plane of polarization of the incident radiation parallel to the crystallographic axes, the 993 cm^{-1} band gave $\rho = 0.10$. The apparent depolarization ratio increased steadily i.e., 15° , $\rho = 0.25$; 30° , $\rho = 0.60$ as the crystal was rotated about the incident beam to a maximum value of $\rho = 0.97$ corresponding to complete depolarization when the plane of polarization was 45° to the crystallographic axes.

6.3.3. Discussion.

The utility of the method for the qualitative identification of polarized bands in isotropic solids is seen from the $\text{Ba}(\text{NO}_3)_2$ example in which the 1047 cm^{-1} band appears significantly polarized ($\rho \approx 0.4$), even when the mismatch of refractive indices ($\eta_{\text{solid}} - \eta_{\text{liquid}}$) is as large

as 0.15. Conversely the method could provide the refractive index of an isotropic solid which exhibits strongly polarized Raman bands.

Unfortunately the results for Na_2SO_4 described above indicate that there are severe limitations to this immersion technique as a method of obtaining accurate depolarization ratios for a powdered anisotropic solid and the method is only effective when the sample is an isotropic solid (e.g., $\text{Ba}(\text{NO}_3)_2$) with a single refractive index. In powdered anisotropic solids, birefringent effects will always operate to increase the apparent ρ value, and high values may be obtained even for a totally symmetric mode, making it virtually impossible to distinguish reliably between polarized and depolarized Raman bands. For this reason the immersion technique was not applied to the study of site splitting in sodium sulphate.

An interesting question that arose from the examination of sodium sulphate is that only two minima were observed at two out of three refractive indices of Na_2SO_4 . This could be due to the symmetric stretch being Raman inactive in the third direction.

Problems may also arise with respect to the immersion liquid. Pairs of liquids which are miscible and yield mixtures which cover a sufficiently wide range of

refractive index are difficult to find; if the solid is reactive this difficulty is increased. Thus it was a great problem to obtain suitable mixtures for the study of powdered nitrate complexes. The most satisfactory liquids in this work have been diiodomethane and di-ethyl ether, which are inert towards ionic nitrates and the majority of monodentate nitrate complexes; however this mixture is unsuitable for many bidentate nitrate complexes because of their reactivity with ether (see section 2.3.5).

6.4. Raman Spectra.

At the time this work was undertaken few laser Raman spectra of anhydrous metal nitrates had been reported. It was considered worthwhile to measure the laser Raman spectra of a representative series of metal nitrates to compliment the already existing i.r. data. The advantages to be achieved by determination of these spectra with depolarization ratios have already been outlined (section 1.3.2), but unfortunately none of the techniques for obtaining depolarization ratios (single crystal, solution or immersion of a powder in a liquid) were suitable for many of the metal nitrates. Also as the Raman spectra here were being obtained, a number of papers appeared in the literature which reported several of these spectra together with

complete factor group analyses. Therefore the spectra of these compounds (Li, Na, K, Rb, Cs, Sr, Ba and Pb nitrates), which agree closely with those published, are presented with only a brief discussion in this thesis. In addition, the i.r. and Raman spectra of the dinitrogen tetroxide adducts of $\text{Be}(\text{NO}_3)_2$ and $\text{Mg}(\text{NO}_3)_2$ are reported for the first time as they indicate significant covalent interactions in these molecules, and because of confusion in the existing literature over the assignment of the i.r. spectra of the two forms of $\text{Cu}(\text{NO}_3)_2$ and interest in possible structure of the β form, the i.r. and Raman of these were determined.

6.4.1. Experimental.

The source or the preparation of the anhydrous metal nitrates examined are presented in Table 6.5. Finely ground anhydrous samples were sealed under an inert atmosphere in 3 mm. diameter borosilicate glass tubes with smoothly rounded ends. Spectra were obtained using the Cary Model 81 Raman Spectrophotometer with 60 mW Spectra-Physics Model 125 He-Ne laser excitation. The infrared spectra were obtained on a Beckman IR-12 spectrometer. In the region 4000 to 400cm^{-1} , nujol and fluorolube mulls on AgCl windows were used, while in the range 500 to 200cm^{-1} vaseline mulls on polyethylene windows were used. All samples were prepared in a dry box and

Table 6.5.

Preparation of Anhydrous Nitrates.

Metal	Source, Purity or Prep'n ^a	Drying		%M		Analytical Method ^c	Ref.
		Temp. °C	Time (hrs)	Found	Calc.		
Li(I)	A 99.0%	105	2				
Na(I)	A 99.5%	105	2				
K(I)	A 99.0%	105	2				
Rb(I)	Aq. HNO ₃	105	2	57.9	58.0	RbClO ₄	2
Cs(I)	B > 97%	105	2				
Be(II)	C	80	8	6.5	6.8	BeO	30
Mg(II)	C	100	8	17.0	16.4	MgO	30
Ca(II)	A 99.0%	150	18				
Si(II)	A 99.0%	105	2				
Ba(II)	A 99.5%	105	2				
Tl(IV)	D	80 ^b	-	16.2	16.2	Tl ₂ O ₃	45
Mn(II)	C	110	10	29.6	30.7	Bismuthate	41
Co(II)	C	110	18	32.0	32.2	Co ₃ O ₄	64
Ni(II)	C	110	18	32.2	32.2	Ni(DMG) ₂	
Cu(II)	C	100	5	32.5	33.4	CuO	1,181
Zn(II)	C	100	18	34.1	34.5	ZnO	41
Ag(I)	F 99.9%	110	4				
Cd(II)	C	110	4	47.4	47.6	CdO	41
Hg(II)	C	100	4			HgO	41
Pb(II)	A 99.0%	110	4				
Sn(IV)	D	40 ^b	-	32.4	32.4	SnO ₂	35

a A, allied Chemical; B, British Drug House; C, N₂O₄/EtOAc; D, N₂O₅; F, Fisher Chemical.

b Sublimation Temperature.

c Analytical Techniques are found in ref. 182, 183.

transferred to the instruments in a desiccator, All samples of α and β $\text{Cu}(\text{NO}_3)_2$ utilized for infrared or Raman spectra were shown to be of the correct form by X-ray powder photographs (59). Raman spectra of α and β copper(II) nitrates were kindly obtained for us by Cary Instruments, Monrovia, Calif., using the $5145\overset{\circ}{\text{A}}$ line of an argon ion laser.

6.4.2. Main Group Metal Nitrates.

The Raman spectra of the alkali metal and silver nitrates are presented in Table 6.6 and the Raman spectra of the isomorphous nitrates of calcium, strontium, barium and lead are presented in Table 6.7. The first Raman spectra of anhydrous metal nitrates appeared in the early 1930's when Krishnamurti (198) and Nisi (199) recorded the Raman spectra of sodium, potassium, barium, lead and ammonium nitrates. These authors were unable to see any multiplet band structure in the ν_3 stretching region. Courture (175) was among the first to see that ν_3 was split into two components. Since 1968, a number of authors have examined the Raman spectra of these compounds in great detail. Factor group analysis, which considers all of the vibrations of the molecules or ions in the complete unit cell as the basis for assigning the bands, has been used to describe the spectra of the nitrates of lithium, sodium, potassium, rubidium, cesium,

Table 6.6.

Raman Spectra of Alkali Metal and Silver Nitrates.

Assignment ^a	Li	Na	K	Rb	Cs	Ag
$2\nu_2(A_1')$	1677 w	1673 w	1657 vw	1597 vw		1618 vw 1605 vw
$\nu_3(E')$	1386 m	1388 m	1361 w 1346 w	1405 w 1349 w	1400 w 1350 w	1348 m 1331 sh
$\nu_1(A_1')$	1071 s,sp	1069 s,sp	1051 s,sp	s057 s,sp	1051 s,sp	1046 s,sp
$\nu_2(A_2'')$						810 vw
$\nu_4(E')$	736 m,sp	726 m,sp	716 m,sp	722 w 707 w	717 m 707 w	734 m 715 m
Lattice Modes	238 s	188 s	130 vw	109 vw	114 w	194 m 136 s 96 m
	125 vw	104 w	85 w 52 vw	58 vw		
Ref. To: i.r.	184, 185, 195	184, 185, 195	184, 185, 195	195	195	
Raman	102, 103, 186, 192, 193	102, 103, 192 - 194	102, 103, 192, 193	102, 103, 193	102, 103, 193	102, 103, 193

^a Based on ionic nitrate with D_{3h} symmetry.

Table 6.7.

Raman Spectra of Calcium, Strontium, Barium, and Lead Nitrates.

<u>Assignment^a</u>	<u>Ca</u>	<u>Sr</u>	<u>Ba</u>	<u>Pb</u>
$2\nu_2(A_1')$	1632 sh 1629 w	1635 sh 1631 m	1636 w	1617 w
$\nu_3(E')$	1419 w 1378 vw	1427 m 1406 m 1371 w	1407 m 1392 m 1358 w	1412 w 1328 m
$\nu_1(A_1')$	1068 s,sp 1040 w	1058 s,sp 1033 w	1048 s,sp 1025 w	1047 s,sp 1029 w
$\nu_2(A_2'')$				814 vw
$\nu_4(E')$	746 m	739 m	733 m	731 m
Lattice Modes	197 w 175 vw	184 m 167 w 132 w 108 w	145 m 133 m 81 s	161 s 145 m 124 m 96 vs

Ref. To:

i.r.	184, 185 196	184, 185, 196	184, 185, 196	41, 196
Raman	103	103	103	103

a Based on ionic nitrate with D_{3h} symmetry.

calcium, strontium and barium (102, 103, 104, 193). Normal coordinate analysis has been carried out for lithium, sodium and potassium nitrates as well (192).

The Raman spectra of beryllium and manganese nitrates and their dinitrogen tetroxide adducts have not previously been reported and are presented along with their infrared spectra in Table 6.8. The symmetric stretching frequency (ν_2 , A_1 for coordinated nitrates) is increased above the free ion by a greater amount in the anhydrous nitrates than in the N_2O_4 adducts. $Be(NO_3)_2$, $Be(NO_3)_2 \cdot 2N_2O_4$ and $Mg(NO_3)_2 \cdot N_2O_4$ all show numerous bands in the region 1550 to 1250 cm^{-1} and this is indicative of strong covalent metal-nitrate interaction (see section 1.3) but does not permit any definite assignment of the mode of nitrate coordination. The relative intensities in the Raman spectra of both the nitrates and N_2O_4 adducts may indicate the mode of coordination, but, without accompanying depolarization ratios, this is only a tentative conclusion. Both the infrared and Raman spectra of the N_2O_4 adducts contain a band close to 2300 cm^{-1} which is assigned as the N-O stretching mode of the nitrosium ion (200). The infrared spectra also contain a medium strength band at approximately 1740 cm^{-1} which has been taken to indicate the presence of un-ionized nitrogen tetroxide in both adducts

Table 6.8. Vibrational Spectra of $\text{Be}(\text{NO}_3)_2$, $\text{Mg}(\text{NO}_3)_2$, $\text{Be}(\text{NO}_3)_2 \cdot 2\text{N}_2\text{O}_4$ and $\text{Mg}(\text{NO}_3)_2 \cdot \text{N}_2\text{O}_4$.

$\text{Be}(\text{NO}_3)_2$ (30)		$\text{Mg}(\text{NO}_3)_2$ (30)		$\text{Be}(\text{NO}_3)_2 \cdot 2\text{N}_2\text{O}_4$		$\text{Mg}(\text{NO}_3)_2 \cdot \text{N}_2\text{O}_4$	
i.r.	R	i.r.	R	i.r.	R	i.r.	R
1600 s	1590 m, sh	1845 w		2274 m	2274 vs	2289 s	2285 vs
1550 s, br	1560 m		1515 w	1747 m	1544 m	1734 m	1485 w
1500 sh			1475 m	1510 vs, br	1512 m	1530 vs	1450 w
1360 s	1400 w		1413 m	1345 vs	1349 s	1320 bs, br	1335 m
			1382 w	1330 vs	1336 sh		
1280 vs, br	1290 s		1101 vs	1310 vs, br	1310 ms		
1070 vs	1075 vs		1076 sh	1250 m			1285 m
1020 sh	1024 sh			1050 w	1054 vs	1065 w	1067 vs
857 m					1019 m	1041 w	1041 m
790 s	795 m	813 vs		832 s	835 vw	810 s, sp	822 w
	777 m	807 vs		800 vs			
743 m	760 w	763 s	753 m	742 w	777 w	764 s	766 m
	732 m		748 sh	615 vs	733 m	743 s	723 m
455 m	500 w, br				615 m		
	450 w, br						486 w
			252 w		258 w		
			190 s		200 w		190 w
			171 w				
			146 m				
			136 m				

(181, 201). Although it is one of the strongest bands in the infrared spectrum on N_2O_4 , the absence of the other equally intense bands at 1600 and 1000 cm^{-1} (202) suggests that $Be(NO_3)_2 \cdot 2N_2O_4$ and $Mn(NO_3)_2 \cdot N_2O_4$ are not just N_2O_4 adducts, but are the nitrosonium salts $[NO^+]_2[Be(NO_3)_4^-]$ and $[NO^+][Mg(NO_3)_3^-]$.

Aluminum(III) trinitrate could not be obtained free of N_2O_5 when it was sublimed (26). The Raman spectrum of indium(III) trinitrate, the only group IIIA metal to form a pure anhydrous trinitrate to date, has been examined by James and Kimber (32). They postulate the presence of bridging nitrate groups in $In(NO_3)_3$ due to the similarity of their spectrum to that of $Sn(NO_3)_4$ and $Ti(NO_3)_4$ and the fact that the samples consistently formed glasses. Their conclusion is probably correct but their reasoning is faulty. The physical properties of indium(III) trinitrate and the similarities of the spectrum to those of $\alpha\text{-Cu}(NO_3)_2$ and $Cu(NO_3)_2 \cdot CH_3NO_2$, which contain bridging nitrates (61, 88, 181) i.e., the highest $\nu(N-O)$ frequency about 1520 cm^{-1} , next highest about 1250 cm^{-1} , suggest that $In(NO_3)_3$ does, indeed, have bridging nitrates. The spectra of $Sn(NO_3)_4$ and $Ti(NO_3)_4$ are entirely different, with the two highest $\nu(N-O)$ frequencies at approximately 1600 and 1190 cm^{-1} (36). Both $Ti(NO_3)_4$ and $Sn(NO_3)_4$ are known to contain only symmetric bidentate nitrate groups (37, 45).

6.4.3. Transition Metal Nitrates.

The Raman spectra of tin(IV) and titanium(IV) tetranitrates are presented in Table 6.9 and that of $\text{Ti}(\text{NO}_3)_4$ in Figure 6.5. The spectrum of $\text{Sn}(\text{NO}_3)_4$ is included here for simplicity, and is very similar to that already reported (36). The Raman spectrum of $\text{Ti}(\text{NO}_3)_4$ is now presented in greater detail than had been previously reported due to the use of a laser source which produces higher quality spectra than the mercury arc source available previously (93, 94). The spectrum can be readily assigned on the basis of D_{2d} symmetry displayed by $\text{Ti}(\text{NO}_3)_4$ (45). The coupling should give rise to components which transform as A_1, B_2 and E in this point group. The differences between the Raman spectrum reported by Addison et. al. (36) for $\text{Ti}(\text{NO}_3)_4$ and that obtained here are: a shoulder on the 1636 cm^{-1} band at 1615 cm^{-1} , which corresponds to the infrared bands in the N-O* region, and these bands must be the B_2 and E components; an additional band in the $\nu_S(\text{N-O}_2)$ region at 992 cm^{-1} , corresponding to the 989 cm^{-1} infrared band, so the B_2 and E components are degenerate, or nearly so, in this region; three Raman bands in the symmetric in-plane bending region, at 797, 785, 775 cm^{-1} ; and three components in the $\nu_{AS}(\text{Ti-O})$ region at 475, 444 and 426 cm^{-1} . The relatively more intense bands at 775 and 444 cm^{-1} may

Table 6.9.

Raman Spectra of Sn and Ti Nitrates.

<u>Assignment (D_{2d})</u>	<u>Sn(NO₃)₄ (36)</u>	<u>Ti(NO₃)₄ (36)</u>
A ₁ v(NO*)	1657 s	1667 s
B ₂ + E v(NO*)	1617 m	1636 m 1615 sh
B ₂ + E v _{AS} (NO ₂)	1228 m	1188 m
A ₁ v _S (NO ₂)	994 s	1006 s,sp
B ₂ + E v _S (NO ₂)	979 m	992 m
A ₁ δ _S (NO ₂)	807 m	797 s,sp
B ₂ + E δ _S (NO ₂)		785 w
+ B ₁ π(O ₂ NO*)		775 m
B ₁ (δ _{AS} NO ₂)		683 w
A ₁ v _{AS} (TiO ₂)		444 m
B ₂ + E v _{AS} (Ti-O ₂)		426 w-m
A ₁ v _S (TiO)	303 m	316 vs
B ₂ + E v _S (TiO)	245 w	282 m
δ(TiO ₂)	200 w	160 vw
Lattice Modes	148 w	137 vw
	98 m	98 m
	75 w	77 w

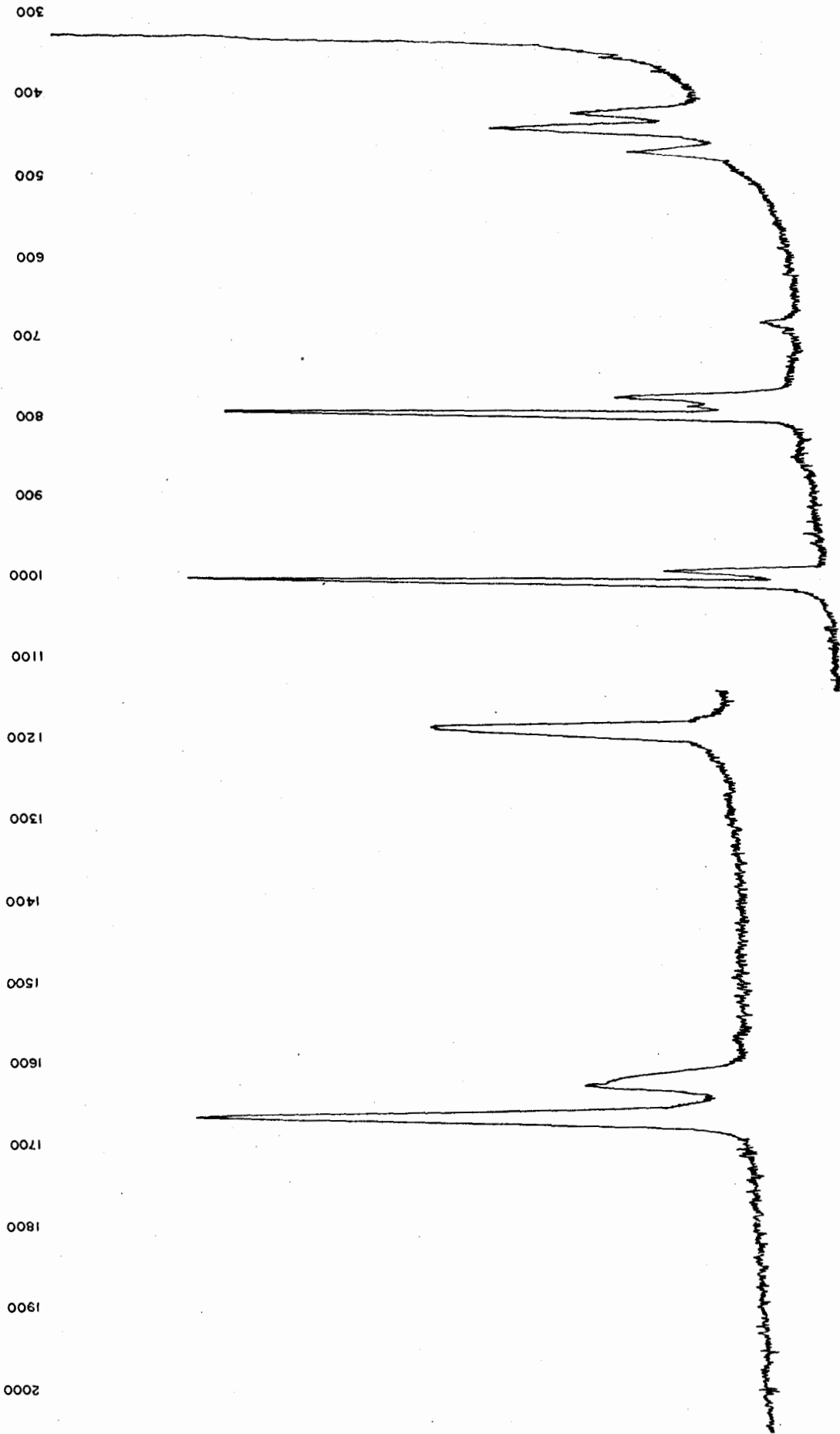


Figure 6.5. Raman spectrum of $Ti(NO_3)_4$

indicate that these are the A_1 modes while the others are the B_2 and E_1 modes.

Vanadium(V) oxide trinitrate was not re-examined as depolarization ratios have already been determined for this compound (36). The colors of chromium(III) trinitrate, nickel(II) and copper(II) dinitrates prevented the determination of their Raman spectra with the He-Ne laser. The Raman spectra of two forms of copper nitrate, obtained with an Ar ion laser, are reported in the next section. The Raman spectra of the dinitrates of manganese(II), cobalt(II), zinc(II), cadmium(II) and mercury(II) are reported in Table 6.10. The Raman and infrared (41) spectra of cadmium nitrate are strictly analogous to those of the ionic alkali and alkaline earth metal nitrates and hence the Raman spectrum may be assigned in the usual manner as due to the NO_3^- ion, viz. $1606, 2\nu_2(A_1')$; 1410 and $1333 \nu_3(E')$; $1073 \nu_1(A_1')$; 750 and $733 \nu_4(E')$; $182, 108$ and 68 cm^{-1} , lattice modes with the conclusion that the interactions in these (41, 51) compounds are predominately ionic. The spectra of mercuric nitrate are more difficult to interpret. They are similar in general composition to the cadmium nitrate spectra, but with the highest Raman band at 1510 cm^{-1} and the ν_1 band at 1036 cm^{-1} , suggesting that there is significant metal-nitrate interaction in this compound. Similarly the spectra of

Table 6.10.

Raman Spectra of Mn, Co, Zn, Cd, and Hg Dinitrates.

<u>ASSIGNMENT^a</u>	<u>Mn (41)</u>	<u>Co (41,198)</u>	<u>Zn (41)</u>	<u>Cd (41)</u>	<u>Hg(41)</u>
$2\nu_2(A_1')$				1606 w	
$\nu(NO^*)$	1447 w	1445 w	1535 w,b	1410 s	1510 w
$\nu_{AS}(NO_2)$	1361 w 1278 w	1380 w 1285 w	1285 w,b	1333 m	1368 w
$\nu_S(NO_2)$	1082 s,sp	1089 s,sp 1081 s,sp 1048 m,sp	1051 s,sp 1039 sh	1073 s,sp 1065 sh	1036 s,sp
$\delta_S(NO_2)$	760 sh	790 b	765 m	750 m	748 m
$\delta_{AS}(NO_2)$	747 m	752 m 742 sh	749 m	733 sh	724 m
Lattice Modes		192 w	181 w 77 m	182 m 108 w 68 w	170 w 135 w

a Assignment for Mn, Co, Zn, and Hg nitrates based on C_{2v} symmetry.

manganese, cobalt and zinc nitrates can be considered to have covalent metal-nitrate interactions since the separations of the two highest $\nu(\text{N-O})$ bands in their Raman spectra are approximately 150 cm^{-1} whereas site splitting in those nitrates that are known to contain ionic nitrates is usually less than 50 cm^{-1} (see Tables 6.6 and 6.7).

6.5. α - and β -Copper(II) Nitrates.

Anhydrous copper(II) nitrate has been shown to exist in two crystalline forms (59); a low temperature α form obtained from $\text{Cu}(\text{NO}_3)_2 \cdot \text{N}_2\text{O}_4$, for which the crystal structure has been determined (61) and a high temperature β form, obtained by vacuum sublimation of the α form, whose structure is unknown. Although a number of authors (17, 60, 181) have examined the infrared spectra of the two forms, there was little agreement between them. For this reason, and as a part of the study of the Raman spectra of anhydrous metal nitrates, the i.r. and Raman spectra of both forms of copper nitrate were obtained and the determination of the crystal and molecular structure of the β form was attempted. The Raman spectra, that were kindly supplied by Cary Instruments, indicated decomposition occurred with the 4880\AA Argon line and the focussed 5145\AA line. When the 5145\AA line was de-focussed, distinct spectra of α - and β - $\text{Cu}(\text{NO}_3)_2$ were obtained, but

the noise level was extremely high and has made location of bands in the 1200 - 1600 cm^{-1} region extremely difficult, see Figures 6.6 and 6.7. Furthermore, attempts to obtain these spectra using the Simon Fraser University Department of Physics Argon laser or the University of Calgary's Argon/Krypton laser were unsuccessful due to decomposition of the samples.

6.5.1. α -Copper Nitrate.

The infrared and Raman spectra are presented in Table 6.11 and Figure 6.6, along with the spectra reported by Logan and Simpson (181) and James and Kimber (60). James and Kimber (60) do not acknowledge Logan and Simpson's paper (181) with which their results are in disagreement, nor Addison and Hathaway's study of the vapor pressure and decomposition of $\text{Cu}(\text{NO}_3)_2$ in the gas phase (1). James and Kimber sublimed both the α and β $\text{Cu}(\text{NO}_3)_2$ samples at 225°C even though Addison and Hathaway found the vapor to be unstable at 226°C. (1), nor do they give X-ray powder patterns they obtained for each form. Thus the results obtained by James and Kimber can not be considered reliable.

The structural determination by Wallwork and Addison (61) of α -copper nitrate indicates that one-half of

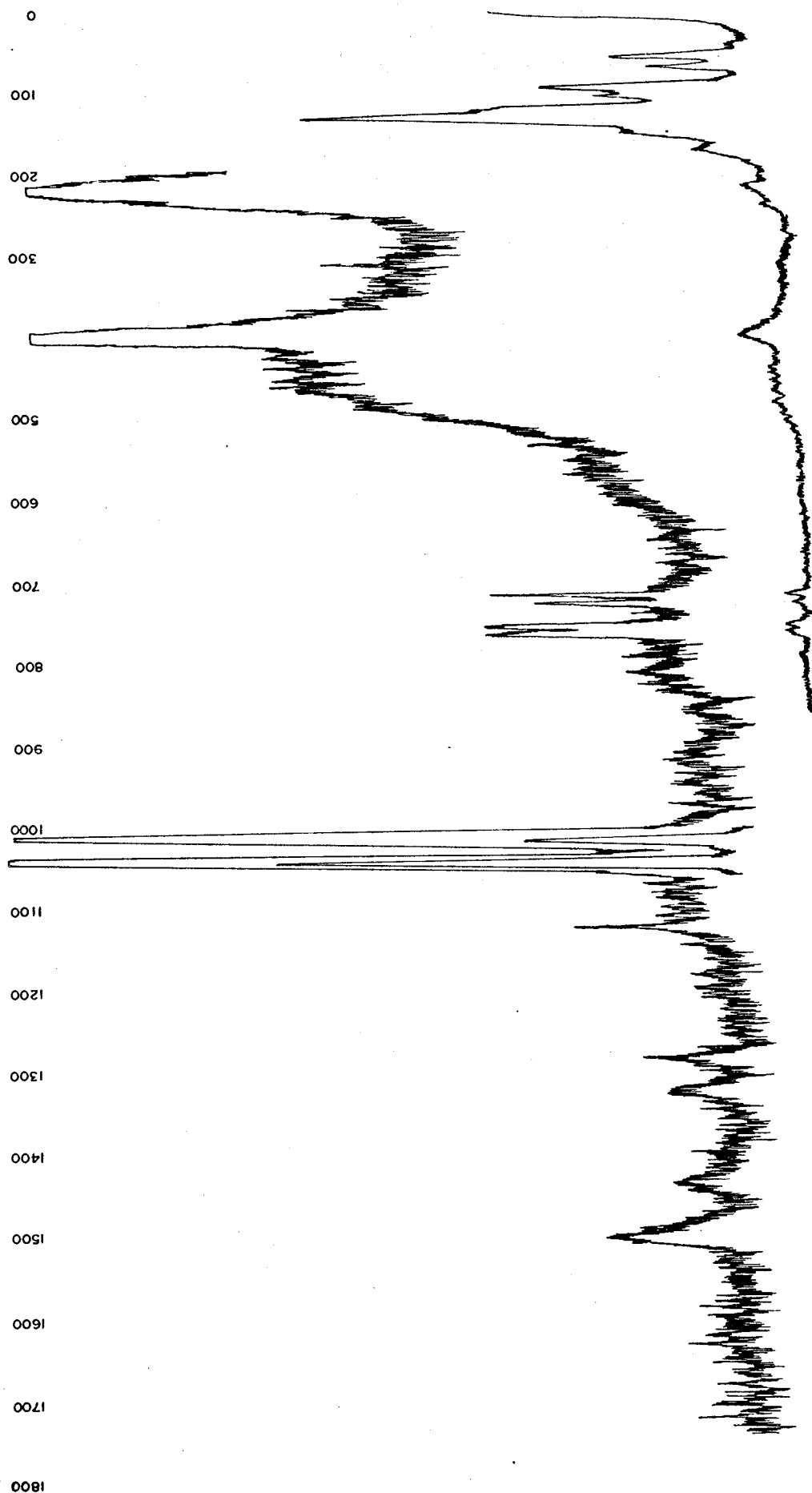


Figure 6.6. Raman spectrum of $\alpha\text{-Cu}(\text{NO}_3)_2$

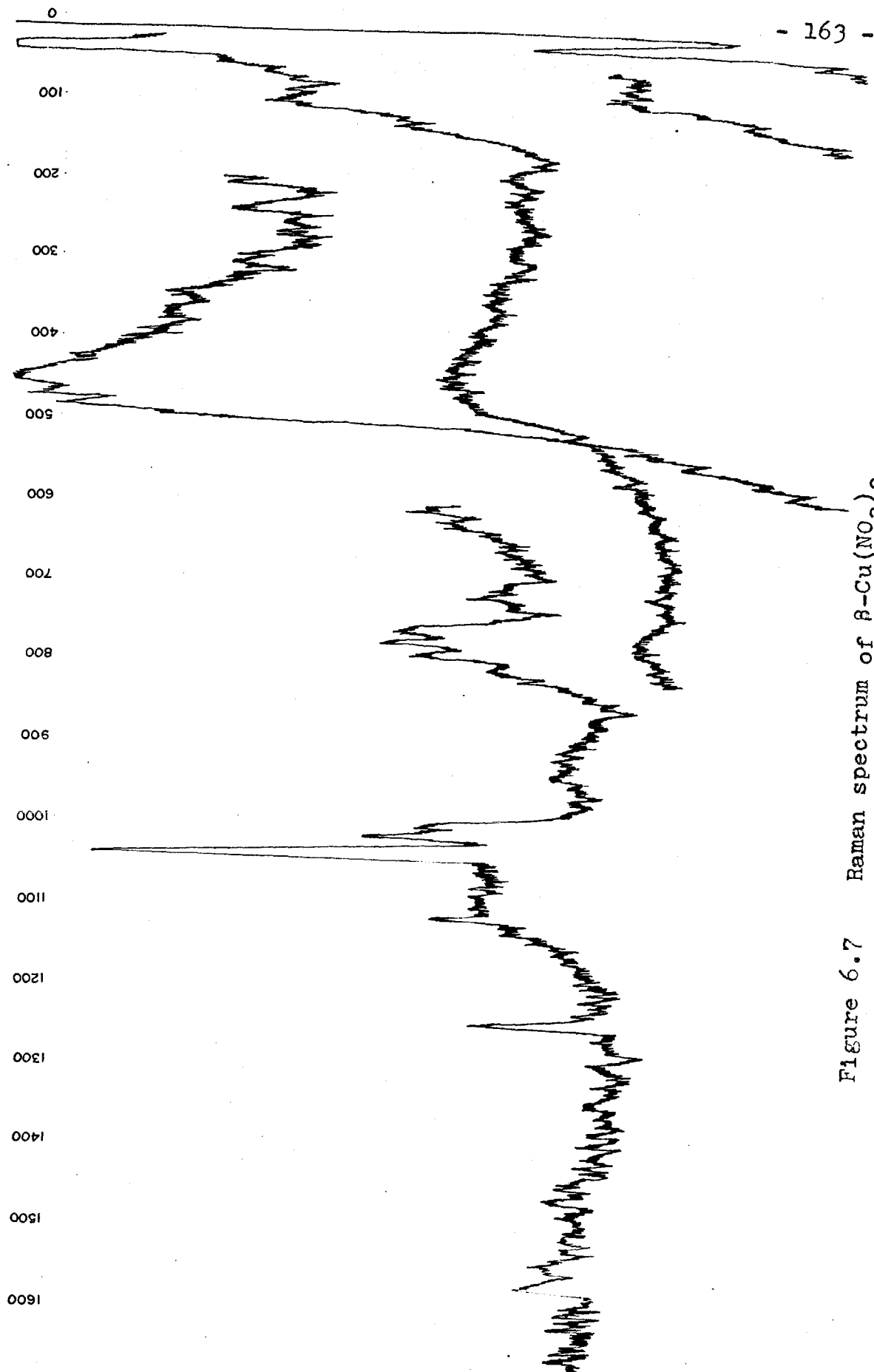


Figure 6.7 Raman spectrum of $\beta\text{-Cu}(\text{NO}_3)_2$

Table 6.11.

Infrared and Raman of α -Cu(NO₃)₂.

<u>Assignment</u>	<u>Logan (181)</u>	<u>James (59)</u>	<u>i.r. (this work)</u>	<u>Raman (this work)</u>
ν (NO*)	1510 vs 1478 vs 1435 vs	1515 m,sh 1464 s,br	1779 w 1520 s,br 1480 s,br 1452 vs,br	1510 s 1430 m
ν_{AS} (NO ₂)	1300 vs,br	1330 s,br 1274 m	1350 sh 1290 vs,br	1318 m 1280 m,br
ν_S (NO ₂)	1049 s 1015 m	1036 m	1054 s 1048 sh 1013 s	1048 vs 1016 m
(2 x 427 cm ⁻¹)		905 w,br	856 w	
δ (Cu-O ₂ N) + π (O ₂ NO)	796 s	807 m	797 s 783 s	
δ_{AS} (ON-O ₂)	759 m 746 w 712 w		760 m 723 m	764 m 756 m 728 m 718 m
ν (Cu-O)		490 m 452 sh 430 s,br	427 s 375 s 351 s,br 310 sh 292 s 240 m,sh	402 m
δ (Cu-O) + Lattice Modes				175 w 136 vs 106 sh 98 sh 70 w 58 w

the nitrate groups form three Cu-O bonds of 2.02, 2.43 and 2.68 \AA and are coordinated as both bridging and asymmetric bidentate nitrates, while the rest form only two bonds of 1.96 and 1.92 \AA and are strictly bridging nitrates. This variety in Cu-O bond lengths, and the fact that bidentate coordination of nitrates should result in a symmetric and asymmetric Cu-O stretching mode, may result in several modes occurring in the Cu-O stretching region (see Table 6.11). The copper-oxygen stretching frequency has been calculated, assuming a force constant of 1 mdyne \AA^{-1} , to be in the region of 360 cm^{-1} (185). Thus the frequencies between 427 - 240 cm^{-1} in the infrared and at 402 cm^{-1} in the Raman spectra are consistent with assignment as $\nu(\text{Cu-O})$ frequencies. The bands below 220 cm^{-1} probably result from $\delta(\text{Cu-O})$ modes and lattice modes.

The nitrogen-oxygen bending region shows two groups of bands centered at 723 and 760 cm^{-1} which may be assigned as the antisymmetric and symmetric in-plane bending modes respectively, and the two infrared bands at 783 and 797 cm^{-1} for which there are no corresponding bands in the Raman could arise from the out-of-plane bending mode of nitrate ligands. The weak infrared band at 856 cm^{-1} is assigned as the first overtone of the $\nu(\text{Cu-O})$ frequency at 427 cm^{-1} .

The $\nu_2(\text{NO}_2)$ region has one set of bands at 1054 and 1048 cm^{-1} and a second set at 1016 and 1013 cm^{-1} . These lower frequency bands seem to be at too low a frequency to be the isotopic species $\text{N}^{16}\text{O}_2^{18}\text{O}^-$ since this has been shown to lie at $(\nu - 20) \text{cm}^{-1}$ (203) approximately 20 cm^{-1} below the $\text{N}^{16}\text{O}_3^-$ species. Thus there seems to be two distinct $\nu(\text{NO}_2)$ modes giving rise to the two groups of bands. This is different from the case of $\text{Mn}(\text{NO}_3)_3 \cdot \text{bipy}$ (chapter 5) in whose i.r. there is only one symmetric stretch seen in this region, even though there are three different types of nitrate coordination in that molecule. The higher frequency stretching region (1200 - 1600 cm^{-1}) shows two distinct groups of bands, the multiplicity of which may be attributed to the numerous types of metal-oxygen interactions in this molecule.

6.5.2. $\beta\text{-Cu}(\text{NO}_3)_2$.

Precession photographs of the 0kl and hkl zones and zero, first and second level Weissenberg photographs were taken of a single crystal of $\beta\text{-Cu}(\text{NO}_3)_2$ using Cu-K_α radiation.

Crystal Data:

$\beta\text{-Cu}(\text{NO}_3)_2$; $M = 187.55$; Orthorhombic,
 $a = 7.46(2)$, $b = 11.20(2)$, $c = 95.0(10)\text{\AA}$, $V = 7890\text{\AA}^3$,
 $\rho_o = 2.49(5) \text{ g. cm}^{-3}$ (flotation, CCl_4 and CH_2I_2),
 $\rho_c = 2.51 \text{ g. cm}^{-3}$; $Z = 64$.

The extremely long axis (95.0\AA) and systematic arrangements of strong and weak reflections on the photographs led to the tentative conclusion of a super-lattice type structure. As the structural determination posed an extensive and difficult crystallographic problem, it was not pursued further.

The infrared and Raman spectra of $\beta\text{-Cu}(\text{NO}_3)_2$ are reported in Table 6.12. The $\nu(\text{Cu-O})$ region is much simpler than that of $\alpha\text{-Cu}(\text{NO}_3)_2$. The occurrence of only one band in each the infrared and Raman spectra in this region leads to the tentative assignment of $\nu_s(\text{Cu-O}) = 330 \text{ cm}^{-1}$ and $\nu_{AS}(\text{Cu-O}) = 335 \text{ cm}^{-1}$. This simple $\nu(\text{Cu-O})$ region may imply that the structure of $\beta\text{-Cu}(\text{NO}_3)_2$ does not have the variety of copper-oxygen bonding types as does $\alpha\text{-Cu}(\text{NO}_3)_2$. It may be seen from tables 6.11 and 6.12 that James and Kimber's i.r. spectrum for $\beta\text{-Cu}(\text{NO}_3)_2$ exhibits many bands in this region that are coincident with the bands observed for $\alpha\text{-Cu}(\text{NO}_3)_2$ in both their own work and the work reported here, but

Figure 6.12.

Infrared and Raman of β -Cu(NO₃)₂.

<u>Assignment</u>	<u>Logan(181)</u>	<u>James (60)</u>	<u>i.r. (this work)</u>	<u>Raman (this work)</u>
v(NO*)	1580 vs 1526 vs 1490 vs	1489 vs	1584 s 1528 s,br 1490 vs	1580 m 1550 m,br 1470 m,br
v _{AS} (NO ₂)	1321 vs 1254 vs,br	1420 s,br 1325 s,br	1324 s,br 1280 sh 1265 vs,br	1255 m,sp
v _S (NO ₂)	1035 m 1013 s 1004 s	1048 m,sp	1038 m 1012 s	1041 s,sp 1017 m
δ _S (NO ₂) + π(O ₂ ,NO)	777 s 764 m	880 w,br 782 m,br 778 m	791 m 774 m	792 m 780 m 765 m
δ _{AS} (NO ₂)	735 m 718 w		731 s 723 m	723 w
v(Cu-O)	336 s 299 sh 253 w,sh	510 m 455 sh 430 s 398 sh 325 m 299 w,sl	335 s,br 299 sh 253 w,sh	330 m 297 m 240 w
Lattice Modes	209 m			210 m
δ(Cu-O)	170 vw 140 vw 94 vw*			140 w 110 m 60 w 40 vs

* This far i.r. data reported are from Ferraro and Walker (177).

which are absent from the spectra reported for β -Cu(NO₃)₂ by Ferraro and Walker (185) and in this work; thus it would appear that the samples examined by James and Kimber are probably a mixture of both forms. The possibility that they may have an oxy-nitrate due to thermal decomposition while subliming the sample also cannot be ignored.

In the δ (NO₂) region, the bands at 723 and 731 cm⁻¹ are assigned as the δ_{AS} (NO₂) and the bands between 760 and 792 cm⁻¹ are assigned as the δ_S (NO₂) modes, on the basis of the relatively strong Raman bands at 780 - 792 cm⁻¹; together with the π (NO) mode which otherwise would not be observed.

The bands at 1038 - 1041 cm⁻¹ must be assumed to be the ν_S (NO₂) mode. The weakness of the Raman spectrum in the region of 1200 to 1600 cm⁻¹ makes the assignment difficult, but bands do appear at approximately 1255 and 1580 cm⁻¹, which by analogy to other bidentate spectra are assigned as the ν_{AS} (NO₂) and ν (NO*) modes respectively.

Appendix A.

Computer Programs Used for Crystal Structure Determination.

Only the features of the various programs that were utilized are described here.

A.1. DATAPR.

A program to convert the intensity data obtained during data collection into structure factor amplitudes ($|F_{hkl}|$) applying both Lorentz (L) and polarization (p) corrections. The correction used was

$$L_p = \frac{1 + \cos^2 2\theta}{2 \sin 2\theta} \quad (A1)$$

and the structure factor amplitude was then expressed as

$$|F_{hkl}| = \frac{KI_{hkl}}{L_p} \quad (A2)$$

where K is a constant determined by crystal size, beam intensity and scale factor arising from variations during data collection, and I_{hkl} is the intensity of the reflection hkl. Output generated the BUCFILE for input into program BUCILS, and listed observed $|F_{hkl}|$, $|F_{hkl}|^2$, $|F_{hkl}|^2/L_p$

and net count for each reflection. The original program was written by F.R. Ahmed, for the National Research Council of Canada and has been modified at Simon Fraser University.

A.2. FORDAP.

A program to compute Fourier syntheses. The Patterson function was based on $|F_{OBS}|^2$ and the Fourier electron density (and Fourier difference syntheses) were based on the signed F_{OBS} (and F_{CALC}). This program was originally written by A. Zalkin. Input includes unit cell dimensions, symmetry information, the observed structure factors with the phases of the calculated structure factors from FORFILE. In the case of the Patterson function, the observed structure factors came from the BUCFILE. Output was in the form of a three-dimensional electron density map and lists of the most intense peaks and troughs on the map. Cards were also obtained to act as input for further computation.

A.3. BUCILS.

A program for calculation of structure factors and full matrix least squares of the scale, atomic positional and thermal parameters in the structure. This program was based on UCILS (Northwestern University and

University of California, Irvine) and has been modified at the University of British Columbia and Simon Fraser University. Input includes unit cell dimensions, symmetry information, scale factor and the appropriate atomic parameters, as well as the observed structure factors obtained from the BUCFILE. BUCILS was used to write the following files:

Forfile: Contained calculated and observed structure factor information for use in the FORDAP program and for analysis of R factors and weights by program RANGER.

ORFILE: Contained atomic coordinates, temperature factors, standard deviations and the correlation matrix of the least square refinement for program ORFE2.

Output from BUCILS could include the scale, atomic coordinates and thermal parameters based on any or all of the cycles of least squares refinement; the shift in parameters from the previous cycle; the correlations between the various parameters and the residual index, R. Cards of the scale, atomic parameters and temperature factors were also obtained for further calculations.

A.4. DANFIG.

A program for calculation of interatomic distances

and angles based on a program by W.H. Baur and modified at the University of British Columbia and Simon Fraser University. Input included symmetry and unit cell information, atomic position and thermal parameter cards from BUCILS or FORDAP. Output listed all atoms closer than a specified distance from all other atoms and listed the bond angles around each atom.

A.5. RANGER.

A program to analyze R factors and weights for different classes of reflections based on $|F_{OBS}|$, $\sin \theta$ or indices. This program was originally written by Dr.P.W.R. Corfield at Northwestern University and modified at the University of British Columbia and Simon Fraser University. Input includes the approximate maximum absolute value of the structure factors, the number of variables and the information in the FORFILE.

A.6. MEANPLANE.

A program to calculate mean planes through various groups of atoms and the deviations of the atoms from that plane. This program was originally written by M.E. Pippy and F.R. Ahmed for the National Research Council and has been

modified at Simon Fraser University. Input includes atomic coordinates with their estimated standard deviations and unit cell dimensions. Output lists the variables from the formula for the plane $Ax^2 + By^2 + Cz^2 + D = 0$; the χ^2 (chi squared) value as an indication of the planarity of the plane; the angles between the planes and the distance of each atom from that plane.

A.7. ORTEP.

A program to plot thermal-ellipsoids for crystal structure illustrations written by C.K. Johnson, Oak Ridge National Laboratory, Oak Ridge, Tennessee and modified at Simon Fraser University. Input includes plotting information, atomic coordinates, thermal parameters and unit cell dimensions. Output is a plot produced by a Calcomp plotter.

A.8. ORFFE2.

A program to calculate inter-atomic distances and angles with standard deviations, to calculate the root-mean-square component of thermal motion along various axes and to calculate inter-atomic distances over thermal motion. The program used was a modified version of the program written by W.R. Busing, K.O. Martin and H.A. Levy at Oak Ridge National Laboratory. Input includes cell dimensions with their

standard errors and the information contained in the ORFFILE.

A.9. FIND H.

A program to position hydrogen atoms, given carbon-hydrogen bond lengths and the remaining coordination of the carbon.

A.10. FILIST.

A program which lists calculated and observed structure factors, for all reflections measured, in a format suitable for the preparation of structure factor tables for publication. This program is based on a program from the University of Canterbury.

Bibliography

1. C.C. Addison and B.J. Hathaway, J. Chem. Soc., 3099 (1958).
2. C.C. Addison and N. Logan, Advan. Inorg. Chem. Radiochem., 6, 71 (1964).
3. B.O. Field and C.J. Hardy, Quart. Rev., 18, 361 (1964).
4. P. Pascal, Nouveau Traite de Chimie Minerale, Masson, Paris, 1959, Vol. VII, p273 - 278.
5. C.C. Addison and D. Sutton, Progr. Inorg. Chem., 8, 195 (1967).
6. A. Zalkin, J.D. Forrester, and D.H. Templeton, J. Chem. Phys., 39, 2881 (1963).
7. C.C. Addison and D.J. Chapman, J. Chem. Soc., 819 (1965).
8. P.P. Gallerzot, D. Weigel and M. Prettre, Acta Cryst., 22, 699 (1967).
9. D. Weigel, B. Imelik and P. Laffitte, Bull. Soc. Chim. France, 345 (1962).
10. B.J. Hathaway, D.G. Holah and M. Hudson, J. Chem. Soc., 4586 (1963).
11. T.J. King, N. Logan, A. Morris and S.C. Wallwork, Chem. Comm., 554 (1971).
12. B.J. Hathaway and A.E. Underhill, J. Chem. Soc., 648 (1960).
13. V. Ya. Rosolovskii, G.N. Shirkova, A.I. Karelin and N.V. Krivtsov, Russ. J. Inorg. Chem., 15, 243 (1970).
14. G.N. Shirkova and V.Ya. Rosolovskii, Russ. J. Inorg. Chem., 16, 1106 (1971).
15. D.J. Millen, J. Chem. Soc., 2606 (1950).
16. I.C. Hisatsune, J.P. Devlin and Y. Wada, Spectrochim. Acta, 18, 1641 (1962).
17. B.O. Field and C.J. Hardy, J. Chem. Soc., 4428 (1964).

18. R.J. Fereday, N. Logan and D. Sutton, J. Chem. Soc. (A), 2699 (1969).
19. D. Bowler and N. Logan, Chem. Comm., 582 (1971).
20. B.O. Field and C.J. Hardy, J. Chem. Soc., 5278 (1963).
21. K.W. Bagnall, D. Brown and J.G.H. duPreez, J. Chem. Soc., 5523 (1964).
22. B.O. Field and C.J. Hardy, Proc. Chem. Soc., 76 (1962).
23. C.C. Addison and D.J. Chapman, J. Chem. Soc., 539 (1964).
24. D. Potts and A. Walker, Can. J. Chem., 49, 202 (1971).
25. C.C. Addison, Chemistry in Nonaqueous Ionizing Solvents, ed. G. Jander, H. Spandau, and C.C. Addison, Pergamon Press, Oxford, 1967, Vol.III, p 1.
26. C.C. Addison, P.M. Boorman and N. Logan, J. Chem. Soc. (A), 1434 (1966).
27. C.C. Addison and J. Lewis, J. Chem. Soc., 1874 (1953).
28. C.C. Addison, R. Davis and N. Logan, J. Chem. Soc. (A), 3333 (1970).
29. C.C. Addison, P.M. Boorman and N. Logan, J. Chem. Soc., 4978 (1965).
30. C.C. Addison and A. Walker, J. Chem. Soc., 1220 (1963)..
31. C.R. Guibert and M.D. Marshall, J. Amer. Chem. Soc., 88, 189 (1966).
32. D.W. James and G.M. Kimber, Aust. J. Chem., 23, 829 (1970).
33. D.G. Tuck, E.J. Woodhouse and P. Carty, J. Chem. Soc. (A), 1077 (1966).
34. D.W. Amos, Chem. Comm., 19 (1970).
35. C.C. Addison and W.B. Simpson, J. Chem. Soc., 598 (1965).
36. C.C. Addison, D.W. Amos, W.H.H. Hoyle and D. Sutton, J. Chem. Soc. (A), 808 (1967).

37. C.D. Garner, D. Sutton, and S.C. Wallwork, J. Chem. Soc. (A), 1949 (1967).
38. D.K. Straub, H.H. Sisler and G.E. Ryschkewitsch, J. Inorg. Nucl. Chem., 24, 919 (1962).
39. M. Schmeisser, Angew. Chem., 67, 493 (1955).
40. K.W. Bagnall, D.S. Robertson and M.A.A. Stewart, J. Chem. Soc., 3633 (1958).
41. C.C. Addison and B.M. Gatehouse, J. Chem. Soc., 613 (1960).
42. C.C. Addison and N. Hodge, J. Chem. Soc., 1138 (1954).
43. J.I. Bullock and D.G. Tuck, J. Chem. Soc., 1877 (1965).
44. T. Moeller and V.D. Aflandilian, J. Amer. Chem. Soc., 5249 (1954).
45. C.D. Garner and S.C. Wallwork, J. Chem. Soc. (A), 1496 (1966).
46. V. Gutmann and H. Tannenberger, Monatsch. Chem., 87, 421 (1956).
47. J.A. Panontin, A.K. Fisher and E.A. Heintz, J. Inorg. Nucl. Chem., 14, 145 (1960).
48. B.O. Field and C.J. Hardy, Proc. Chem. Soc., 11 (1963).
49. K.W. Bagnall, D. Brown and P.J. Jones, J. Chem. Soc., 717 and 2396 (1964).
50. D. Brown and P.J. Jones, J. Chem. Soc. (A), 733 (1966).
51. W.W. Ewing and C.F. Glick, J. Amer. Chem. Soc., 62, 2174 (1940).
52. D.K. Straub, R.S. Drago, J.T. Donoghue, Inorg. Chem., 1, 848 (1962).
53. J. Drummond and J.S. Wood, J. Chem. Soc. (A), 226 (1970).
54. D.J. Lovejoy and A.J. Vosper, Chem. Comm., 1205 (1968).

55. J.G. Bergman and F.A. Cotton, *Inorg. Chem.*, 5, 1208 (1966).
56. J. Hilton and S.C. Wallwork, *Chem. Comm.*, 871 (1967).
57. C.C. Addison and B.G. Ward, *Chem. Comm.*, 819 (1966).
58. C.C. Addison and B.G. Ward, *Chem. Comm.*, 155 (1966).
59. N. Logan, W.B. Simpson and S.C. Wallwork, *Proc. Chem. Soc.*, 341 (1964).
60. D.W. James and G.M. Kimber, *Inorg. Nucl. Chem. Letters*, 5, 609 (1969).
61. W.E. Addison and S.C. Wallwork, *J. Chem. Soc.*, 2925 (1965).
62. R.E. LaVilla and S.H. Bauer, *J. Amer. Chem. Soc.*, 85, 3596 (1963).
63. C.D. Garner and S.C. Wallwork, *Chem. Comm.*, 108 (1969).
64. C.D. Garner and S.C. Wallwork, *J. Chem. Soc. (A)*, 3092 (1970).
65. A. Walker and J.R. Ferraro, *J. Chem. Phys.*, 43, 2689 (1965).
66. T.A. Beineke and J. Delgaudio, *Inorg. Chem.*, 7, 715 (1968).
67. J.R. Ferraro, L.I. Katzin and G. Gibson, *J. Amer. Chem. Soc.*, 77, 327 (1955).
68. W.W. Wendlandt and J.L. Bear, *J. Inorg. Nucl. Chem.*, 12, 276 (1960).
69. J.L. Ryan, *J. Phys. Chem.*, 64, 1375 (1960).
70. J.L. Ryan, *J. Phys. Chem.*, 65, 1099 (1961).
71. C.C. Addison, H.A. Champ, N. Hodge and A.H. Norbury, *J. Chem. Soc.*, 2354 (1964).
72. G.A. Barclay, T.M. Sabine and J.C. Taylor, *Acta Cryst.*, 19, 205 (1965).

73. C.C. Addison, N. Logan, S.C. Wallwork and C.D. Garner, Quart. Rev., 25, 289 (1971).
74. F.W.B. Einstein, E. Enwall, D.M. Morris and D. Sutton, Inorg. Chem., 10, 678 (1971).
75. E. Yasaki, I. Oonishi, H. Kawaguchi, S. Kawaguchi, and Y. Komiyama, Bull. Chem. Soc. Japan, 43, 1354 (1970).
76. A.F. Cameron, D.W. Taylor and R.H. Nuttall, J.C.S. Dalton, 422 (1972).
77. M. Mathew, G.J. Palenik and A.J. Carty, Can. J. Chem., 49, 4119 (1971).
78. H. Nakai, S. Ooi, H. Kuroya, Bull. Chem. Soc. Japan, 43, 577 (1970).
79. N.A. Bailey and S.J. Bowler, J. Chem. Soc. (A), 1763 (1971).
80. G.W. Bushnell and M.A. Khan, Can. J. Chem., 50, 315 (1972).
81. R.E. Drew and F.W.B. Einstein, Acta Cryst. B 28, 345 (1972).
82. M. ul Hague, C.N. Caughlan, F.A. Hart and R. VanNice, Inorg. Chem., 10, 115 (1971).
83. N.K. Dalley, M.H. Mueller and S.H. Simonsen, Inorg. Chem., 10, 323 (1971).
84. A.F. Cameron, D.W. Taylor and R.H. Nuttall, J.C.S. Dalton, 58 (1972).
85. A.F. Cameron, K.P. Forrest, R.H. Nuttall and D.W. Taylor, Chem. Comm., 210 (1970).
86. A.F. Cameron, K.P. Forrest, R.H. Nuttall and D.W. Taylor, J. Chem. Soc. (A), 2492 (1971).
87. G.S. Brownlee, A. Walker, S.C. Nyburg, and J.T. Szymanski, Chem. Comm., 1073 (1971).
88. B. Duffin and S.C. Wallwork, Acta Cryst., 20, 210 (1966).
89. R.V. Biagetti, W.G. Bottjes and H.M. Haendler, Inorg. Chem., 5, 379 (1966).

90. W. Nowacki and R. Scheidegger, *Helv. Chim. Acta*, 35, 375 (1952).
91. M. ul Hague, F.A. Hart and C.N. Caughlan, *Chem. Comm.*, 1240 (1970).
92. G.G. Messmer and G.J. Palenik, *Inorg. Chem.*, 8, 2750 (1969).
93. Raman Spectroscopy, H.A. Szymanski, ed; Plenum Press, New York, 1967, p 7.
94. T.R. Gilson and P.J. Hendra, Laser Raman Spectroscopy, John Wiley and Sons, New York, 1970, p 64.
95. H. Brintzinger and R.E. Hester, *Inorg. Chem.*, 5, 980 (1966).
96. R.E. Hester and W.E.L. Grossman, *Inorg. Chem.*, 5, 1308 (1966).
97. N.F. Curtis and Y.M. Curtis, *Inorg. Chem.*, 4, 804 (1965).
98. G. Topping, *Spectrochim. Acta*, 21, 1743 (1965).
99. R.H. Nuttall and D.W. Taylor, *Chem. Comm.*, 1417 (1968).
100. J.I. Bullock and F.W. Parrett, *Chem. Comm.*, 157 (1969).
101. A.B.P. Lever, E. Mantovani and B.S. Ramaswamy, *Can. J. Chem.*, 49, 1957 (1971).
102. M.H. Brooker and D.E. Irish, *Can. J. Chem.*, 48, 1183, (1970).
103. D.W. James and W.H. Leong, *J. Chem. Phys.*, 49, 5089 (1968).
104. M.H. Brooker, D.E. Irish and G.E. Boyd, *J. Chem. Phys.*, 53, 1083 (1970).
105. W.H. Hartford and M. Darrin, *Chem Rev.*, 58, 1 (1958).
106. M. Schmeisser and D. Lutzow, *Angew. Chem.*, 66, 230 (1954).

107. E.E. Aynsley, J. Chem Soc., 2425 (1958).
108. A. Engelbrecht and A.V. Grosse, J. Amer. Chem. Soc., 76, 2042 (1954).
109. D.J. Chapman, PhD. Thesis, University of Nottingham, (1965).
110. R.J. Fereday and D. Sutton, Chem. Comm., 510 (1966).
111. M.A. Hepworth and K.H. Jack, Acta Cryst., 10, 345 (1957).
112. Von R. Hoppe, W. Liebe and W. Dähne, Zeit.Anorg. and Allgem. Chemie, 307, 276 (1961).
113. S. Emori, M. M. Kiskita and M. Kubo, Inorg. Chem., 8, 1385 (1969).
114. A.J. Edwards, J. Chem. Soc.(A), 2653 (1971).
115. R. Dingle, Inorg. Chem., 4, 1287 (1965).
116. G.C. Allen, G.A.M. El-Sharkawy and K.D. Warren, Inorg. Chem., 10, 2538 (1971).
117. A.Cretien and G. Varga, Bull.Soc. Chim. France, Ser. 5, 3, 2385 (1936)..
118. T.S. Davis, J.P. Fackler and M.J. Weeks, Inorg. Chem., 7, 1994 (1968)..
119. I. Bernal, N. Elliott, T. Lalancette, Chem. Comm., 803, 1971.
120. W.E. Hatfield, R.C. Fay, C.E. Pfluger and T.S. Piper, J. Amer. Chem. Soc., 85, 265 (1963).
121. W. Levason, C.A. McAuliffe and S.E. Murray, Inorg. Nucl. Chem. Letters, 8, 97 (1972).
122. Inorganic Syntheses, ed. W.C. Fernelius, McGraw-Hill, NewYork, 1946, Vol. II, p 213.
123. J.R. Fowler and J Kleinberg, Inorg. Chem., 9, 1005 (1970).
124. G.H. Cartledge and W.P. Ericks, J. Amer. Chem. Soc., 58, 2061 (1936).

125. T.S. Piper and L. Carlin, J. Chem. Phys., 35, 1809 (1961).
126. Inorganic Syntheses, ed. J. Kleinberg, McGraw-Hill, New York, 1963, Vol VII, p 183.
127. S. Pinchas, B.L. Silver and I. Laulicht, J. Chem. Phys., 46, 1506 (1967).
128. R.D. Hancock and D.A. Thornton, Inorg. Nucl. Chem. Letters, 3, 419 (1967).
129. M. Mikami, I. Nakagawa and T. Shimastouchi, Spectrochim. acta, 23A, 1037 (1967).
130. G. Brauer, Handbook of Preparative Inorganic Chemistry, Academic Press, New York, 1965 Vol 2, p. 1469.
131. C.P. Prabhakaran and C.C. Patel, J. Inorg Nucl. Chem., 30, 867 (1968).
132. M. Bartlett and G.J. Palenik, Chem. Comm. 416 (1970).
133. W.M. Reiff and W.A. Baker, Inorg. Chem., 9, 570 (1970).
134. A. Van den Bergen, K.S. Murray, M.J.O'Connor and B.O. West, Aust. J. Chem., 22, 39 (1969).
135. R.L. Collin and W.N. Lipscomb, Acta Cryst., 2, 104 (1949).
136. R. Norrestam, Acta Chem. Scand., 21, 2871 (1967).
137. S. Asbrink, to be published, see ref. 134.
138. R. Dev and G.H. Cady, Inorg. Chem., 10, 2354 (1971).
139. E. Contreras, V. Riera and R. Uson, Inorg. Nucl. Chem. letters, 8, 287 (1972).
140. H.A. Goodwin and R.N. Sylva, Aust. J. Chem., 18, 1743 (1965).
141. H.A. Goodwin and R.N. Sylva, Aust. J. Chem., 20, 629 (1967).
142. H. Funk and H. Kreis, Zeit. Anorg. Allgem. Chemie, 349, 45 (1967).

143. L.J. Boucher, J. Amer. Chem. Soc., 90, 6640 (1968).
144. L.J. Boucher, J. Amer. Chem. Soc., 92, 2725 (1970).
145. B.J. Bulkin, J. Opt. Soc. Amer., 59, 1387 (1969).
146. D.F. Shriver, Appl. Spect., 23, 552 (1969).
147. L.F. Fieser and M. Fieser, Reagents for Organic Synthesis, John Wiley and Sons, New York, 1967, p 637.
148. Inorganic Syntheses, W.L. Jolly, ed. McGraw-Hill, New York. 1968, Vol XI, pp 56 - 61.
149. B.N. Figgis and R.S. Nyholm, J. Chem Soc., 4190 (1958).
150. R.J. Fereday, PhD. Thesis, University of Nottingham (1968).
151. C.C. Addison, Coord. Chem. Rev., 1, 58 (1966).
152. C.C. Addison, Adv. in Chem Series #35, C.B. Colburn, ed., Amer. Chem. Soc., 1962. p 131.
153. J.F. Olsen and L. Burnelle, J. Amer. Chem. Soc., 92, 3659 (1970).
154. T.W. Martin, L.L. Swift and J.H. Venable, J. Chem. Phys., 52, 2138(1970).
155. T.W. Martin, J.M. Burk, and A. Henshall, J. Amer. Chem. Soc., 88, 1097 (1966).
156. A.J. Carty and D.G. Tuck, J. Chem. Soc. (A), 1081 (1966).
157. J.J. Patel, D.B. Sowerby and D.G. Tuck, J. Chem. Soc, (A), 1187 (1967).
158. W.R. McWhinnie and J.D. Miller, Adv. Inorg. Chem. Radiochem, 12, 135 (1969).
159. J.D. Donaldson and D.G. Nicholson, J. Chem. Soc.(A), 145 (1970).
160. D. Davenport, H. Burkhardt and H. Sisler, J. Amer. Chem. Soc., 75, 4175 (1953)
161. D.R. Sears and J.L. Hoard, J. Chem. Phys., 50, 1066 (1969).

162. A.J. Edwards, J. Chem. Soc.(A), 3074 (1971).
163. B. Morosin and J.R. Bratkevode, Acta Cryst., 17, 705 (1964).
164. P.M. Plaksin, R.C. Stoufer, M. Mathew and G.J. Palenik, J. Amer. Chem. Soc., 94, 2121 (1972).
165. R.F. Stewart, E.F. Davidson and W.T. Simpson, J. Chem. Phys., 42, 3175 (1965).
166. International Tables for X-Ray Crystallography, Kynoch Press, Birmingham, 1962, Vol III, p 202.
167. International Tables for X-Ray Crystallography, Kynoch Press, Birmingham, 1962, Vol III, p 213.
168. E.L. Muetterties and C.M. Wright, Quart. Rev., 21, 109 (1967).
169. J. C. Taylor, M.H. Mueller and R.L. Hitterman, Acta Cryst., 20, 842 (1966).
170. D. Britton and J.D. Dunitz, Acta Cryst., 19, 815 (1965).
171. F.A. Cotton, D.M.L. Goodgame and R.H. Soderberg, Inorg. Chem., 2, 1162 (1963).
172. S. Scavnicar and B. Matkovic, Acta Cryst., B 25, 2046 (1969).
173. M.S. Hussain and H. Hope, Acta Cryst. B 25, 1866 (1969).
174. C.C. Addison, P.M. Boorman and N. Logan, J. Chem. Soc., 5146 (1965).
175. L.Couture and J.P. Mathieu, Compt Rend., 225, 1140 (1947).
176. W.F. Murphy, M.V. Evans and P. Bender, J. Chem. Phys., 47, 1836 (1967).
177. "Polarization Measurements with the Cary 81 Raman Spectrometer", Cary Instruments, Monrovia, Calif.

178. A.B.P. Lever, *Inorg. Chem.*, 4, 1042 (1965).
179. S.D. Ross, *Spectrochim. Acta*, 18, 1572 (1962).
180. G. Herzberg, *Infrared and Raman Spectroscopy of Polyatomic Molecules*, Van Nostrand, New York, 1955, p 167.
181. N. Logan and W.B. Simpson, *Spectrochim. Acta*, 21, 857 (1965).
182. W.F. Hillebrand, G.E.F. Lundell, H.A. Bright and J.I. Hoffman, *Applied Inorganic Analysis*, J. Wiley and Sons, New York, 1953.
183. L. Erdey, *Gravimetric Analysis*, Pergamon Press, Oxford, 1956.
184. K. Buijs and C.J.H. Schutte, *Spectrochim. Acta*, 18, 307 (1962).
185. J.R. Farraro and A. Walker, *J. Chem. Phys.*, 42, 1273 (1965).
186. R.E. Miller, R.R. Getty, K.L. Trevil and G.E. Leroi, *J. Chem. Phys.*, 51, 1385 (1969).
187. A.P.I. Project 44, Raman Spectral Data # 64.
188. F.L. Voelz, F.F. Cleveland and A.G. Meister, *J. Opt. Soc. Amer.*, 43, 1061 (1953).
189. C.W. Brown, R.J. Obsernski, J.R. Allkins and E.R. Lippincott, *J. Chem Phys.*, 49, 4806 (1968).
190. D.H. Whiffen, *J. Chem. Soc.*, 1350 (1950).
191. P.R. Griffiths and H.W. Thompson, *Proc. Roy. Soc.*, 298A, 51 (1967).
192. I. Nakagawa and J.L. Walker, *J. Chem. Phys.*, 51, 1389 (1969).
193. M.H. Brooker, *J. Chem. Phys.*, 53, 2670 (1970).
194. D.L. Rousseau, R.E. Miller, and G.E. Leroi, *J. Chem. Phys.*, 48, 3409 (1968).

195. J. Greenberg and L.J. Hallgren, J. Chem Phys., 33, 900 (1960).
196. D. Bloor, Spectrochim. Acta, 21, 133 (1965).
197. C.C. Addison and D. Sutton, J. Chem Soc., 5553 (1964).
198. P. Krishnamurti, Indian J. Physics, 5, 1 (1930).
199. H. Nisi, Chem. Abstracts, 27, 5248 (1933).
200. D.W.A. Sharp and J Thorley, J. Chem. Soc., 3357 (1963).
201. C.C. Addison and B. Hathaway, J. Chem. Soc., 1468 (1960).
202. R.H. Pierson, A.N. Fletcher and E. St. Clair Gantz, Anal. Chem, 28, 1218 (1956).
203. M.H. Brooker and D.E. Irish, Can J. Chem, 48, 1198 (1970).
204. G.M. Kimber and D.W. James, Inorg. Nucl. Chem. Letters, 5, 771 (1969).